

**DESIGN AND CONTROL OF  
COMPONENTS-BASED  
INTEGRATED SERVO  
PNEUMATIC DRIVES**

**July 2006**

**Hongtao Pan**

**A Thesis Submitted For the Award of  
Doctor of Philosophy Degree By  
Department of Engineering and Technology  
De Montfort University**

## **Declaration**

No part of the work described in this thesis has been submitted in support of an application for any other degree or qualification of this or any other University or any other Institution of learning.

## Acknowledgement

I would like to give my sincere gratitude to my research supervisors, Dr Junsheng Pu and Mr. B. C. Wong, for their supervision and encouragement. In particular, I would like to express my appreciation to them for their interest and enthusiasm, and for making time to read, modify and comment on the manuscript.

I would like to thank Professor Philip R Moore for his help; I would like to thank all the members of Mechatronics Research Group (MRG) at De Montfort University.

Finally, and most importantly, I would like to express my sincere appreciation to my beloved wife Dongmei Xue, my son, my parents and other members of my family. Their love and encouragement have made my research at De Montfort University a bright remembrance.

## Synopsis

On-off traditional pneumatic drives are most widely used in industry offering low-cost, simple but flexible mechanical operation and relatively high power to weight ratio. For a period of decade from mid 1980's to 1990's, some initiatives were made to develop servo pneumatic drives for most sophisticated applications, employing purpose-designed control valves for pneumatic drives and low friction cylinders. However, it is found that the high cost and complex installation have discouraged the manufacturer from applying servo pneumatic drives to industrial usage, making them less favourable in comparison to their electric counterpart. This research aims to develop low-cost servo pneumatic drives which are capable of point-to-point positioning tasks, suitable for applications requiring intermediate performance characteristics. In achieving this objective, a strategy that involves the use of traditional on-off valve, simple control algorithm and distributed field-bus control networks has been adopted, namely, the design and control of Components-based Integrated Pneumatic Drives (CIPDs).

Firstly, a new pneumatic actuator servo motion control strategy has been developed. With the new motion control strategy, the processes of positioning a payload can be achieved by opening the control valve only once. Hence, low-speed on-off pneumatic control valves can be employed in keeping the cost low, a key attraction for employing pneumatic drives. The new servo motion control strategy also provides a way of controlling the load motion speed mechanically. Meanwhile, a new PD-based three-state closed-loop control algorithm also has been developed for the new control scheme. This control algorithm provides a way of adapting traditional PID (Proportional Integral Derivative) control theories for regulating pneumatic drives. Moreover, a deceleration control strategy has been developed so that both high-speed and accurate positioning control can be realised with low cost pneumatic drives. Secondly, the

effects of system parameters on the transient response are studied. In assisting the analysis, a second order model is developed to encapsulate the velocity response characteristics of pneumatic drives to a step input signal. Stability analyses for both open loop and closed-loop control have also been carried out for the CIPDs with the newly developed motion control strategy. Thirdly, a distributed control strategy employing LonWorks has been devised and implemented, offering desirable attributes, high re-configurability, low cost and easy in installation and maintenance, etc to keep with the traditional strength for using pneumatic drives. By applying this technology, the CIPDs become standard components in “real” and “virtual” design environments. A remote service strategy for CIPDs using TCP/IP communication protocol has also been developed.

Subsequently a range of experimental verifications has been carried out in the research. The experimental study of high-speed motion control indicates that the deceleration control strategy developed in the research can be an effective method in improving the behaviour of high speed CIPDs. The verification of open loop system behaviour of CIPDs shows that the model derived is largely indicative of the likely behaviour for the system considered, and the steady state velocity can be estimated using the Velocity Gain  $K_v$ . The evaluation made on a pneumatically driven pick-and-place machine has also confirmed that the system setup, including wiring, tuning, and system reconfiguration can be achieved in relative ease. This pilot study reveals the potential for employing CIPDs in building highly flexible cost effective manufacturing machines. It can thus be concluded that this research has developed successfully a new dimension and knowledge in both theoretical and practical terms in building low-cost servo pneumatic drives, which are capable of point-to-point positioning through employing traditional on-off pneumatic valves and actuators and through their integration with distributed control technology (LonWorks) by adopting a component-based design paradigm.

# Contents

<b>DECLARATION.....</b>	<b>II</b>
<b>ACKNOWLEDGEMENT.....</b>	<b>III</b>
<b>SYNOPSIS.....</b>	<b>IV</b>
<b>CONTENTS.....</b>	<b>VI</b>
<b>LIST OF FIGURES.....</b>	<b>XII</b>
<b>LIST OF TABLES.....</b>	<b>XVI</b>
<b>NOMENCLATURE.....</b>	<b>XVI</b>
<b>ABBREVIATION.....</b>	<b>XVI</b>
<b>CHAPTER 1 INTRODUCTION.....</b>	<b>1</b>
1.1 RESEARCH BACKGROUND.....	1
1.1.1 <i>Advantages of servo pneumatic drives.....</i>	<i>1</i>
1.1.2 <i>The drawback in building traditional servo pneumatic drives.....</i>	<i>3</i>
1.1.3 <i>The way forward in building servo pneumatic drives.....</i>	<i>5</i>
1.2 THE RESEARCH OBJECTIVE.....	8
1.3 THESIS ORGANISATION.....	9
<b>CHAPTER 2 LITERATURE SURVEY.....</b>	<b>11</b>
2.1 INTRODUCTION.....	11
2.2 RESEARCHES ON SERVO PNEUMATIC SYSTEM.....	11
2.2.1 <i>Studies on fundamental knowledge of pneumatic system.....</i>	<i>12</i>
2.2.1.1 Studies on characteristics analysis and modelling, control approaches, and design models of pneumatic servo drives.....	13
2.2.1.2 Studies on development of servo pneumatic components.....	20
2.3 FLEXIBLE MANUFACTURING SYSTEMS AND DISTRIBUTED CONTROL.....	21

2.4	FRAMEWORK OF COMPONENTS-BASED DISTRIBUTED CONTROL SYSTEMS .....	23
2.4.1	<i>Studies on application of distributed control technology</i> .....	24
<b>CHAPTER 3 ARCHITECTURE OF COMPONENTS-BASED INTEGRATED PNEUMATIC DRIVES.....</b>		<b>29</b>
3.1	INTRODUCTION .....	29
3.2	OVERVIEW OF THE COMPONENTS-BASED INTEGRATED PNEUMATIC DRIVES	30
3.3	ARCHITECTURE OF THE COMPONENTS-BASED INTEGRATED PNEUMATIC DRIVES CONTROL NETWORK.....	31
3.4	COMPOSITION OF A COMPONENTS-BASED INTEGRATED PNEUMATIC DRIVE.	33
3.5	HARDWARE COMPOSITION OF COMPONENTS-BASED INTEGRATED PNEUMATIC DRIVES .....	37
3.5.1.1	Composition of Integrated Pneumatic Actuator Module (IPA).....	38
3.5.1.2	Composition of Integrated Direction Control Module (IDC).....	41
3.5.1.3	Composition of Integrated Speed Control module (ISC) .....	43
<b>CHAPTER 4 MOTION CONTROL OF COMPONENTS-BASED INTEGRATED PNEUMATIC DRIVES.....</b>		<b>45</b>
4.1	INTRODUCTION .....	45
4.2	PNEUMATIC ACTUATOR MOTION CONTROL STRATEGY EMPLOYED WITHIN CIPDs .....	46
4.2.1	<i>Cylinder motion control strategy of CIPDs with a symmetric pneumatic cylinder</i> .....	46
4.2.2	<i>Pneumatic circuit with an asymmetric pneumatic cylinder</i> .....	48
4.3	SERVO MOTION CONTROL OF THE CIPDs .....	50
4.3.1	<i>Three significant motion states of a full motion process</i> .....	50
4.3.2	<i>Servo control algorithm of the CIPDs</i> .....	53
4.3.3	<i>Generation of three-state control signal</i> .....	57
4.4	HIGH-SPEED MOTION CONTROL STRATEGY OF CIPDs.....	60
4.4.1	<i>Minimum Start-Stop Displacement</i> .....	60
4.4.2	<i>Approaches for increasing positioning accuracy</i> .....	62
4.4.3	<i>Acceleration and deceleration control of CIPDs</i> .....	63

**CHAPTER 5 NETWORK SERVICE OF COMPONENTS-BASED INTEGRATED PNEUMATIC DRIVES.....66**

5.1 INTRODUCTION .....66

5.2 CONNECTIVITY OF COMPONENTS-BASED INTEGRATED PNEUMATIC DRIVES NETWORK WITH BUSINESS NETWORKS .....67

5.3 COMPOSITION OF GATEWAY DEVICE.....68

5.4 AN EXAMPLE OF GATEWAY DEVICE .....69

    5.4.1 *Gateway device Internet self-configuration and auto-registration processes* ..... 71

    5.4.2 *Hardware composition of the example gateway device*..... 71

**CHAPTER 6 MATHEMATICAL ANALYSIS OF THE PNEUMATIC SYSTEM OF COMPONENTS-BASED INTEGRATED PNEUMATIC DRIVES .....74**

6.1 INTRODUCTION ..... 74

6.2 BASIC ASSUMPTIONS ..... 75

6.3 BASIC GOVERNING EQUATIONS AND THEIR LINEARIZATION ..... 75

    6.3.1 *The flow relationships of the control valves* ..... 76

    6.3.2 *Dynamic flow relationship within the actuator chambers*..... 79

    6.3.3 *Piston and payload dynamics* ..... 80

6.4 MODELLING OF OPEN-LOOP SYSTEM .....82

    6.4.1 *The open-loop transfer function of moving state of motion*..... 82

    6.4.2 *The state-space representation of moving state of motion*..... 85

    6.4.3 *State-space presentation of the stopping state of motion*..... 86

    6.4.4 *State-space presentation of a complete motion process* ..... 88

6.5 THE SYSTEM TRANSIENT-RESPONSE SPECIFICATIONS ..... 89

6.6 STABILITY ANALYSIS OF OPEN-LOOP CONTROLLED INTEGRATED PNEUMATIC DRIVES ..... 90

    6.6.1 *Stability analysis of open-loop system at the moving state of motion*.. 90

    6.6.2 *Stability analysis of the stopping state of motion*..... 91

6.7 STABILITY ANALYSIS OF PD-BASED THREE-STATE CLOSED-LOOP CONTROLLED INTEGRATED PNEUMATIC DRIVES ..... 92



6.7.1	<i>Energy variation within a complete motion process</i> .....	93
6.7.1.1	The kinetic energy during moving state of motion.....	94
6.7.1.2	The maximum dissipation of load kinetic energy during the stopping state of motion.....	95
6.7.1.3	Potential energy .....	96
6.7.2	<i>Stability analysis and Simulink verification</i> .....	98
6.7.2.1	Simulink model composition of closed-loop control system.....	98
6.7.2.2	Stability analysis .....	98
6.8	DETERMINATION OF THE NON-DRIVING CHAMBER PRESSURE.....	103
6.9	EFFECT OF THE EXHAUST ORIFICE SIZE ON LOAD VELOCITY RESPONSE .....	105
<b>CHAPTER 7</b>	<b>EXPERIMENTAL SYSTEM SETUP .....</b>	<b>108</b>
7.1	INTRODUCTION .....	108
7.2	SETUP OF ES-I (MATHEMATICAL ANALYSIS VERIFICATION SYSTEM) .....	108
7.2.1	<i>Structure of the ES-I</i> .....	108
7.2.2	<i>Specifications and characteristics of the ES-I</i> .....	113
7.2.2.1	NextMove Digital Motion Controller .....	114
7.2.2.2	Airflow rate regulator .....	115
7.3	SETUP OF ES-II (SYSTEM FOR HIGH-SPEED MOTION CONTROL OF CIPDs ) .....	117
7.4	SETUP OF ES-III (TWO AXES GANTRY TYPE PICK-AND-PLACE MACHINE). .....	120
7.5	CONSTRUCTION OF TWO AXES GANTRY TYPE PICK-AND-PLACE MACHINE .....	121
7.6	TP/FT-10 CONTROL MODULE BASED SERVO MOTION CONTROLLER .....	124
7.6.1	<i>Assistant circuits of the TP/FT-10 Control Module</i> .....	124
7.6.1.1	Power supply:.....	125
7.6.1.2	Position measurement: .....	126
7.6.1.3	Home position sensor block:.....	126
7.7	PROGRAMMING OF THE SERVO MOTION CONTROLLER.....	127
7.7.1	<i>Closed loop control update timer</i> .....	127
7.7.2	<i>Use of Integer in control algorithm programming</i> .....	128
<b>CHAPTER 8</b>	<b>EXPERIMENTAL STUDIES.....</b>	<b>132</b>
8.1	INTRODUCTION .....	132

8.2	FRICION CHARACTERISTICS OF THE ES-I (MATHEMATICAL ANALYSIS SYSTEM) .....	132
8.2.1	<i>Static friction of the ES-I</i> .....	133
8.2.2	<i>The system viscous friction and Coulomb friction</i> .....	135
8.3	VERIFICATION OF MATHEMATICAL MODELLING OF CIPDs .....	136
8.3.1	<i>Verification of open loop system transfer function of the CIPDs</i> .....	137
8.3.2	<i>Verification of the Velocity Gain <math>K_v</math> of the CIPDs</i> .....	137
8.3.3	<i>Verification of pulse-input response using state-space presentation of the CIPDs</i> .....	139
8.4	EXPERIMENTAL STUDIES OF HIGH-SPEED MOTION CONTROL OF CIPDs ....	141
8.5	EXPERIMENTAL STUDIES ON THE TWO AXES GANTRY TYPE PICK-AND-PLACE MACHINE (ES-III).....	144
8.5.1	<i>Nodes within the two axes gantry type pick-and-place machine network</i> .....	144
8.5.2	<i>Test of the motion controller performance</i> .....	146
8.5.3	<i>The Commander</i> .....	149
8.5.4	<i>Experimental results of control of the Pick-and-place Machine</i> .....	151
<b>CHAPTER 9</b>	<b>CONCLUSIONS .....</b>	<b>153</b>
9.1	RESEARCH CONTRIBUTIONS.....	153
9.1.1	<i>Development of “on-off” control strategy for pneumatic cylinder motion</i> .....	153
9.1.2	<i>Development of PD-based three-state control algorithm for the “on-off” control strategy</i> .....	154
9.1.3	<i>Development of components-based architecture of integrated pneumatic drives</i> .....	154
9.1.4	<i>Mathematical analyses of pneumatic system with the new cylinder motion control approach and the “on-off” control strategy</i> .....	156
9.1.5	<i>Discovery of the Velocity Gain of pneumatic system with the new motion control strategy</i> .....	157
9.1.6	<i>Application considerations of Neuron Chip 3150 for distributed control of pneumatic drives</i> .....	157
9.1.7	<i>Research of high-speed motion control of pneumatic drives</i> .....	157

9.2	RECOMMENDATIONS FOR FURTHER RESEARCH WORK .....	158
9.2.1	<i>Further research on performance of pneumatic drives with the new motion control strategy using other control algorithm.....</i>	<i>158</i>
9.2.2	<i>Research on velocity profile control of pneumatic drives with the new motion control strategy.....</i>	<i>158</i>
9.2.3	<i>Research on the application of other network technology in the CIPDs .....</i>	<i>159</i>
<b>APPENDIX LONWORKS TECHNOLOGY.....</b>		<b>160</b>
A.1	<i>Motorola MC143150 Neuron Chip.....</i>	<i>162</i>
A.2	<i>Echelon TP/FT-10F Control Module.....</i>	<i>164</i>
A.3	<i>Programming language - Neuron C.....</i>	<i>166</i>
A.4	<i>Network communications .....</i>	<i>168</i>
A.4.1	Communications between devices using network variables.....	168
A.4.2	Communications between devices using application messages .....	170
<b>LIST OF REFERENCES.....</b>		<b>172</b>

## List of Figures

<i>Figure 1-1 A typical architecture of traditional servo pneumatic drive.....</i>	<i>3</i>
<i>Figure 1-2 Necessary components required to build a servo pneumatic drive (excluding servo motion controller).....</i>	<i>4</i>
<i>Figure 3-1 Architecture of Components-based Integrated Pneumatic Drives system</i>	<i>31</i>
<i>Figure 3-2 The relationship among the distributed control system image, the database and the practical control system.....</i>	<i>32</i>
<i>Figure 3-3 Composition of a components-based integrated pneumatic drive.....</i>	<i>33</i>
<i>Figure 3-4 CIPD component image for control system.....</i>	<i>35</i>
<i>Figure 3-5 Connection of components in virtual environment design .....</i>	<i>36</i>
<i>Figure 3-6 Composition of a Components-based Integrated Pneumatic Drive .....</i>	<i>37</i>
<i>Figure 3-7 Pneumatic circuit diagram of CIPD.....</i>	<i>38</i>
<i>Figure 3-8 Composition of Integrated Pneumatic Actuator component .....</i>	<i>39</i>
<i>Figure 3-9 Hardware composition of the integrated TP/FT-10F Control Module.....</i>	<i>41</i>
<i>Figure 3-10 Composition of IDC component .....</i>	<i>42</i>
<i>Figure 3-11 Composition of ISC component.....</i>	<i>43</i>
<i>Figure 4-1 Simplified pneumatic circuit diagram of the CIPDs.....</i>	<i>47</i>
<i>Figure 4-2 Pneumatic circuit of the CIPDs during A direction motion of piston .....</i>	<i>48</i>
<i>Figure 4-3 Pneumatic circuit of the CIPDs during B direction motion of piston .....</i>	<i>48</i>
<i>Figure 4-4 The pneumatic circuit diagram of the CIPDs using an asymmetric pneumatic cylinder.....</i>	<i>49</i>
<i>Figure 4-5 Three significant motion states of a full motion process.....</i>	<i>51</i>
<i>Figure 4-6 Relationship between load position, load velocity, control signals for Valves A and B and tree-state control signal.....</i>	<i>52</i>
<i>Figure 4-7 Block diagram of a process with a feedback controller .....</i>	<i>54</i>
<i>Figure 4-8 Block diagram of the servo control loop of CIPDs .....</i>	<i>56</i>
<i>Figure 4-9 Procedures of converting analogue signal to valve control signals.....</i>	<i>58</i>

<i>Figure 4-10 The function of the Interpreting Block.....</i>	<i>58</i>
<i>Figure 4-11 Relationship between the servo control demand and the three-state control signal. ....</i>	<i>59</i>
<i>Figure 4-12 Relationship between the valve control signal, the valve response and the load velocity.....</i>	<i>61</i>
<i>Figure 4-13 Deceleration control strategy of CIPDs.....</i>	<i>64</i>
<i>Figure 4-14 Pneumatic circuit of high-speed CIPDs with four speed valves.....</i>	<i>64</i>
<i>Figure 5-1 Proposed architecture of CIPDs network services.....</i>	<i>68</i>
<i>Figure 5-2 Composition of gateway device .....</i>	<i>69</i>
<i>Figure 5-3 Types of messages between control network and business network.....</i>	<i>70</i>
<i>Figure 5-4 Block diagram of Gateway device used in the research.....</i>	<i>72</i>
<i>Figure 6-1 Schematic diagram of the system when the Chamber B is driving chamber .....</i>	<i>76</i>
<i>Figure 6-2 Friction model: (a) nonlinear Coulomb friction and stiction; (b) linear viscous friction; (c) combination friction model.....</i>	<i>81</i>
<i>Figure 6-3 Schematic diagram of the system at stopping state of motion.....</i>	<i>87</i>
<i>Figure 6-4 Simplified block diagram of CIPD's servo control loop.....</i>	<i>92</i>
<i>Figure 6-5 The relationship between valve control signal and the load velocity.....</i>	<i>93</i>
<i>Figure 6-6 Illustration of potential energy of CIPD.....</i>	<i>97</i>
<i>Figure 6-7 Composition of closed-loop control system Simulink model.....</i>	<i>98</i>
<i>Figure 6-8 Simulation result: velocity profile when the closed-loop control CIPD is a stable system .....</i>	<i>99</i>
<i>Figure 6-9 Simulation result: Positioning profile when the closed-loop control CIPD is a stable system.....</i>	<i>100</i>
<i>Figure 6-10 Simulation result: velocity profile when the closed-loop control CIPD is an asymptotically stable system.....</i>	<i>101</i>
<i>Figure 6-11 Simulation result: positioning profile when the closed-loop control CIPD is an asymptotically stable system .....</i>	<i>101</i>
<i>Figure 6-12 Simulation result: velocity profile when the closed-loop control CIPD is an unstable system .....</i>	<i>102</i>
<i>Figure 6-13 Simulation result: positioning profile when the closed-loop control CIPD is an unstable system.....</i>	<i>103</i>

<i>Figure 6-14 The relationship between ratio of chamber pressure-supply pressures and ratio of inlet-outlet orifice area .....</i>	<i>105</i>
<i>Figure 7-1 Simplified construction views of the EP-I.....</i>	<i>109</i>
<i>Figure 7-2 The block diagram of the closed loop control system.....</i>	<i>110</i>
<i>Figure 7-3 The symbol of FESTO® MPYE-5-1/8HF-010B valve .....</i>	<i>112</i>
<i>Figure 7-4 The flow characteristic of FESTO® MPYE-5-1/8HF-010B valve .....</i>	<i>113</i>
<i>Figure 7-5 Configuration of pneumatic control valves for EP-I.....</i>	<i>113</i>
<i>Figure 7-6 Block diagram of NextMove Digital Motion Controller configuration with EP-I and data analysing host.....</i>	<i>115</i>
<i>Figure 7-7 Dimensions of the Connector and the Orifice Regulation Plate .....</i>	<i>116</i>
<i>Figure 7-8 Setup of the airflow rate regulator .....</i>	<i>116</i>
<i>Figure 7-9 Simplified construction views of the Experimental Study System.....</i>	<i>118</i>
<i>Figure 7-10 The block diagram of the closed loop control system.....</i>	<i>119</i>
<i>Figure 7-11 3-D view of pneumatically driven pick-and-place machine .....</i>	<i>121</i>
<i>Figure 7-12 Simplified construction views of pick-and-place machine.....</i>	<i>122</i>
<i>Figure 7-13 Schematic diagram of motion for the pick-and- place machine .....</i>	<i>123</i>
<i>Figure 7-14 Block diagram of CIPD motion controller .....</i>	<i>125</i>
<i>Figure 7-15 Encoder connection to the Neuron Chip .....</i>	<i>126</i>
<i>Figure 7-16 Circuit diagram of home position sensor block.....</i>	<i>127</i>
<i>Figure 7-17 General processing procedure of control algorithm calculation.....</i>	<i>129</i>
<i>Figure 7-18 Processing procedure of variable calculation of CIPDs.....</i>	<i>130</i>
<i>Figure 8-1 The definitions for the piston positions and motion direction.....</i>	<i>134</i>
<i>Figure 8-2 Static friction distribution of the experimental system .....</i>	<i>134</i>
<i>Figure 8-3 Comparison of simulation and experimental results of transfer function of the CIPDs.....</i>	<i>137</i>
<i>Figure 8-4 Simulation results of velocity profile with different sizes of exhaust orifice .....</i>	<i>138</i>
<i>Figure 8-5 Experimental results of velocity profile with different sizes of exhaust orifice .....</i>	<i>139</i>
<i>Figure 8-6 Comparison of experimental and simulation results of pulse-input velocity response .....</i>	<i>140</i>
<i>Figure 8-7 Comparison of experimental and simulation results of pulse-input driving</i>	

<i>chamber pressure response</i> .....	140
<i>Figure 8-8 Difference between the transfer function and state-space presentation for simulation of step-input response</i> .....	141
<i>Figure 8-9 Experimental results showing the relationship between position, velocity, and speed valve control signals of high-speed CIPDs</i> .....	142
<i>Figure 8-10 Effect of speed valves controlled exhaust orifice size on the deceleration regulation</i> .....	143
<i>Figure 8-11 Positioning profile of two experiments with different size of exhaust orifices</i> .....	144
<i>Figure 8-12 Network of the two axes gantry type pick-and-place machine</i> .....	145
<i>Figure 8-13 An example web page stored in the Gateway and displayed by Microsoft Internet Explorer</i> .....	146
<i>Figure 8-14 Flowchart of closed-loop control computation simulation program</i> ....	147
<i>Figure 8-15 Performance of simulation program with 4 ms execution interval</i> .....	148
<i>Figure 8-16 Control panel of the Commander</i> .....	149
<i>Figure 8-17 Sequence of sending out the target position by the Commander</i> .....	150
<i>Figure 8-18 Corresponding actions of the pick-and-place machine</i> .....	150
<i>Figure 8-19 Positioning profile of X, Y-axis responding to network variables of target positions</i> .....	151
<i>Figure 8-20 Positioning profile of distributed controlled the X, Y-axis</i> .....	152
<i>Figure A-0-1 Typical composing of a LonWorks node</i> .....	161
<i>Figure A-0-2 Simplified block diagram of an MC143150 Neuron Chip</i> .....	163
<i>Figure A-0-3 Simplified block diagram of TP/FT-10F Control Module</i> .....	165
<i>Figure A-0-4 Top view of TP/FT-10F Control Module</i> .....	166

# PAGE NUMBERING AS ORIGINAL



## List of Tables

<i>Table 3-1 Connection with the Integrated Direction Control Module .....</i>	<i>39</i>
<i>Table 3-2 Connection with the Integrated Speed Control Module .....</i>	<i>40</i>
<i>Table 4-1 An example of user definable Speed Valve Control Criteria Table used in the deceleration control strategy .....</i>	<i>65</i>
<i>Table 6-1 The Routh table of the system at moving state of motion .....</i>	<i>90</i>
<i>Table 7-1 Parameters and operating conditions of the EP-I.....</i>	<i>111</i>
<i>Table 7-2 Parameters and operating conditions of the Mathematical Analysis System .....</i>	<i>120</i>
<i>Table 7-3 Floating-point math performance (ms.) .....</i>	<i>129</i>
<i>Table 8-1 Experimental results of testing <math>C_f</math> and <math>F_c</math> .....</i>	<i>135</i>
<i>Table 8-2 Parameters used in MatLab simulation .....</i>	<i>136</i>

## Nomenclature

<p><math>a, b</math> subscripts for Chamber A and Chamber B respectively</p> <p><math>A</math>: piston area</p> <p><math>c_f</math> viscous damping coefficient</p> <p><math>C_d</math> discharge coefficient</p> <p><math>C_{ov}</math> exhaust orifice area-control signal voltage coefficient</p> <p><math>D</math> pipe inner diameter</p> <p><math>e</math> motion error</p> <p><math>K_p</math> proportional servo loop gain</p> <p><math>F_f</math> frictional force</p> <p><math>F_l</math> total load force</p> <p><math>F_t</math> total resistant force</p> <p><math>i</math> subscript to designate initial condition</p> <p><math>K_d</math> derivative servo loop gain</p> <p><math>l</math> stroke length of cylinder</p> <p><math>m</math> mass of gas</p> <p><math>\dot{m}</math> mass flow rate</p> <p><math>M</math> payload</p> <p><math>P</math> pressure</p> <p><math>P_{atm}</math> atmosphere pressure</p> <p><math>P_d</math> down stream pressure</p> <p><math>P_e</math> exhaust pressure</p> <p><math>P_r</math> downstream / upstream pressure ratio</p> <p><math>P_s</math> supply pressure</p> <p><math>P_u</math> up stream pressure</p> <p><math>R</math> gas constant</p>	<p><math>T_s</math> supply temperature</p> <p><math>T_u</math> up stream temperature</p> <p><math>V</math> volume</p> <p><math>Vol_{a,b}</math>: on-off valve control signal voltage</p> <p><math>w</math> port width</p> <p><math>X</math> spool displacement of valve</p> <p><math>Y</math> load position</p> <p><math>\dot{Y}</math> load velocity</p> <p><math>\ddot{Y}</math> load acceleration</p> <p><math>Y_d</math> demand load position</p> <p><math>\dot{Y}_d</math> demand load velocity</p> <p><math>\ddot{Y}_d</math> demand load acceleration</p> <p><b>Constants for air:</b></p> <p><math>r = 1.4,</math></p> <p><math>C_d = 0.82,</math></p> <p><math>C_k = \sqrt{\frac{2}{r-1} \left(\frac{r+1}{2}\right)^{\frac{r+1}{r-1}}} = 3.864</math></p> <p>,</p> <p><math>C_r = \left(\frac{2}{r+1}\right)^{\frac{r}{r-1}} = 0.528</math></p> <p><math>C_0 = \sqrt{\frac{r}{R((r+1)/2)^{(r+1)/(r-1)}}} = 0.04</math></p>
---	---

## Abbreviation

AUV:	Autonomous Underwater Vehicles
BCD:	Binary Coded Decimal
BGSMs:	Business network Gateway Service Messages
BSMs:	By-pass Service Messages
CGSMs:	Control network Gateway Service Messages
CIM:	Computer Integrated Manufacturing
DCS:	Distributed Control Systems
DHCP:	Dynamic Host Configuration Protocol
ES-I:	First Experimental System(mathematical analysis verification system)
ES-II:	Second Experimental System(high-speed motion control study system )
ES-III:	Third Experimental System
FMS:	Flexible Manufacturing System
IDC:	Integrated Direction Control module
IPA:	Integrated Pneumatic Actuator module
ISC:	Integrated Speed Control module
PWM:	Pulse Width Modulation
RAE:	Region of Acceptable Errors
SVs:	Speed control Valves

# Chapter 1 Introduction

## **1.1 Research Background**

Traditionally, pneumatic drives have been used to automate simple tasks, e.g. simple on/off tasks where accurately control of the transient behaviour of the drive is not needed. This is largely because of their inherent ability to provide a low cost, compact, safe and simple power source. When only simple motion control is required, pneumatic drives with mechanical end stops have proved to be adequate cost effective and popular.

For a period of decade from mid 1980's to 1990's, some initiatives were made to develop servo pneumatic drives for most sophisticated applications, employing purpose-designed control valves for pneumatic drives and low friction cylinders. However, it is found that the high cost and complex installation have discouraged the manufacturer from applying servo pneumatic drives to industrial usage, making them less favourable in comparison to their electric counterpart. This research has thereafter been directed to develop low-cost servo pneumatic drives which are capable of point-to-point positioning tasks, suitable for applications requiring intermediate performance characteristics.

### **1.1.1 Advantages of servo pneumatic drives**

Pneumatic drives have been with us for many years within industrial processes and it was adopted earlier than hydraulics as a principal source for transmitting a force. Compared with their counterpart, pneumatic drives have some particular advantages, in terms of speed, simplicity, safety, cleanliness,

cost-effectiveness, robustness and direct acting. In addition pneumatic drives require far less maintenance than their competing systems.

Servo pneumatic drives have already proven their usefulness in hundreds of automation systems worldwide, and offer the machine designer a cost-effective solution for a wide range of intelligent motion applications. Manufacturers have started to consider the use of servo pneumatic drives for more advanced applications.

Servo pneumatic drives with very carefully designed components, which manufactured at relatively high cost when compared with conventional pneumatic components, have offered reliable performance for a rang of application systems. It has been shown that the servo pneumatic drives can now provide speed in excess of 2 m/sec. By choosing a cylinder with proper diameter, loads of several hundred pounds can be positioned, although research shows that as much as 65% of the positioning tasks typically require loads from 0.9 – 11.3 Kg (2 to 25 lb). Positioning tolerances of  $\pm 0.1$  mm can be achieved. This accounts for at least 70% of positioning system requirements. A particularly significant attribute of pneumatic drives is the high acceleration capability up to  $100 \text{ m/s}^2$ . Further more, cost increases due to load handling ability are mainly dependent on actuator and valve size. Pneumatic components do not increase in price nearly as fast as electric motors do; hence further savings for heavy-duty requirements.

It can be concluded that the best applications for servo pneumatics are those requiring:

- Rapid point-to-point positioning
- High load carrying capacity-to-size ratio
- Mechanical simplicity
- Ease of maintenance
- Low cost

### 1.1.2 The drawback in building traditional servo pneumatic drives

Building up a servo pneumatic drive normally requires several pneumatic components, such as: pneumatic control valve, position sensor, home sensor, fittings, pipes, motion controller hardware and software, structure mechanisms, and so on. Some advancement in pneumatic components has been made since the introduction of the concept of servo pneumatics. The FESTO MPYE-5 series proportional pneumatic valves, for example, have integrated with electronic amplifier with feedback loop to linearize the relationship between the airflow rate and the input control signal. The advanced pneumatic components have significantly reduced the complexity in building servo pneumatic drives. However, there are still having some difficulties for none-specialists to build a servo pneumatic drive.

Figure 1-1 shows a typical architecture of traditional servo pneumatic drive with a 5-port proportional pneumatic valve, while Figure 1-2 shows the necessary components required for building such servo pneumatic drive (excluding servo motion controller). Some of servo pneumatic drives employ more components, e.g. more control valves, airflow rate regulator, pressure sensor, and so on.

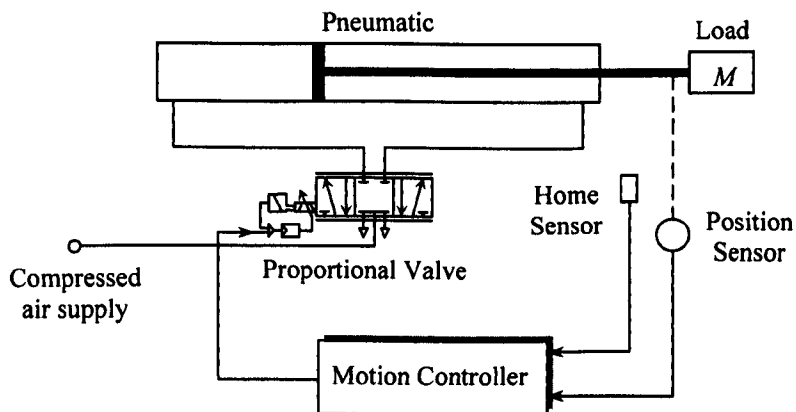


Figure 1-1 A typical architecture of traditional servo pneumatic drive

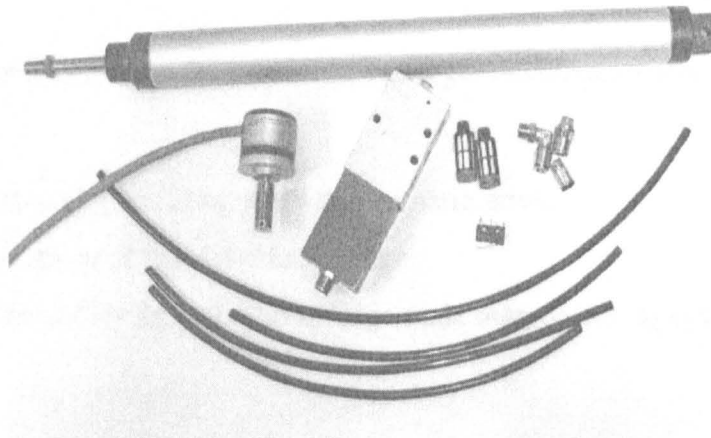


Figure 1-2 Necessary components required to build a servo pneumatic drive  
(excluding servo motion controller)

To build such servo pneumatic drive, the engineers firstly must have the knowledge of using the every component including mechanical and electronic interface. The engineers also have to specially program and tune the motion controller according to individual application specification. This is the most important and difficult procedure in building a servo pneumatic drive because that both the professional knowledge and experience are required in the programming and the tuning of servo pneumatic drive. However, there are less engineers and users that are qualified to do such work. Although in today's market, some motion controllers are commercially available for building servo pneumatic drives (e.g. FESTO SPC200 Servo-pneumatic positioning controller), users still need to learn some programming skill to setup motion profile to the controller.

Furthermore, traditional servo pneumatic drives have less flexibility in rebuilding large scale manufacturing system because that traditional pneumatic drives only support "real" design environment instead of supporting both "real" and "virtual" design environments. When changes are required for large scale manufacturing system due to the change of product, for example, traditional

servo pneumatic drives often require many works on rewiring and programming to meet the changes.

In short, some drawback of traditional servo pneumatic drives can be concluded as follows:

- Complexity in building a servo pneumatic drive.
- Requirement of specialist knowledge
- Less flexibility for re-building large scale manufacturing system.

### **1.1.3 The way forward in building servo pneumatic drives**

Nowadays, the world marketplace becomes increasingly customer-driven. To satisfy the needs of global competitive markets, more and more industrial sectors need to manufacture a wide variety of product models, which typically have a short product life, in short lead-times and in variable production volumes to retain competitive advantage. Even for the same model type, certain features variants are common to meet individual preferences. Therefore, the adoption of concurrent engineering and agile manufacturing has been advocated as a way forward in meeting such requirements. By agility, it means that manufacturing machine systems are able to respond rapidly and cost effectively to production changes both in terms of volume and variety.

The agility, re-configurability, re-usability and extendibility of the manufacturing machine systems are highly desirable to have embodied from an early phase in the design and implementation process. One prevalent approach to achieve enhanced re-configurability of machine systems is to adopt modular design and the use of standard components, so that agility is at least in part realised by re-using and re-configuring machine elements, in response to new or changed application.



The significant development of computing sciences has also greatly affected the design and control of modern manufacturing machine systems. As many powerful simulation tools currently are on market, the requirements and benefits for virtual design or engineering have emerged (Eriksson and Moore, 1994). The virtual design provides an efficient method for the design of large scale manufacturing systems by utilising various discrete-event simulation tools for layout design, bottleneck analysis, throughput analysis, and so on. In the virtual design, the control system image or the virtual control system is seen to be the same as the real physical control system. By this way, simulation tools can be used for evaluating different automation designs and equipment capabilities, in particular industrial robot based applications.

One of the devisal to efficiently meet such design paradigm shift is using “components-based methodology” towards a more distributed components-based configurable orientation in both software and hardware, with close interaction and mapping between the “virtual” and “real” worlds for both machine system and their control system (Pu and Moore, 1998).

The components-based methodology provides an effective way for interfacing/integration between “virtual” and “real” worlds. This is realised through the separation of two basic properties in a component, i.e. the “image of a component” and its “substance” (physical component). The image of a component or the virtual component is seen as the same for that of the real component. However, the image of a component only relates to the I/O functions of a real component and does not consider its physical existence. If the physical existence of a component is changed and its I/O functions are not changed, then the image of the component will not be changed. After using a picture to express a real component, some suitable tools can be employed to edit or analyse a component, or do any thing it is useful. 3-D graphical modelling and simulation tools, for example, have proven to be highly effective for rapid prototyping, visualisation and testing ‘what-if’ scenarios in the manufacturing engineering domain.

Meanwhile, as modern manufacturing machine systems become more sophisticated, distribution of intelligence is an important design philosophy for manufacturers and system builders to gain competitive advantage. By benefiting from the availability of high-speed microprocessors/microcontroller and the advancement in digital signal processing, 'Intelligence' can now be distributed to the component level, which provides a new dimension in building manufacturing machines and/or production systems. With such approaches the wiring and installation costs are greatly reduced. Maintenance of the system and equipment is simplified and the control capabilities should improve. The control elements can now be considered truly 'distributed' not only in conceptual terms but also in physical forms.

In distributed control systems, the process of aggregating "components" is through "message" connection in reference to the "control system image". A control system image, which defines the logical relationship and information flow between these components, is the synergistic view on the relational or ordering of the components' image. In other words, the relationship of the I/O functions of the input and output events of the components are governed by its control system image resident with that control system. The control system re-configuration can be done through the rewiring of the I/O pins of components' image in the control system image or the logical binding of the I/O functions of the components. Thus, through manipulating the control system image of a distributed control system, the behaviour of that control system is ultimately changed.

The provision of distributed control system re-configuration without involving recompilation is seen as one way to achieve efficient modification as requirements change. When such modifications are conducted on part of a machine or system, the operation of rest of the machine or system can still be functioning. In this way, the time for system setup, re-configuration, or maintenance can be also kept to minimum.

Therefore, a components-based integration paradigm is identified as the way forward in building next-generation servo pneumatic drives, which should exhibit the following characteristics

- An easy way to achieved high re-configurability or flexibility.
- Controlling complex systems by using simple building blocks.
- Dramatic reduction in wiring and increased modularity.
- Minimised machine's life cycle costs through improved fault self-diagnosis and lower downtime.
- Applying an open industry standard for communications.
- Low cost, easy set up
- Provision for system integration

## **1.2 The Research Objective**

A major purpose of the proposed research aims to develop low-cost servo pneumatic drives namely Components-based Integrated Pneumatic Drives (CIPDs). The proposed CIPDs provide capability of point-to-point positioning, and suitable for applications requiring intermediate performance characteristics. Meanwhile, the proposed CIPDs also provide some features such as easy in setup, supporting both “real” and “virtual” design environments, supporting remote service access via Internet. The following issues are suggested for the research:

- To devise a new point-to-point motion control strategy for the proposed CIPDs. The strategy involves the use of traditional on-off valve to reduce the manufacturing cost.
- To develop a new control algorithm for CIPDs. The new control algorithm should be simple so that it requires less specialist knowledge to the users.
- To design some modularized pneumatic components that supporting easy setup, easy tuning, easy maintenance.
- To adopt distributed control technology into the CIPDs. Distributed control technology is seen as a significant factor that allows

requirements of modern control system design, such as: re-configurability, re-usability, and extendibility, to be realised cost-effectively and efficiently.

- To provide Internet connectivity to the proposed CIPDs for the purpose technical and other remote service access.
- To carry out mathematical modelling and system stability analysis for the CIPDs.

### **1.3 Thesis Organisation**

This thesis is organised into 9 chapters. The following paragraphs present the outlines of the remaining chapters of this thesis

Chapter 2 is the literature survey. This chapter reviews the efforts made by previous researchers on modelling, control and energy efficient operating of servo pneumatic system. It also introduces some knowledge of distributed control systems including advantages and disadvantages.

Chapter 3 presents the proposed architecture of the Components-based Integrated Pneumatic Drives (CIPDs). It also details the CIPD network architecture and composition of CIPD.

Chapter 4 gives technical details of the CIPDs including the pneumatic actuator motion control strategy, servo control of the CIPDs, and high-speed motion control of CIPDs.

Chapter 5 introduces the remote service access strategy of CIPDs. An example of gateway device is given in this chapter.

Chapter 6 covers the modelling study and dynamic characteristic analysis of the CIPD. The modelling developed in both frequency domain and time domain.

The open-loop system and closed-loop system stability are investigated.

Chapter 7 describes the experimental system setup. Two experimental systems are presented. Some hardware parameters are given in this chapter. The experimental data processing method is also included.

Chapter 8 presents the experimental results. It includes the test of friction characteristics of the experimental system. The model verifications have been conducted by comparing open-loop system step input and pulse input response obtained through simulation and experiments.

Chapter 9 is conclusion which states the contribution of the research to the servo control technology of pneumatic drives and the suggestion of further research work.

The Appendix and the List of References are the last part of the thesis. The Appendix provides some information about the LonWorks Technology which has been employed in this research as a distributed control technology. This section also includes details about the hardware that used in the research. The List of References section provides all the publications that have been studied during this research.

# Chapter 2 Literature Survey

## **2.1 Introduction**

Designing a components-based integrated pneumatic drive is a complex task. It includes technologies from different disciplines such as computer sciences, pneumatic system modelling and control and so on. This chapter presents a review of literature focused on the researches on modelling and control of pneumatic drives, distributed control systems including general information and identified research areas.

## **2.2 Researches on Servo Pneumatic System**

Servo control of pneumatic drives has been an interesting topic for many researchers and engineers driven by the advantages of pneumatic actuators. During the last two decades or so, research and development efforts have significantly advanced the fundamental knowledge. It has been shown that the servo pneumatic drives can now provide speeds in excess of 2 m/sec. By choosing the proper diameter of cylinder, loads of several hundred pounds can be positioned, although research shows that as much as 65% of the positioning tasks typically require loads from 0.9-11.3 kg (2 to 25 lb.). Accuracy is somewhat less than that of competing technologies, but tolerances of  $\pm 0.1$  mm can now be achieved. This accounts for at least 70% of positioning system requirements (Sandoval and Latino, 1997). A particularly significant attribute of pneumatic drives is the high acceleration capability up to  $100\text{m/s}^2$ . Further, cost increases due to load handling ability are mainly dependent on actuator and valve size. Pneumatic components do not increase in price nearly as fast as electric motors do, offering further savings for heavy-duty requirements. Servo

pneumatic drives are becoming a competitive alternative to hydraulic servomechanisms where especially high accuracy is not required and when moderate response and output stiffness are acceptable.

Servo control of pneumatic actuators proves to be a significant advance but still with some limitations, such as: difficult to achieve constant piston speed and maintain accurate position; low energy efficiency; low load capacity and so on. Pneumatic servos are still not as stiff as their competing technologies. However, some of the limitations have been resolved. With continuous development of servo pneumatic drives controlling technology, the applications will be expanded and increased to many areas hitherto not known for adopting pneumatic technology.

### **2.2.1 Studies on fundamental knowledge of pneumatic system**

Traditionally, pneumatic drives have been used to automate simple industrial tasks. One of the first attempts to analyse pneumatic power control systems was reported by Shearer (1956) who studied an open-loop system consisting of a pneumatic servomotor driving an inertia load acted upon by an external force. The fundamental equations for the description of pneumatic systems were set up in his work. Burrows et al (1966) have extended Shearer's work using the root-locus technique to provide a simpler design procedure and more insight into the effect of parameter changes on system performance. Shearer subsequently reported work on a closed loop pneumatic system with mechanical position feedback between the load and the valve. The system was of high-pressure type using air at a supply pressure of about 54 bars. The results of his work were successfully applied first in spacecraft and missile engine control.

### ***2.2.1.1 Studies on characteristics analysis and modelling, control approaches, and design models of pneumatic servo drives***

During the last two decades, with advances in microelectronics and an increasing trend towards automated manufacture, the use of electronics for machine control systems has accelerated the development of servo pneumatic significantly. The development of programmable servo controlled motion has been stimulated so that automated processing equipment can be fabricated with sufficient operational flexibility, this gives much benefit to pneumatic systems to be considered for more complex processes and systems which require high performance capabilities. There has been some research and development in producing pneumatic servos. The research on pneumatic servo systems is almost a reflection of modern control engineering. New research initiatives on designing and producing analogously and digitally controlled servo pneumatic systems have emerged. This brief overview tries to give a skeleton picture of former research works in this area.

Some of the earliest works in pneumatic servo technology can be attributed to the research by Shearer et al. (Shearer, 1956; Burrows and Webb, 1966; Vaughan, 1965). These researches were carried out based on a nominal transfer function model obtained by linearizing the system around a specific operating condition. These early works provided the foundation for much of the later research and development, and established the underlying principles for the understanding and control of servo pneumatic system.

One of the main difficulties associated with the use of air as a fluid-power source is the fine tolerances required in servo-valves to prevent leakage. This, together with the cost of manufacturing proportional-acting servo-valve, suggests the use of on-off valve which present less sealing problem and are cheaper to produce. One other important consideration in the use of on-off control is that this form of control provides the theoretical time optimum response.



Burrows and Webb (1968) described an analogue computer simulation of an on-off pneumatic servomechanism comprising a polarized relay with dead zone and hysteresis and an on-off four-way valve supplying air to a cylinder driving an inertia load acted upon by viscous damping and Coulomb friction. The effect of varying the amount of friction, position, velocity, and acceleration feedback is studied. The effect of the addition of stabilizing tanks is also considered.

Weston, Moore et al (1984) studied microprocessor-based low cost pneumatic servo drives with a Martonair proportional pneumatic valve. A fourth-order linearised model of pneumatic systems was derived based on Burrows's (1969) linearised analysis of pneumatic drives, with the assumption of an inertia load and negligible friction. The approximate model was used as an aid to design a suitable control strategy for pneumatic drives. Based on the linearised model, a three-loop controller with position, velocity and acceleration feedback was implemented and the approach incorporated digital compensation for variation in system parameters, such as the loop gains  $K_p$ ,  $K_v$  and  $K_a$ . When positioning loads in a "point to point" mode with brake sub-system, it was possible to achieve a significant improvement in both the static and dynamic performance of the drive. For example, the positioning accuracy of  $\pm 0.1$  mm was achieved and the system bandwidth was increased by nearly threefold.

The research reported by Morgan (1985) indicated that programmable positioning using electro-pneumatic drives is not only technically feasible but can also be commercially attractive.

Bublitz and Pindel et al. (1992) have pointed out that the advantages of using electronic control networks cannot be realized without incorporating actuators, valves, and pumps into the control and feedback loop. Control networks allow improving machine performance, uptime, and reliability as well as plant productivity and product quality because information can readily be exchanged between supervisors, departments, and machines. This information can be monitored, analysed, and revised to optimise procedures – all without disrupting operations. Interfacing fluid power components with the control

networks provides the data required for modern management information systems.

An optimised solution to the control of non-linear pneumatic system is often “localised” and position dependent, Moore and Weston et al. (1984) proposed a general-purpose gain-scheduling control scheme, which can be used to tackle the above problems and be tailored to suit a specific application instance

Backé (1986 and 1993) has developed a three-loop controller (position, velocity and acceleration feedback with velocity and acceleration derived from position signal) and applied on a Martonair rodless cylinder with an IHP high performance pneumatic servo valve. The system stiffness and damping were improved significantly by the three-loop controller and the best positioning accuracy achieved was  $\pm 0.01$  mm with a stroke of 200 mm, a load of 100N and a maximum velocity of 2.5 m/s. It was emphasized in his research that the positioning performance of servo pneumatic systems was strongly affected by the quality and the time response of the servo valve and the friction behaviour. A rapid acting and accurate pneumatic servo or proportional valve is essential for achieving good positioning accuracy. An adaptive force control gripper was also studied in Backé’s research.

Pu and Weston (1990) introduced new approaches and design models aimed at determining the steady behaviour of pneumatic servo drives. They have established the relationships characterising actuator velocity and chamber pressure with respect to valve displacement. Certain parameter ratios are defined and a novel analytical solution is offered. Pu and Moore (1991a) gave the aspects of the operating characteristics of pneumatic systems and described control methods for pneumatic servomotors. Both analytical and experimental approaches were considered. The results show that digital-controlled air motors have the potential of providing an alternative solution to their electric and hydraulic motor counterparts. Air servomotors, through inherent low cost, good power-to-weight ratio and intrinsically safe operation, can thus be utilised to control industrial machines in certain application areas. Pu and Moore

et al (1991b) have studied the feasibility in employing such drives to achieve simple motion profile following through adopting a high-gain control approach. A new design model which differs from previous research studies and provides the basis for formulating the control approach are used. A vane-type reciprocating actuator has been chosen for this study. The effects of various controller gain terms on dynamic responses and system stability are illustrated. A tuning procedure is thus identified on the basis of analytical and experimental observations. Pu and Moore (1991c) have also considered the use of “profile-planning” to improve the performance attributes and to simplify the tuning problems found with pneumatic servo drives.

A simulation model of a rotary pneumatic servo system has been developed and verified by Tillett and Vaughan, et al (1997) against an experimental system. The double-acting rotary actuator is a novel device utilizing flexible inflatable bladders. The device differs from conventional pneumatic cylinders in that it exhibits low levels of friction, as it has no sliding seals, but it does suffer from hysteresis caused by bladder distortion. The objective of their study was to develop a tool with which to investigate the effect of various forms of hysteresis and other parameters on system performance. The dynamic model utilizes a linearized analysis of pneumatic components based on earlier studies. The principal advance described in their paper relates to the inclusion of non-linear elements. These are hysteresis caused by friction or the distortion of flexible components, and a digital controller implementation. The simulation predicted all major modes of behaviour. Simplified models of rubber and coulomb friction-induced hysteresis modified simulation performance in line with experimental results. An investigation in simulation showed that coulomb friction-induced hysteresis had a greater damping effect than that caused by distorting the bladders. This result applies only to position control, as hysteresis has been shown not to provide damping in trajectory control applications.

Shih and Tseng (1994) have concerned with the practical application of PID-self-tuning control on position control of a pneumatic servo cylinder. Instead of the complicated system equation-deriving process, a second-order

mathematical model is found by the system identification method, which is used for the controller design. A PID-self-tuning controller, whose control parameters  $K_p$ ,  $K_i$ ,  $K_d$  are time variant and self-adjusted, is designed and implemented in a microcomputer to control the position of the pneumatic cylinder.

Richer and Yildirim (2000, 2000b) have developed a detailed mathematical model of dual action pneumatic actuators controlled with proportional spool valves. They provide an accurate model of a pneumatic actuator system controlled by a proportional spool valve. The model is targeted to develop force controllers that perform at significantly more demanding operating conditions. For this purpose, the model takes into consideration the friction in the piston seals, the difference in active areas of the piston due to the rod, inactive volume at the ends of the piston stroke, leakage between chambers, valve dynamics and flow nonlinearities through the valve orifice, and the time delay and flow amplitude attenuation in valve-cylinder connecting tubes. Since the ultimate purpose of the modelling effort is for control applications, the proposed equations should be suitable for on-line implementation. They also designed special experiments in order to identify the un-known characteristics of the pneumatic system, such as: valve discharge coefficient, valve spool viscous friction coefficient, and piston friction forces. The model was finally tested using two experiments that allowed the measurement of the actuator force output and piston displacement. The experimental results were compared with the results obtained by numerical simulation.

Slotine and Sastry (1983) presented a methodology of feedback control which is developed to achieve accurate tracking in a class of non-linear, time-varying systems in the presence of disturbances and parameter variations. The methodology uses in its idealized form piecewise continuous feedback control, resulting in the state trajectory 'sliding' along a time-varying sliding surface in the state space. This idealized control law achieves perfect tracking; however, non-idealities in its implementation result in the generation of an undesirable high-frequency component in the state trajectory. To rectify this, it is

shown how continuous control laws may be used to approximate the discontinuous control law to obtain robust tracking to within a prescribed accuracy without generating undesirable high-frequency signal. The method is applied to the control of a two-link manipulator handling variable loads in a flexible manufacturing system environment. However, this methodology has several important drawbacks, particularly high control authority and control chattering. Chattering is generally undesirable in practice, since it involves extremely high control activity, and further may excite high-frequency dynamics neglected in the course of modelling. Also, in particular, the methodology involved a trade-off between tracking precision and robustness to un-modelled high-frequency dynamics. Slotine (1984) subsequently quantified the precise nature of this trade-off, and complete the methodology by showing how to achieve optimal tracking performance given bandwidth requirements and (perhaps time-varying) modelling uncertainties.

A robust feedback linearization methodology is introduced by Xiang and Wikander (1998) for a pneumatic actuator servo control system. By the presented method, that effective friction compensation, with the dynamic friction model, was obtained. High motion and force control performance were achieved with the presented techniques. Stability and robustness analysis with respect to uncertainties and linearization residual are also included.

Shih and Ma (1998) have also introduced a control law, which combines the sliding mode and modified differential PWM (M-D-PWM) control method. A M-D-PWM controller is designed and implemented in a microcomputer to control the position of a pneumatic rodless cylinder. Instead of using a servo valve, two cheap high-speed solenoid valves are applied in the system. The experimental results show that the pneumatic system has the advantages both good performance and low cost with the proposed controller.

Pneumatic servo axes controlled by PWM piloted digital valves are a suitable economic solution in all those cases in which high precision is not required. Unfortunately this kind of system is strongly non-linear, and hence

fuzzy logic is a powerful instrument to solve the control problem. The application of this technique requires the definition of dedicated membership functions for the fuzzy sets, while a unique set of control rules can be defined for every kind of actuator. An algorithm for the automatic tuning of the membership function was developed and tested by Mattiazzo and Mauro et al. (1998).

The fuzzy control approach has been found to be an effective alternative to deal with complicated, ill-defined and poorly mathematically modelled dynamically process. Without relying on detailed mathematical model, the fuzzy control algorithm is developed by incorporating human knowledge and experience directly into implementations. Hence, fuzzy control can be used to overcome difficulties of parameter identification.

Wang and Chang (1999) reported an experimental implementation of decoupling self-organizing fuzzy control to a TITO (Two-Input Two-Output) pneumatic position control system. By using the concept of decentralized control, a TITO control structure is decomposed into two separate control channels. Each channel is associated with a self-organizing fuzzy control (SOFC) for single-axial pneumatic control system and a decoupling SOFC for structure interactions. The experimental results show that the proposed control algorithm can achieve high control accuracy, and it is robust to various operating conditions.

Pneumatic servo positioning system contains several non-linearities such as the air flow-pressure relationship through the variable area orifice of the valve, the compressibility of air, and the friction between the contacting surfaces of the slider-piston system. To overcome the disadvantages of a pneumatic servo positioning system and for purpose of control and simulation, all the non-linearities of the system must be modelled. The problem can be treated to the end of constructing a complete and effective model that can be used for simulation and accurate control of such systems (Bashir and Farid, 2000).

### ***2.2.1.2 Studies on development of servo pneumatic components***

“Bubbler” is a new type of pneumatic rubber actuator that designed and developed by Suzumori (1999) to realize linear motion. This actuator consists of a silicone rubber slab, and its interior is divided into many chambers. When pressure is applied to successive chambers sequentially, the surface of the rubbers lab produces linear travelling waves that drive objects placed on the actuator. Bubbler can be applied as a mobile robot base or a conveyor. The characteristics of the actuator can be estimated by applying a simple linear analysis method for various driving conditions: frequency, length, and duty ratio of the generated waves, vertical loads, and horizontal loads. Slip ratio or the error between the theoretical and experimental velocity of the actuator is within 20%. “Pneumatic wobble motor” is also a new type of pneumatic stepping motor (Suzumori and Hori 1999). A pneumatic wobble motor consists of a donut shaped wobble generator made of silicone rubber, a wobble ring made of metal, and an output shaft. The output shaft is encased in the wobble ring, which the wobble generator covers. The wobble generator has six chambers and injecting air into each sequentially causes the wobble ring revolution, which makes the output shaft to rotate. The characteristics of this motor were analyzed theoretically. Two prototypes with different designs are fabricated and tested. The features of pneumatic wobble motor are (1) big torque (more than 10 times that of conventional small-size electromagnetic motors). (2) simple structure and (3) waterproof and dustproof.

A new design of pneumatic motor and its application to parallel robot mechanism have also been reported (Suzumori and Hashimoto et al, 2002). This motor consists of a pair of bevel gears and three pneumatic cylinders. It achieves gear meshing with high efficiency, resulting in small noise and vibration. The motor achieves 0.5-degree stepping increment without any electrical devices or sensors mounted on the servomechanism. This makes the motor possible to be used under hazard conditions such as in water and in the strong magnetic fields where conventional electromagnetic motors cannot be used. Characteristics of the motor have been analyzed theoretically and

experimentally. The application shows that the motors can be used as a direct servo motor for robot mechanisms.

Akagi and Dohta et al (1999) have describes an extension of a optical servo system, which can be used in hazardous environments, is a novel and attractive control system, to a more normal scale system using a normal pneumatic rodless cylinder with a full stroke of 600 mm. First, two kinds of opto-pneumatic servo system using the rodless cylinder are explained briefly. Second, the control performance of the first system, which uses two flow amplifiers in the market, is investigated. Finally, the optical servo valve is designed and improved by using the analytical model proposed previously. And the control performance of the second system using the improved valve is investigated. As a result, it is shown that the improved optical servo valve is more useful in a normal scale control system compared with the flow amplifier.

Air pressure measurement is an important application in process industries. A microprocessor based new pressure-measuring device, which is claimed that improves sensitivity over other conventional pressure sensors, is proposed by Balasubramanian and Guven (1994). The sensor consists of a diaphragm and a string fixed inside a hollow cylinder attached to a pneumatic medium. While one side of the diaphragm is exposed to pneumatic pressure, the string is stretched on the other side. With the use of a microprocessor, the string is periodically excited through an electromagnet and the vibrating frequency is measured from the signal obtained at an opto-coupler. The frequency is calibrated to indicate the pressure.

### ***2.3 Flexible manufacturing systems and distributed control***

In order to prosper today manufacturers may well forced to use new production techniques, especially for products that are made in small to moderate quantities. The profitability, productivity, and market share of manufactures now is being affected by many factors, including price increases, a failure to



understand customers and markets, poor use of capital. Many economists, engineers, and managers believe that steps need to be taken to increase productivity through automating both product design and production facilities. Product and process improvements are widely acclaimed to provide economic gains and to increase flexibility, resulting in fast responses and rapid adaptability to changing market conditions (Chen and Adam, 1991). The concept of computer-integrated-manufacturing (CIM) comes as a consequence of developments in computer-aided design and factory automation. It includes the ability to control planning through design to shipping. It embraces the integration of office automation, computer-aided design and manufacturing, automatic storage and retrieval system, distributed data processing, and so on (Deane, 1980). The CIM provides the systematic approach to integrated system development involving system engineering method to define the problem and technique for establishing the architecture of CIM.

Implementation of flexible manufacturing systems (FMS) started in the late 1970's on the conventional mechanical engineering shop-floor (Mo, 1989). Since then the number of installations kept increasing at a constant rate.

Distributed control systems (DCS), which were introduced in the 1970s, have long been a dream of engineers seeking to automate factories, warehouses, homes, and other complex systems where the sensing and control tasks are spread out over too large an area for central control to be effective. DCS gained rapid popularity starting in the 1980s because of their high reliability and superior functions and performance. In distributed control system, all transducers – sensors and actuators – have embedded intelligence and are therefore referred to as smart. They are interconnected by networks of various topologies which come under the generic name of fieldbuses. Design of distributed control involves decomposing a complex system or a machine into many simple parts (components). Each part or component implements a special task or some functions. All parts or components are connected using networks and formed a whole system or a machine.

Compared with the control system employing a centralised architecture, some of advantages and disadvantages of distributed control systems have been pointed out (Xie, 1999; Lesser and Corkill, 1981; Chapman, 1990; Heck and Wills et al, 2003; Callen, 1998), such as:

- 1). Lower installation costs of wide spread systems.

Data communication realised through a fast serial bus instead of multi-wire connecting cables. The resulting savings are expected to be dramatic.

- 2). Increased reliability and flexibility for system modification or extension.
- 3). Unlimited processing ability and lower processing cost.
- 4). Reduced software complexity.

The principle difficulty in implementing such a system is that unless the system is open whereby a set of standards are agreed allowing a true multi-vendor system employing best of class principles, it can only be realised by a single vendor solution which can never be optimal and carries significant risk.

Until now, the hardware of building control systems has undergone an evolution in which the processing has been increasingly distributed onto the plant under control. Advances in DCSs and the field devices which provide field information to DCSs have been driven by the proprietary technology of a number of vendors. In recent years, however, this field has felt the impact of the trends toward open standards, downsizing, and lower prices.

#### ***2.4 Framework of components-based distributed control systems***

The components-based distributed control for mechatronic systems consist of many devices and a fieldbus. A device is a copy of a component which stands for the device type. Each device has an individual device name and identity (ID) which is used to distinguish different copies of the same component. All the devices communicate each other via fieldbus. For example, a building

automation system may have many temperature sensors with the same I/O functions. This means that these temperature sensors are copies of a temperature sensor component. Each temperature sensor is called a device and has its device name and ID.

#### **2.4.1 Studies on application of distributed control technology**

Over the last decade great strides have been made in the area of application of distributed control technology. In the study of distributed control systems, researchers have focused their attentions to wide aspects of envelopment and application of distributed control technology. Some researchers have focused on modelling, scheduling and simulation of distributed control systems (Pascal and Frederique et al, 1993; Huvenoit and Bourey et al, 1995; Moriwaki and Ueda et al, 1993; Lee, 1997; Zheng and Wang, 2000). Other researchers have focused on the system structure design, characteristic analysis, and application of distributed control systems (Darwish and Soliman, 1988; Hirose, 1985; Huliehe and Lee et al, 1993; Harissis and Abdelrazik et al, 1990; Jung and Jeong et al, 1994). Distributed control is also a favourable technology in the design of computer-controlled vehicles (Xie, 1999; Callen, 1998; Smith, 1994; Dai, 2002).

Sensor networks are gaining a central role in the research community. Sinopoli and Sharp et al (2003) addressed some of issues arising from the use of sensor networks in control applications. Classical control theory proves to be insufficient in modelling distributed control problems where issues of communication delay, jitter, and time synchronization between components are not negligible. They presented their hardware and software platforms while proposing an open architecture to help rich distributions. They reviewed useful models of computation and then suggested a mixed model for design, analysis, and synthesis of control algorithms within sensor networks. They also suggested a general approach to control design using a hierarchical model composed of continuous time-triggered components at the low level and discrete event-

triggered components at the high level.

Real-time control systems, involving continuous measuring and monitoring of physical quantities, need often to take into account fault-tolerance capabilities to guarantee a correct behaviour (even in the presence of a given amount of hardware faults and software errors) or, at least, to provide gracefully degradable performances. Piuri (1994) has presented an integrated approach to dimensioning the distributed system and to allocating the computation for real-time control applications. They reversed the classical approach of software allocation on a fixed architecture, and allocated the software components onto a virtual architecture having no predefined constraints. The actual hardware structure is assembled following guidelines of optimum software allocation. Fault tolerance has been included in the design methodology as a basic feature for any critical system. Different strategies have been analyzed. Their integration in the homogeneous frame for system design has been introduced. The use of their methodology has been experimented also in some real-life cases concerning chemical industries, robotics, and electrical power plants; in such cases, it has been proved effective in reducing the costs (about 20% less than traditional methodologies) while guaranteeing a high degree of fault tolerance.

Benamara and Moreno (1997) have solved some problems related to the distribution by considering a virtual distributed system. Real-time distributed applications have stricter distribution requirements than classical distributed systems. Generally, the solutions are built in a “bottom-up” way by combing existing solutions in the domain of control and distribution. However, the distribution of control application on them is complex (synchronisation problems, consistency of data, concurrency, and so on). At this time, it is possible to dispatch data to all modules sharing industrial network, but expressing global behaviour is more difficult without a complete modelling of mechanism ensuring this behaviour. Therefore, in order to migrate the systems to a common hardware and software platform a new concept must be considered. This platform must integrate re-configurable entities, model

their behaviours and perform their communication mechanisms. They have reported the concepts related to their virtual automation and the construction of a distributed system as a combination of disparate collaborating control agents. The development of the control system is based on an object-oriented method using a systemic approach. The need of two complementary models is also introduced: a behavioural model based on cognitive and expert systems, and an architectural model that hides the physical distribution of the application.

Traditional generations of mobile robots/vehicles are typically wire guided with low functionality. Usually the vehicle follows a guide track to navigate to its target or a human operator controls the vehicle by means of a hand-held controller or remote controller. However, the operator mistakes (e.g. misjudging the vehicle speed or the distance between the obstacle and the vehicle) might damage the vehicle, loads and the vehicle work environment. Dai (2002) has designed a smart sensing system using distributed control technology. The smart sensing system integrated in a semi-autonomous vehicle facilitates a level of perception to support the enhanced behaviours of the system. The smart laser scanner component can provide raw data or extracted data for autonomous navigation mode. In the component, specialised perception algorithm extracts the necessary information, whereby: perception is conducted on a need-to-know basis. Multiple parallel processes that fit the semi-autonomous vehicle's different behavioural requirements were used. The research has achieved results in the area of distributed control, intelligent sensors and systems integration within automation systems using the flexibility offered by the approach. This approach combines advanced control and sensing techniques (i.e. reactive behavioural control architecture and smart sensing) with the state-of-the-art enabling technologies (i.e. distributed control and component-based design) to the realisation of semi-autonomous vehicles being enhanced.

Chen and Wang (2002) proposed a standard-based scalable framework for distributed application systems. The framework is featured with Internet-based distributed real-time systems with visualization device methods and remote service capabilities. These devices are among the most critical parts of

processes and production lines, since they handle all functions related to dynamic behaviours of distributed real-time systems. The framework will handle event and time triggered real-time scheduling. It covers multi-tier architecture with language independent interfaces, nodes and applications. Built-in dependability technologies at the application level enable the users to implement customized applications and to easily integrate them into a distributed control system. The programmable and re-configurable built-in dependability mechanisms provide a flexible platform for distributed real-time application.

LonWorks technology is a complete platform for implementing control network systems. This technology was developed by Echelon Corporation and put on the market in 1990. Echelon's efforts were focused on obtaining a standard communications protocol together with the necessary tools which provide an easy and fast implementation of the nodes in a network. Hence, LonWorks technology includes all of the elements required to design, deploy and support control networks.

Smith (1994) reported an application of LONTalk, a Local Operating Network protocol, to a distributed control system for the Ocean Voyager II Autonomous Underwater Vehicles (AUVs). A detailed description of the OV II's distributed sensing and control architecture is given, in addition to the salient features of LONTalk and its associated hardware. The Ocean Voyager II is one of a new generation of small long-range inexpensive AUVs for oceanographic data collection. The goal behind developing a distributed control system was to simplify construction of the vehicle while increasing reliability and re-configurability. With specific examples from the OV II development, the advantages and disadvantages of using the distributed control and the LONTalk protocol are discussed. A comparison between SAIL and LonWorks, and potential for cost-effective interoperability of sensor, actuator, and computation systems in AUVs using LonWorks, are also made in the report.

Alonso and Ribas et al (2000) presented a new distributive control system for fluorescent lighting applications based on LonWorks technology. The system features the following elements: microprocessor controlled fluorescent lamp electronic ballast, communication system using the power line as communication media, and control software for Windows 95 environment. With this structure, a low-cost distributive control system for lighting applications has been achieved, allowing both energy saving and increase in the reliability of the fluorescent lighting system.

# Chapter 3 Architecture of Components-Based Integrated Pneumatic Drives

## 3.1 Introduction

Pneumatic drives are the most widely used in industry in terms of total number of units. This is because, in comparison with their counterparts, pneumatic drives have some particular advantages. The main advantages of pneumatic drives are their economy, simplicity, robust, and direct acting when compared to other technologies of equivalent performance. Pneumatic drives require far less maintenance than their competing systems, which often need a set of complex mechanisms between actuator and load such as lead screws, gearboxes or belt drives.

In the last 20 years or so, with renewed interest in the application of servo pneumatic drives, a significant amount of research has been carried out into the control of servo pneumatic drives including static and dynamic control characteristics, servo motion control strategy, and so on. In practice, most of servo pneumatic drives are designed as an individual control system with a dedicated computing element (motion controller) for the implementation of servo motion control strategy. Some of servo pneumatic drives have been designed to support some common data transfer protocols such as: LAN, RS232, RS458 and so on. However, these types of individual system normally only support the manufacturing machine/system design and control in the “real” environment.

The Components-based Integrated Pneumatic Drives (CIPDs) that are developed in this research, not only support the design of control system in the



“real” environment, but also support the design in “virtual” environments. This chapter presents the architecture of CIPDs system, and the composition of individual CIPD.

### ***3.2 Overview of the Components-based Integrated Pneumatic Drives***

The CIPDs are designed to provide point-to-point motion processes. A CIPD consists of three integrated CIPD modules: Integrated Pneumatic Actuator Module (IAP), Integrated Direction Control Module (IDC), and Integrated Speed Control Module (ISC). According to different application requirements, users are allowed choose the models with different parameters to build a cost effective servo pneumatic drive. The CIPDs employ a new pneumatic actuator motion control strategy. With such strategy, the speed of motion can be controlled by mechanism adjustment rather than programming the motion controller. The motion controller is pre-installed with a common motion control application program, which is independent to the other models of a CIPD. Hence, the users are totally released from learning skills for programming the motion controller. The CIPDs are also integrated with distributed control technology and digital feedback control technology. These technologies ensure that CIPDs are easy to be set up; flexible in configuration; having high positioning accuracy, and to be components-based devices in a distributed control system, and so on.

In short, compared with traditional servo pneumatic drives, the following specific features can be summarised:

- Only three models are needed to build up a servo pneumatic drive.
- No need of specialist to build up a servo pneumatic drive.
- No need of programming skill to program the CIPDs at user stage.
- Motion speed can be adjusted mechanically.
- Positioning accuracy of  $\pm 0.1$  mm can be easily achieved.
- Multiple-media communication ability.

- Re-configurable, re-usable, low cost, and easy for setup.

### 3.3 Architecture of the Components-based Integrated Pneumatic Drives Control Network

Figure 3-1 illustrates the architecture of a large scale manufacturing system that is built by CIPDs with remote service access support.

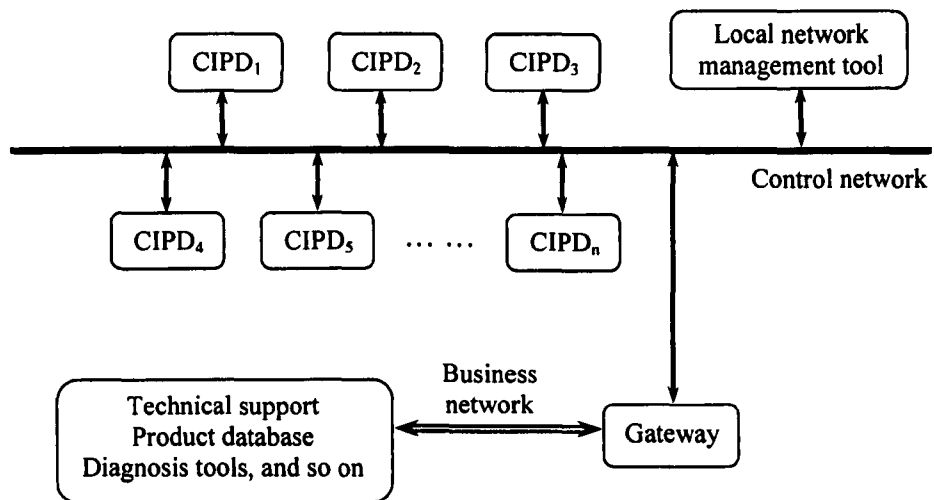


Figure 3-1 Architecture of Components-based Integrated Pneumatic Drives system

A CIPDs network system consists of a number of CIPDs, a local control network fieldbus, and a gateway device. Each CIPD has an individual name and identity which is used to distinguish different CIPD in the same control system. All the CIPDs and the gateway device communicate each other via the control network fieldbus. The gateway device also connects the control system to Internet for technical services support, product monitoring, and system maintenance, and so on.

The local control network is built based on distributed control technology. A distributed control system has a system image used in virtual design environment. The system image is a virtual expression of the system made up by a group of component images and their connection. The connection lines to the I/O pins of the components and represents the message exchange among the input and output events of the components within the distributed control system. The distributed control system images provide a good visual representation of distributed control system design platform. By using this platform, the design of distributed control system is similar to the design of an electronic circuit. A control system designer mainly considers what components will be used and how to connect these components together to build up a distributed control system. A database, which is hidden within the control system image, links up the control system image and the practical distributed control system. When the control system image is modified, the database and the practical control system are also modified. Figure 3-2 shows the relationship among the distributed control system image, the database and the practical control system

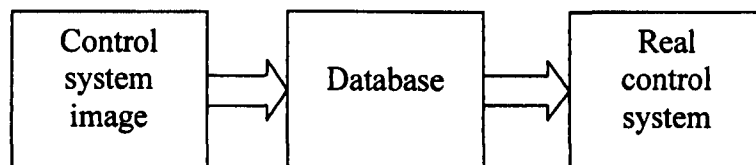


Figure 3-2 The relationship among the distributed control system image, the database and the practical control system

### 3.4 Composition of a Components-based Integrated Pneumatic Drive

A CIPD in a distributed control system is an entity which is designed to perform a certain function or tasks and can be used to compose more complex entities for given purpose. A CIPD includes:

- 1). A physical component (or a real component) which consists of a set of hardware (entity) and software (application program),
- 2). An CIPD component image (virtual component), and
- 3). An I/O function database.

Figure 3-3 illustrates the composition of a components-based integrated pneumatic drive.

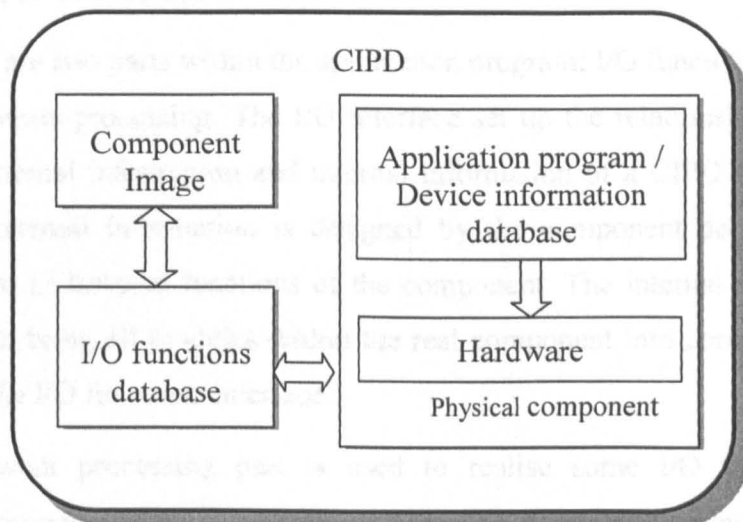


Figure 3-3 Composition of a components-based integrated pneumatic drive

The physical component of a CIPD is needed to build a real distributed control system. A real CIPD component includes the following two parts:

i). Hardware

The hardware means the physical entities of a CIPD component including mechanical structures, electric devices, and some others. Each CIPD component must at least have a CPU to implement events and communicate with others. There is no flexibility between these physical entities, so it cannot easily be modified. However, the other components within a CIPD are designed as standard models but with different parameters, hence users can easily change the relative physical entities to meet the different application requirements.

A CIPD component is physically connected to other components within the control system via its communication I/O. Within the local network, the communication among components is through the same communication protocol. There is a gateway device inserted between the local network and Internet for access of remote services.

ii). The application program

There are two parts within the application program: I/O functions interface and events processing. The I/O interface set up the relationship between the external information and internal information of a CIPD component. The external information is designed by the component developer and used to understand functions of the component. The internal information used to bring all modules within the real component into correspondence with the I/O functions interface.

The event processing part is used to realise some I/O functions or input/output events, some control algorithms, network communication, and some others. The control module will communicate with the I/O function interface and other modules, such as the sensor module, so that it can get enough information to realise the control.

The CIPD component image is a virtual component used in the virtual environment of component design and control system design. In control system design, the component image could be expressed as a picture (a kind of symbol) and associated I/O pins. The picture stands for the entity and the functions of CIPD component. The CIPD component image could be thought as a black box from the viewpoint of a control system designer. The functions of a component are embedded within the black box. The visible aspects for a control system designer are the incoming and outgoing events. This means that a control systems designer only needs to know what functions or events will be implemented by a component, how to use these components to realise the control system solution by connecting suitable I/O pins (network variable), and does not need to know how the functions of events will be achieved within a component. Therefore, designing a control system is similar to designing an electronic schematic. Figure 3-4 illustrates the CIPD component image for control system design in virtual environment.

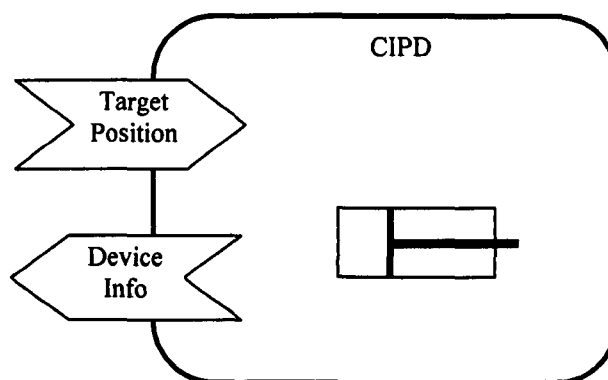


Figure 3-4 CIPD component image for control system

The I/O pins represent the virtual connections which are event driven to this component or other components. An event is a stimulus from one component to another for: a) passing a message; b) asking it to do something; or c)

invoking an operation. In other words, the I/O pins are used to set up the logic connection with other components. Each pin has a pin type name which stands for the event type name, such as temperature, pressure, and so on. The pin type name is also called a network variable name in a control system. Each pin has an input or output characteristics and some pins of a component may have the same pin type name, but a different pin name. Figure 3-5 shows the example of virtual connection between a sensor node and a CIPD node in virtual environment design.

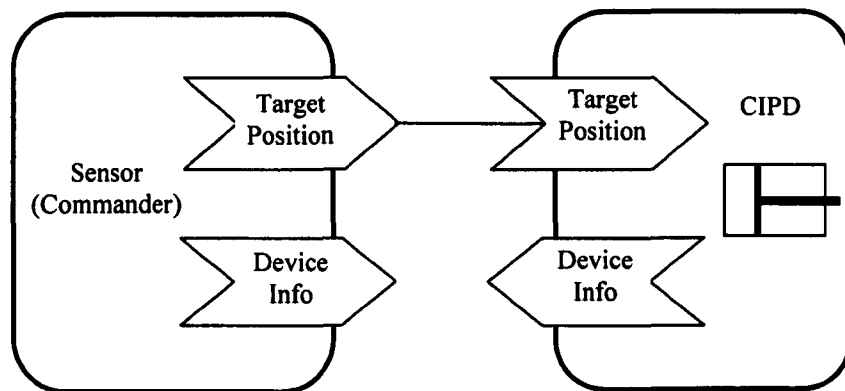


Figure 3-5 Connection of components in virtual environment design

The I/O functions database is a bridge between the virtual image and the real physical component. In other words, it is a logical interface to a CIPD physical component. This database consists of: a) the program ID, b) the types of input/output events, c) the names of input/output events, d) the direction of messages (input/output), and e) the connection attributes of input/output events (Priority, Authenticated, and so on). It is also used to set up the relationship between the control system virtual design and the real system.

### 3.5 Hardware Composition of Components-based Integrated Pneumatic Drives

A CIPD involves three integrated physical components (modules), they are: Integrated Pneumatic Actuator Module (IPA), Integrated Direction Control Module (IDC), and Integrated Speed Control Module (ISC). These integrated CIPD physical components include all necessary elements to build a servo pneumatic drive. These components are also Plug & Play devices; hence a CIPD can be setup in a few minutes without any configuration process.

Figure 3-6 shows hardware composition of a CIPD (with a pneumatic cylinder as an example) that developed in this research, it also shows the relationship of the three physical components and the airflow path within a CIPD. Figure 3-7 shows the pneumatic circuit diagram of a CIPD. The details about each component are presented in the following sections.

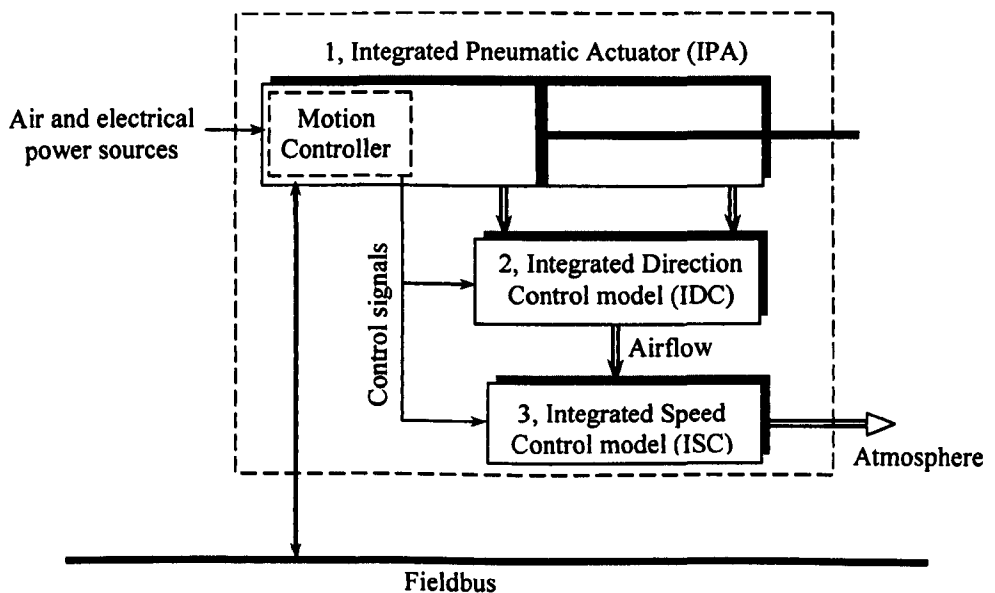


Figure 3-6 Composition of a Components-based Integrated Pneumatic Drive



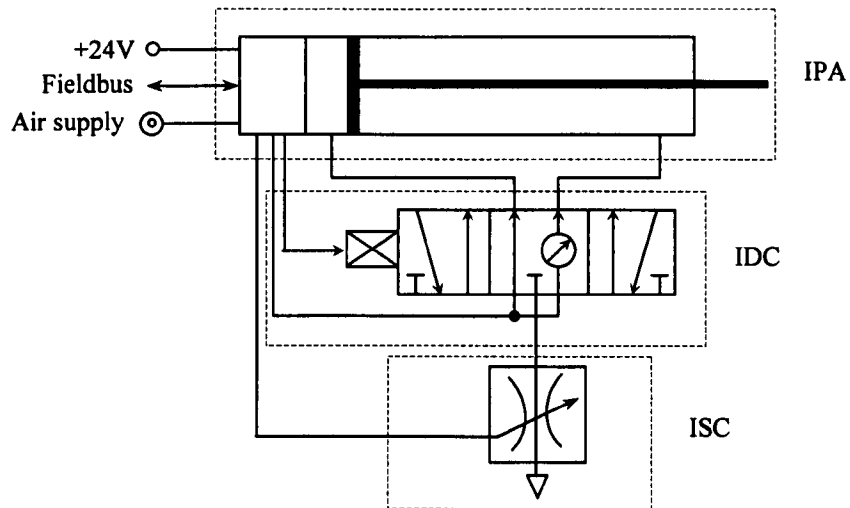


Figure 3-7 Pneumatic circuit diagram of CIPD

### 3.5.1.1 Composition of Integrated Pneumatic Actuator Module (IPA)

The Integrated Pneumatic Actuator Module (IPA) proposed in this research is an intelligent component based on a pneumatic actuator (pneumatic cylinders are used in this research). This module is integrated with a TP/FT-10F Control Module (manufactured by Echelon) for network processing and application implementation. This module is also integrated with position sensor and home sensor for the load position feedback and initializing the load to a referenced position. An electrical power supply regulation unit is included for the motion controller. Figure 3-8 shows the composition of the IPA module.

In practice, this module can be regarded as a usual pneumatic actuator that generates motion force. According to different application requirement for the motion force, user should choose an IPA with a suitable size actuator inside the module, to optimize the cost effective.

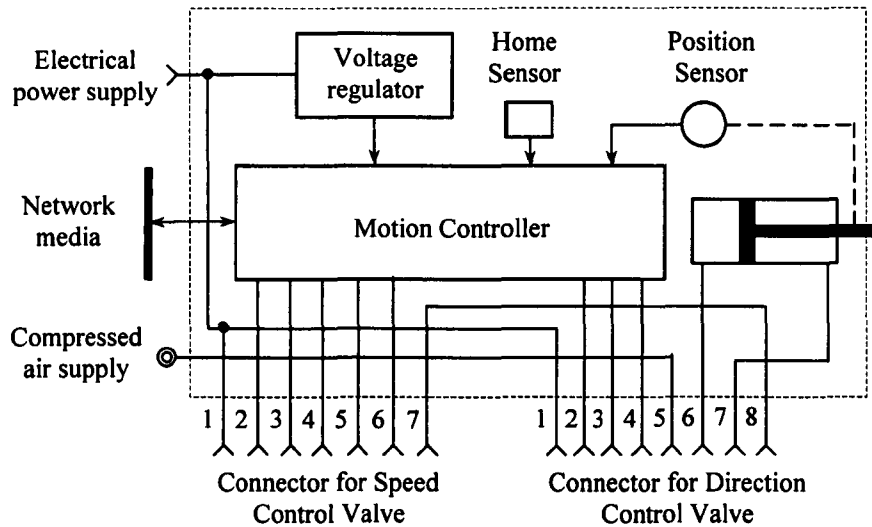


Figure 3-8 Composition of Integrated Pneumatic Actuator component

This module has some connections with other two modules (Integrated Direction Control Module and Integrated Speed Control Module) including compressed air supply and valve control signals. Table 3-2 and Table 3-1 list the connections. This module also has the connection to the network fieldbus.

Table 3-1 Connection with the Integrated Direction Control Module

Pin No.	Function
1	Power supply
2	Control signal for valve A
3	Control signal for valve B
4	GND
5	Compressed air supply
6	Cylinder port
7	Cylinder port
8	Released air port

Table 3-2 Connection with the Integrated Speed Control Module

Pin No.	Function
1	Power supply
2	BCD signal line 1
3	BCD signal line 2
4	BCD signal line 3
5	BCD signal line 4
6	GND
7	Released air port

The integrated TP/FT-10F Control Module, which is manufactured by Echelon, includes a Neuron 3150 chip that is integrated with LonWorks Technology. A Neuron 3150 Chip includes three processors inside the chip: MAC Processor, Network Processor, and Application Process. The Application Process is specially provided to users to run an application program. A Neuron 3150 chip also provides 11 programmable I/O pins with 34 selectable modes of operation, and two 16-bit timer/counters for frequency and timer I/O. The LonWorks Technology is a complete platform for implementing distributed control network systems. Through the network, any motion command from other devices, e.g. target position command, emergency stop command, and so on, can be transmitted as network variables via the fieldbus. LonWork Technology includes all of the elements required to design, deploy, and support control networks. It also supports multiple communication media including Power-line, Twisted-pair cable, Radio Frequency, and so on. Figure 3-9 illustrates the hardware composition of the integrated TP/FT-10 Control Module.

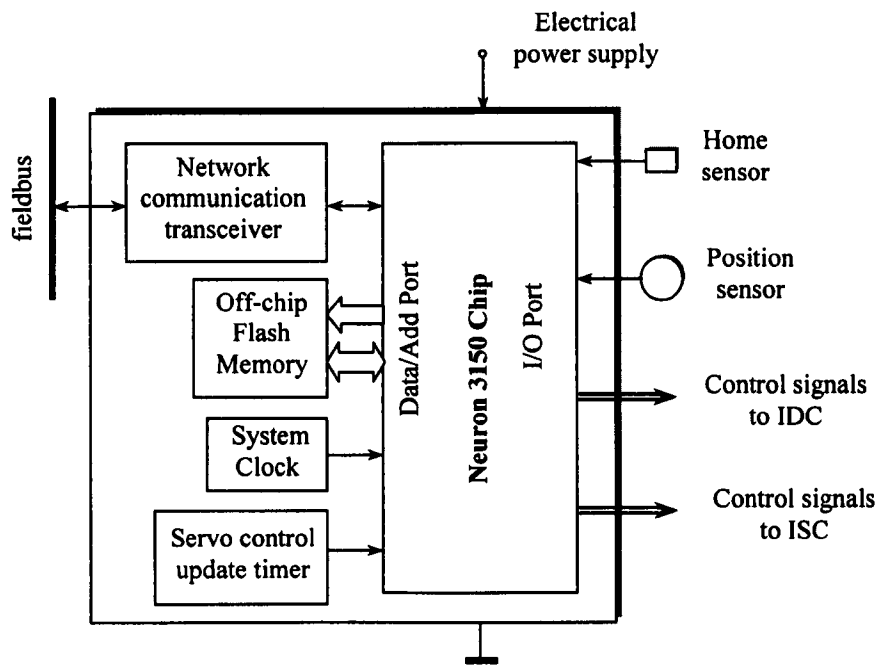


Figure 3-9 Hardware composition of the integrated TP/FT-10F Control Module

### 3.5.1.2 Composition of Integrated Direction Control Module (IDC)

The Integrated Direction Control module (IDC) proposed in this research is a none-intelligent component. It consists of two 3-port 2-position on-off solenoid pneumatic valves, one pressure regulator, one non-return valve, and one 2-channel amplifier for the valves. The IDC is placed between the IIPA module and the ISC module (as shown in Figure 3-6). The function of the IDC is controlling the motion direction the pneumatic actuator.

Figure 3-10 shows the composition of IDC module. The pin functions of its interface are listed in Table 3-1.

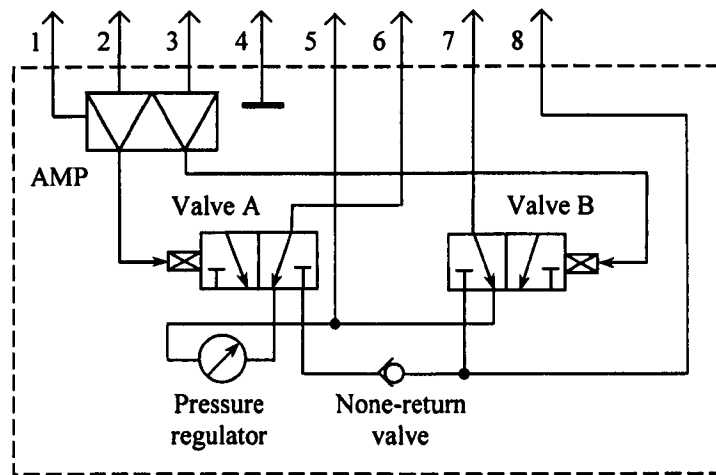


Figure 3-10 Composition of IDC component

The CIPDs employ a new pneumatic cylinder motion control strategy. Under this motion control strategy, the velocity of motion is proportional to the orifice size of the exhaust port (details are presented in Section 6.9). The port size of the two on-off control valves in the IDC affects the maximum motion velocity of the CIPD. By integrating the two on-off control valves and other associational parts to be one module, users have flexibility to choose different IDC to meet the application specification of maximum motion speed. Hence, the cost-effective feature of the CIPD can be significantly improved by avoiding using a large size IDC to build a slow moving drive.

In practice, if an IPA which based on an asymmetric pneumatic actuator is selected for a CIPD, users are required to adjust the Pressure Regulator inside the IDC to make the cylinder stable at stand-by state (no motion target position variable is received by the motion controller). The reason for doing so is explained in next chapter.

### 3.5.1.3 Composition of Integrated Speed Control module (ISC)

The Integrated Speed Control (ISC) module proposed in this research is non-intelligent component. It consists of several 2-port on-off pneumatic valves, and each of them is associated with a size adjustable port orifice. The function of the ISC is to control the size of exhausting port of the CIPD, so that the velocity of the load can be controlled (details are presented in Section 4.4 and Section 6.9). The control signal from the motion controller is a BCD (Binary Coded Decimal) signal hence, for example, four control signal wires can control up to fifteen objects.

Figure 3-11 shows the composition of the ISC module. The pin functions of its interface are listed in Table 3-2.

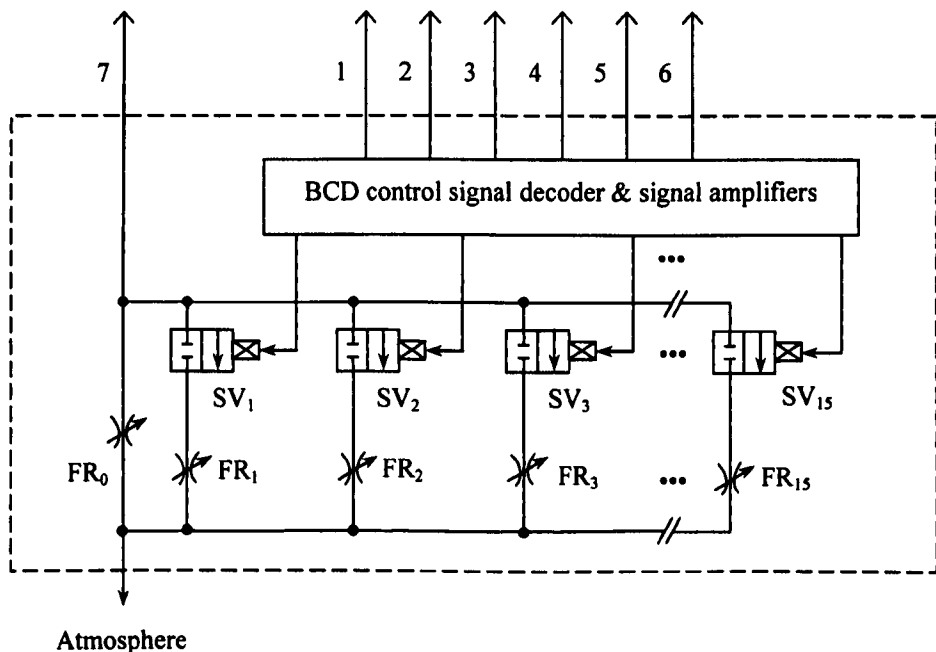


Figure 3-11 Composition of ISC component

From Figure 3-11 it can be seen that, by controlling the state of on-off valves,

the total size of the orifice (between the Pin 7 to the port connected to atmosphere) can be controlled. The minimum orifice size is controlled by the  $FR_0$  when all of the on-off valves are at closed state. The number of the on-off valves is flexible, but it will affect the performance of the CIPD in acceleration and deceleration phase, and positioning accuracy as well (details about is explained in Section 4.4.3). Changing the number of on-off valves dose not affects the application program pre-installed in the motion controller in IPA. Hence, users are allowed to choose different ISC with different number of valves, to meet their application specification to have a cost-effective CIPD

The ISC is connected to the IPA module via its external interface. After this component is installed, users are required to adjust the orifice size of each on-off valve to set the maximum motion speed and a suitable motion deceleration rate.

# Chapter 4 Motion Control of Components-Based Integrated Pneumatic Drives

## 4.1 Introduction

Most of the previous research on the servo control of pneumatic drives is based on the traditional motion control strategy. In such strategy, a motion control of pneumatic actuator is achieved by charging compressed air into pneumatic actuator chambers. When the drive is in stand by state, the pressures in the chambers are equal to the atmospheric pressure, or lower than the air supply pressure. To achieve a good control performance, one or more cooperative high-bandwidth proportional or on-off control valves are placed between the compressed air source and the pneumatic actuator. However, from the manufacturing point of view, the cost of either the high bandwidth proportional or on-off valves is expensive. This is one of the factors that deter the manufacturer from applying this kind of system, thus making them less favourable.

The CIPDs, which are developed in this research, employ a new motion control strategy. In this new control strategy, both chambers of the pneumatic actuator are directly connected to the compressed air source when the system is in stand by state. The motion control of the actuator is achieved by releasing the compressed air from one of chambers. Thus, air pressure in only one of the chambers is being controlled (the other remain as supply pressure). By using this method, not only the air in the chambers is more controllable but also low-bandwidth pneumatic valves can be employed, hence providing a lower cost pneumatic system. This chapter introduces such motion control strategy and the corresponding pneumatic circuit.



## **4.2 Pneumatic actuator motion control strategy employed within CIPDs**

Pneumatic actuators can be largely classified in to two classes: symmetric pneumatic actuators and asymmetric pneumatic actuators. The symmetric pneumatic cylinders have same piston area in two chambers. When the two chambers are charged by a same compressed air supply, the piston will not move because the force, that crossing the piston generated by the compressed air, are balanced. However, asymmetric pneumatic cylinders have different piston areas in the two chambers, when the two chambers are charged with a same compressed air supply, the piston can be moving if the force crossing the piston is larger than frictional forces of the system. Therefore, the pneumatic circuit of CIPDs with symmetric actuators is slightly different to CIPDs with asymmetric actuators. In the following sections, a pneumatic cylinder is used as an example of pneumatic actuator for presenting the pneumatic circuit of the new pneumatic actuator motion control strategy.

### **4.2.1 Cylinder motion control strategy of CIPDs with a symmetric pneumatic cylinder**

Figure 4-1 is a simplified pneumatic circuit diagram of CIPDs with a symmetric pneumatic cylinder at stand-by state. The system mainly consists of one pneumatic cylinder, two 3-port 2-position on-off pneumatic solenoid valves (Valve A ,B) and two airflow rate regulators ( $FR_{A,B}$ ).

At ready-to-work state, both the Chamber A and B are directly connected to the compressed air supply, hence the pressures of both chamber ( $P_a$  and  $P_b$ ) are equal to the compressed air supply pressure  $P_s$ . At this state, the load ( $M$ ) does not move because pressure difference between the Chamber A and B is zero.

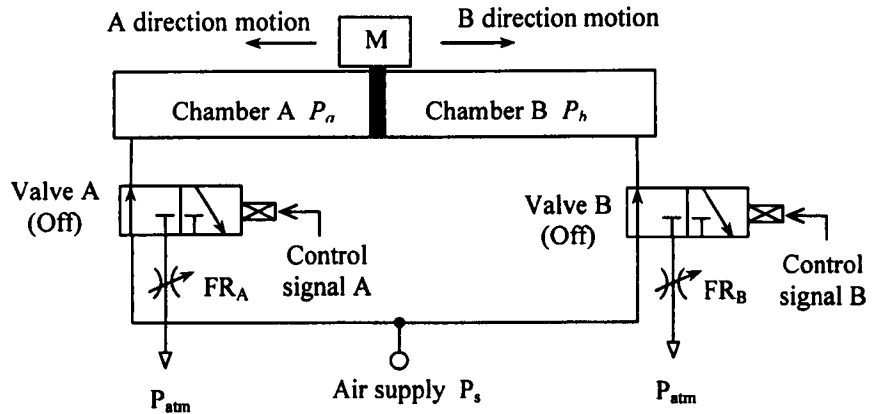


Figure 4-1 Simplified pneumatic circuit diagram of the CIPDs

When an A direction motion of load is required, the control valve A will be turned from “off” state to “on” state by the valve control signal A, then the pneumatic circuit becomes one as shown in Figure 4-2. At this state, the Chamber A is connected to the atmosphere through the airflow regulator A ( $FR_A$ ), hence compressed air in the Chamber A is being exhausted. This will cause the chamber pressure  $P_a$  to be lower than the supply pressure  $P_s$ . When a force difference crossing the piston, which is caused by the pressure difference of  $P_a$  and  $P_b$ , is larger than the system frictional forces of the system, the load start to move.

When the load reaches target position, the valve control signal A will turns the Valve A from the “on” state to the “off” state, then the pneumatic diagram becomes one same as Figure 4-1. At this state, the Chamber A is re-charged to the compressed air supply, and the force cross the piston is zero. This will cause the load to be stopped by the frictional force of the system.

Figure 4-3 is pneumatic circuit diagram of CIPDs when load is moving towards B direction. Its working theory can be easily understood by referring above description.

In this research, the two motion control valves, Valve A and Valve B, are referred as Direction Control Valves.

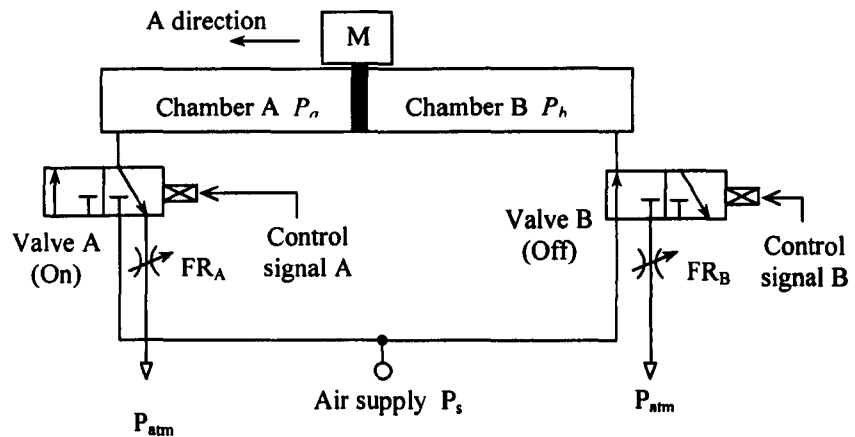


Figure 4-2 Pneumatic circuit of the CIPDs during A direction motion of piston

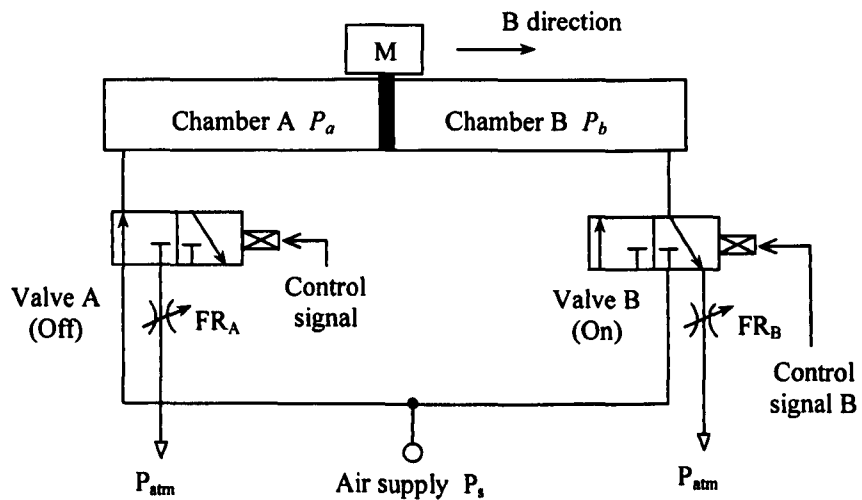


Figure 4-3 Pneumatic circuit of the CIPDs during B direction motion of piston

#### 4.2.2 Pneumatic circuit with an asymmetric pneumatic cylinder

An asymmetric pneumatic cylinder normally is associated with a difference of effective piston area, that is  $A_a \neq A_b$ . To control the piston to be stable

at stand-vy state, a relationship that  $P_a A_a = P_b A_b$  must be satisfied. This can be achieved by applying different chamber pressures  $P_a$  and  $P_b$  in two chambers; in other words, the pressure of compressed air supply to the two chambers should be different.

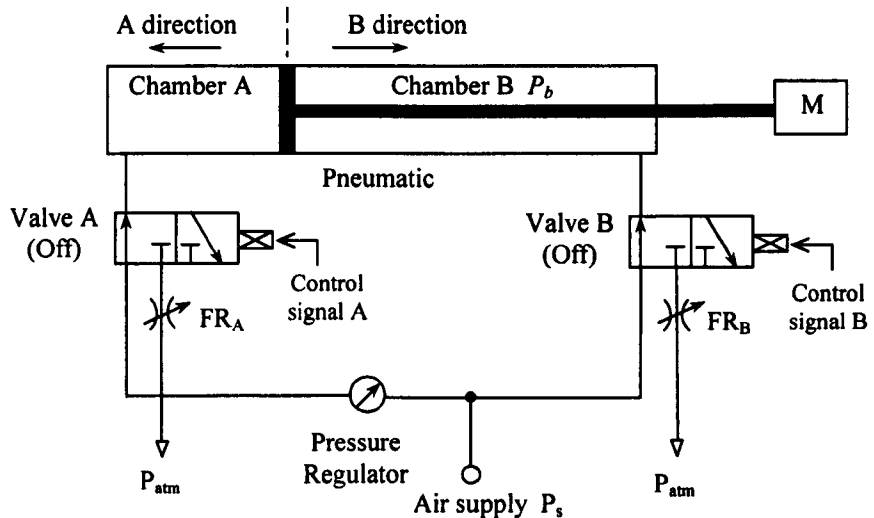


Figure 4-4 The pneumatic circuit diagram of the CIPDs using an asymmetric pneumatic cylinder

A simplified pneumatic circuit of CIPDs with an asymmetric pneumatic cylinder is shown in Figure 4-4. In this circuit, a pressure regulator is inserted between the compressed air supply and the control valve that controls the air in the chamber associated with the large piston area. Therefore, the relationship,  $P_a A_a = P_b A_b$ , can be satisfied by setting up two different supply pressures. The theory of the motion control strategy of CIPD with an asymmetric actuator is same as theory described in Section 4.2.1.

### **4.3 Servo motion control of the CIPDs**

The CIPDs employ two 3-port 2-position on-off pneumatic valves as direction control valves. On-off pneumatic valves only accept the logical control signal 0 or 1. In other words, on-off valves cannot correctly response to an analogue control signal. However, most of well-developed modern control technologies are based on analogue signal calculations. PWM (Pulse Width Modulation) is a well known approach that likely to be chosen to transfer an analogue signal to a object digitally. Many successful electrical applications proved that the PWM is a sufficient way in automation control system. For the application of servo pneumatic system, PWM normally requires wide bandwidth on-off control valves (e.g. 100 Hz) to achieve relatively good performance; however, the wide bandwidth on-off pneumatic valves are normally low capacity and high cost.

To benefit from modern control technology, a three-state control algorithm is developed during this research. This control algorithm is based on an analogue control algorithm, however its outputs are two valve control signals. Any well-developed analogue control algorithm, for example, PID-based control algorithm, can be directly applied to the three-state control algorithm.

#### **4.3.1 Three significant motion states of a full motion process**

As described in Section 4.2, the motion control of the pneumatic cylinder in achieved by releasing the air in the corresponding chamber. According to the state of the direction control valves (“On” state or “Off” state), the full motion process could be divided into three significant states as illustrated in Figure 4-5.

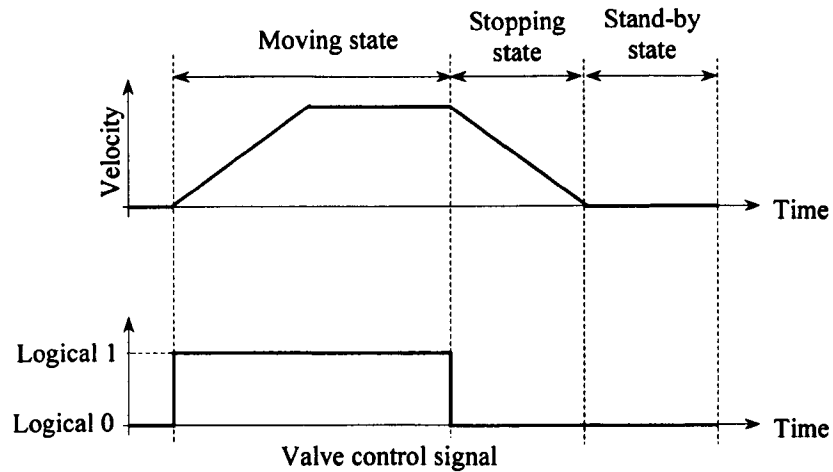


Figure 4-5 Three significant motion states of a full motion process

- 1). ***Moving State***: this state includes the period from the time, at which the control signal to a control valve is turned from logical 0 to logical 1, to the time at which the control signal is turned from logical 1 to logical 0.
- 2). ***Stopping State***: this state includes the period from the time just after the control signal is turned from logical 1 to logical 0 to the time at which the load is stopped by the system frictional force.
- 3). ***Stand-by State***: this state includes the period from the time, at which the piston (load) is stopped, to the time at which the piston (load) starts to move for next motion command.

According to the pneumatic actuator motion control strategy described in Section 4.2, the relationship between load position, load velocity and

control signals of Valves A and B can be schematically illustrated in Figure 4-6. It can be seen that a three-state control signal can present the state of control signals for Valves A and B. The relationship between the three-state control signal and control signals of Valves A and B is also illustrated in Figure 4-6.

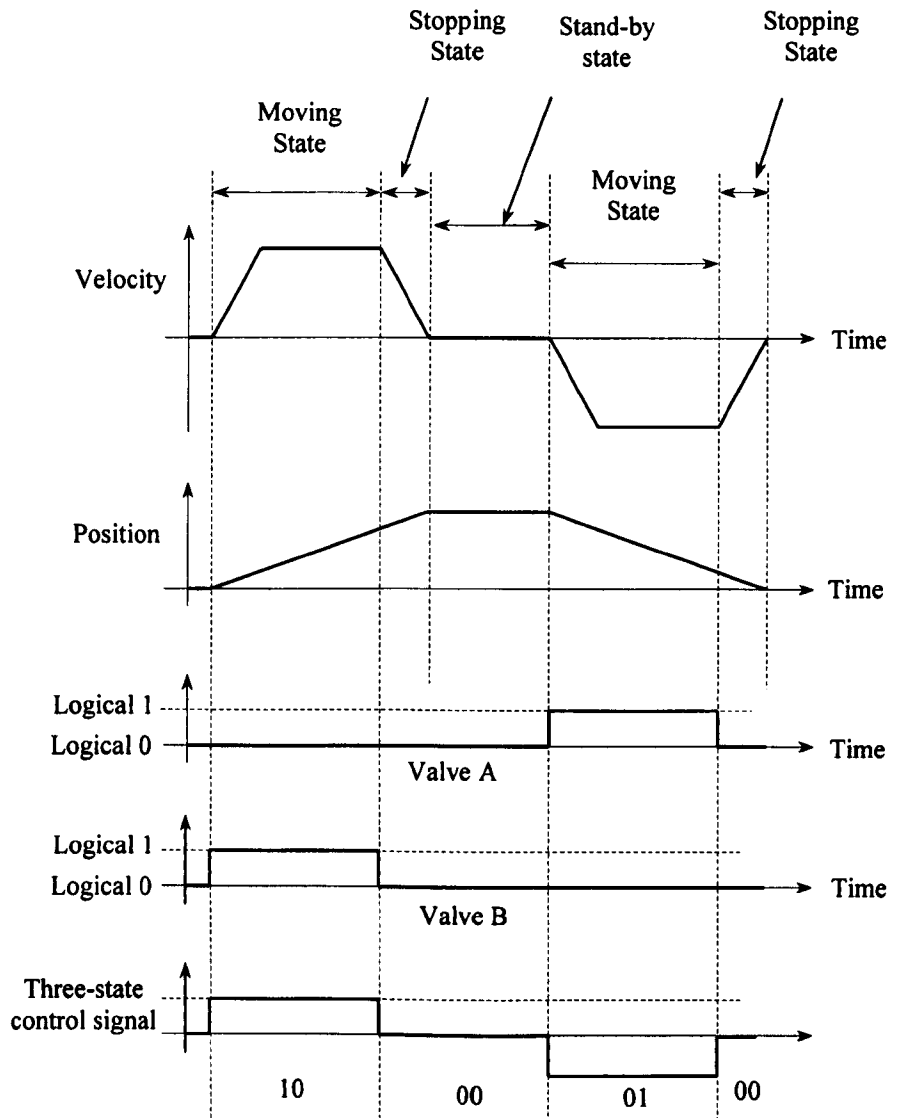


Figure 4-6 Relationship between load position, load velocity, control signals for Valves A and B and tree-state control signal

The three states of the control signal are:

- State 1: this controls Valve A to be open and Valve B to be closed. At this state, the piston (load) is controlled to move for an A direction motion. In three-state control signal, this state is denoted by “10”.
- State 2: this controls both Valve A and Valve B to be closed. At this state, the piston (load) is decelerated or stopped. In three-state control signal, this state is denoted by “00”.
- State 3: this controls Valve A to be closed and Valve B to be open. At this state, the piston (load) is controlled to move for a B direction motion. In three-state control signal, this state is denoted by “01”.

#### **4.3.2 Servo control algorithm of the CIPDs**

It is very difficult for pneumatic servo actuators to achieve high control performance due to their extraordinary high non-linearities. Many factors contribute to the non-linearities associated with a pneumatic actuator. These include the non-linearity of friction and compressibility of air, and other factors like time delay of control valves.

Feedback linearization is one of the well-known techniques for a control system with non-linearities. With this technique, a non-linear system can be controlled like a linear one. The principle of feedback control can be expressed as the following (Åström and Hägglund, 1995):



*Increase the manipulated variable when the process variable\* is smaller than the setpoint\*\* and decrease the manipulated variable when the process variable is larger than the setpoint.*

This type of feedback is called negative feedback because the manipulated variable moves in opposite direction to the process variable. Virtually any feedback controller is intended to generate an output that causes some corrective effort to be applied to a process so as to drive a measurable process variable towards demand. The block diagram shown in Figure 4-7 illustrates the negative feedback principle.

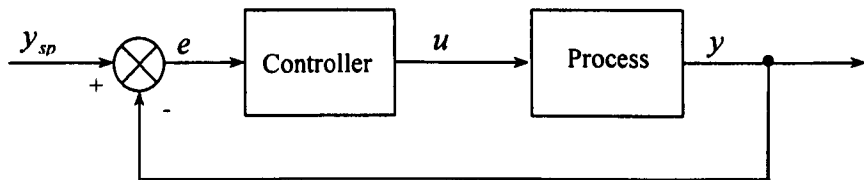


Figure 4-7 Block diagram of a process with a feedback controller

PID-based control is the most commonly used control method for servo control. It is simple to be implemented and there exist some well-developed tuning knowledge and strategies. The effect of each mode in a PIDVF (Proportional, Integral, Derivative, Velocity feedback, Velocity feed-forward) 5-term control algorithm on servo pneumatic system control using proportional valve has been studied previously (Pan, 2002). The followings are the summaries of the reported results.

- 
1. \* The process output is called process variable (PV) in this research.
  2. \*\* The desired value of the process variable is called the setpoint (SP) in this research. It is denoted by  $y_{sp}$ .

- **Proportional mode (P):** Proportional mode produces a correction that is proportional to the error and adjusted with the proportional gain factor  $K_p$ . This correction is then added to the control input, and the error is then reduced. With an increase in proportional gain, system's stiffness is increased, thereby resulting in reduced positioning error. However, there is a limit, beyond which the system will become unstable or oscillatory.
- **Integral mode (I):** Integral mode produces a control action; the action is proportional to the integral of the error with time. A constant error signal will produce an increasing correcting signal. The correction continues to increase as long the error persists.
- **Derivative mode (D):** Derivative mode produces a control action that is proportional to the rate at which the error is changing. When there is a sudden changing in the error signal the controller gives a large correcting signal. When there is a gradual change only a small correcting signal is produced. Derivative control can be considered to be a form of anticipatory control in that the existing rate of change of error is measured, a coming larger error is anticipated, and a correction applied before a larger error has arrived.
- **Velocity feedback mode (V):** Velocity feedback mode is used to reduce the onset of instability in the servo loop algorithm. It acts to resist rapid movement of the actuator and hence allows the proportional gain to be set higher before oscillation sets in.
- **Velocity feed-forward mode (F):** Velocity feed-forward mode is used to reduce time delay/acceleration response and position following error. With pure feedback, relatively large position error is needed in order to produce a command signal which can maintain the system at the desired velocity. The introduction of a velocity feed-forward term can reduce the large positioning error caused while trying to achieve the desired velocity.

The feedback control technology has been chosen for the control of the CIPDs. However, according to the nature characteristics of the CIPDs, it is concluded that integral, velocity feedback, velocity feed-forward modes are ignorable. This is because that, firstly, the CIPDs are point-to-point positioning drives, control of velocity profile in a motion processing is not required, secondly, the three-state control signal will ignore any control action produce by integral, velocity feedback, velocity feed-forward modes due to the exist of the Region of Acceptable Errors (RAE, details about three-state control signal generation are presented in next section). Therefore, a PD-based servo control loop is employed within the CIPDs. The block diagram of the servo control loop of CIPDs is shown in Figure 4-8.

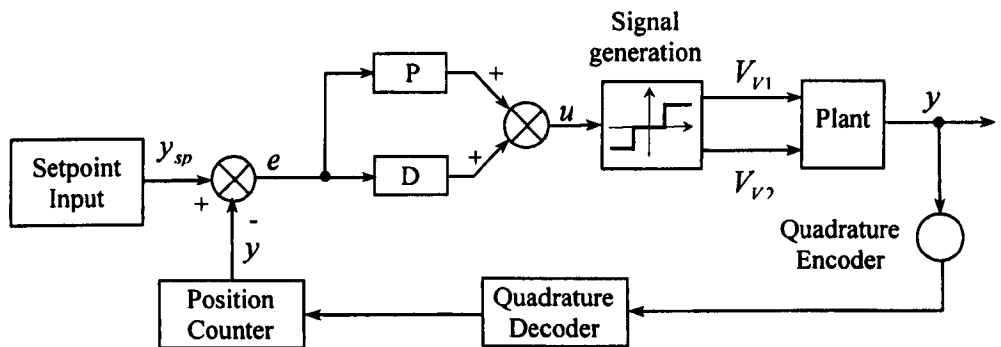


Figure 4-8 Block diagram of the servo control loop of CIPDs

The actuator is controlled to minimise the error between the setpoint and the process variable (measured position) fed by the incremental/decremental encoder. The controller samples the measured position of the load ( $y$ ), compares the setpoint and the measured position ( $y$  and  $y_d$ ) and generates a new servo control demand ( $u$ ) by running the control algorithm. The controller then converts the control demand to a three-state control signal, and outputs the valve control signals ( $V_a, V_b$ ), which drive the on-off valves through their signal amplifiers.

The relationship between the control demand ( $u$ ) and the positioning error is described as Equation (4-2).

$$u = K_p \cdot e + K_d \frac{\Delta e}{\Delta \tau} \quad (4-1)$$

where

$u$  : control demand

$K_p$  : proportional gain

$K_d$  : derivative gain

$e$  : following error

$\Delta \tau$  : servo update period

### 4.3.3 Generation of three-state control signal

Figure 4-9 shows the procedure of generating three-state control signal from an analogue control signal. The two valve control signals are generated from the interpretation of the three-state control signal. In practice, this procedure can be implemented through one of the following method:

- Programming,
- Electronic circuit, or
- Combination of programming and electronic circuit.

A function block, referred as Interpreting Block, will convert the control demand signal ( $u$ ) to a three-state signal, and outputs cooperated valve control signals  $V_A$  and  $V_B$ . The input signal of Interpreting Block is a servo control demand ( $u$ ), which is an analogue signal of a closed loop control algorithm calculation. Figure 4-10 shows detailed function of this block.

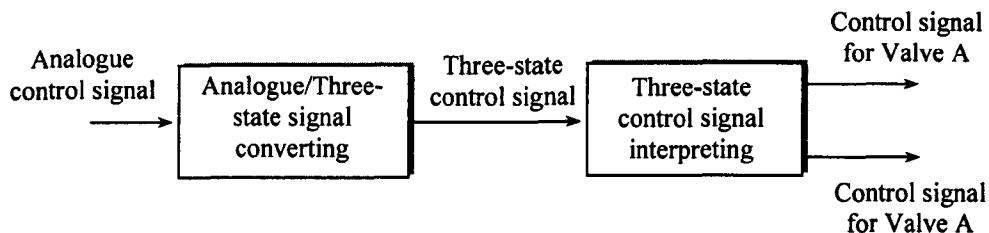


Figure 4-9 Procedures of converting analogue signal to valve control signals

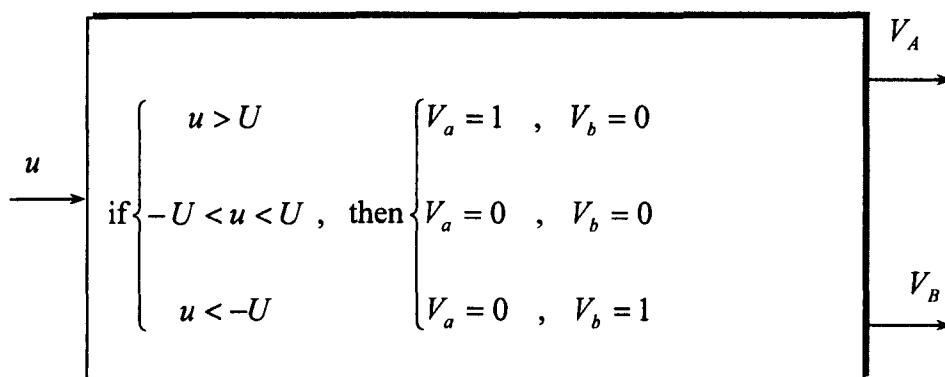


Figure 4-10 The function of the Interpreting Block

In Figure 4-10,

$u$  : the servo control demand;

$U$  : boundary value of servo control demand defined by Region of Acceptable Errors (RAE) ;

$V_a$  : control signal of Valve A;

$V_b$  : control signal of Valve B;

0: logical signal for “off” state of valve control voltage;

1: logical signal for “on” state of valve control voltage;

To convert an analogue control demand signal to a three-state control signal, a region, defined as Region of Acceptable Errors (RAE), must be set up. From

Equation (4-1), it can be seen that when the load is stopped, then  $U = K_p \cdot e$ , hence the RAE has also indirectly defined a region of acceptable final positioning errors. Therefore, the setting of width of RAE also indirectly controls the final positioning error.

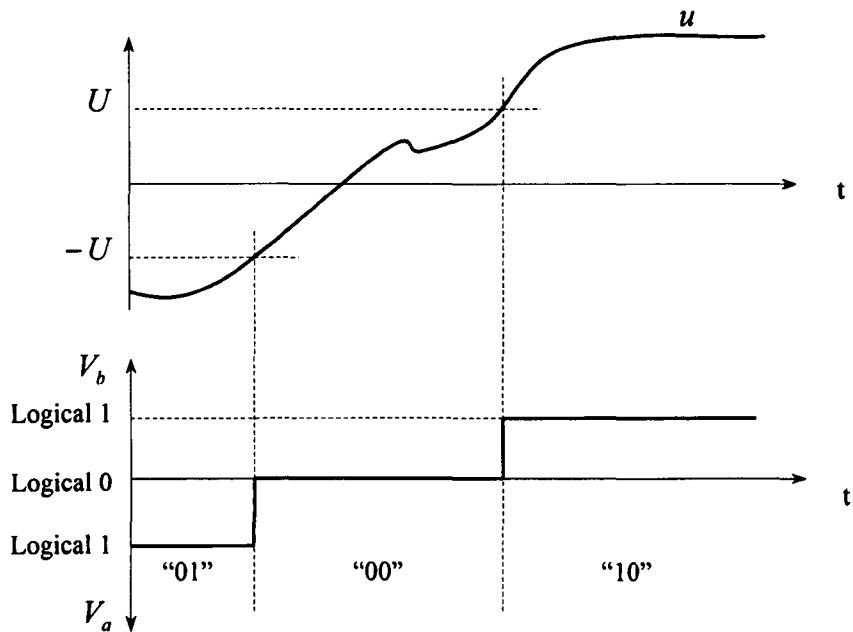


Figure 4-11 Relationship between the servo control demand and the three-state control signal.

When the control command  $u$  is within the RAE defined by  $-U$  and  $U$ , the Interpreting Block outputs a “00” state control signal ( $V_a = 0, V_b = 0$ ), any control demand made by the analogue control algorithm to further reduce the positioning error will be ignored. Figure 4-11 graphically shows the relationship between the control demand ( $u$ ) and the three-state control signal.

#### 4.4 High-Speed Motion Control Strategy of CIPDs

Modern manufacturing processes are characterised by a high degree of automation, with electronics controlling the processing and handling machinery. A wide spectrum of manufacturing industries requires more and more complicated units for high-speed handling, transportation, assembling, and so on. Servo pneumatic drives, with its advantages in terms of speed, simplicity, safety, cleanliness, cost-effectiveness, and direct acting, still can be the first choice.

For high-speed point-to-point machinery, fast operating cycle times and good positioning accuracy with very small or without overshoot is often a prerequisite. This section discusses the factors affecting the positioning ability of the CIPDs, the approach employed in the CIPDs for increasing the position accuracy, and a control strategy developed for deceleration regulation to reduce the settling overshoot.

##### 4.4.1 Minimum Start-Stop Displacement

In any actuation system, once the motion is initiated, the actuator will move some displacement before it stops. The minimum displacement between start and stop is as defined Minimum Start-Stop Displacement (MSSD). That is

$$d_{mssd} = d_{st} - d_{si} \quad (4-3)$$

where

$d_{mssd}$ : minimum start-stop displacement;

$d_{st}$ : stop position;

$d_{si}$ : initial position.

The MSSD is a key parameter that indicates the system positioning accuracy.

Reducing the MSSD of the system is one of the efficient methods to increase the system positioning accuracy.

Figure 4-12 schematically shows the practical relationship between the valve control signal, the response of valve, and the load velocity within a complete motion process. It can be seen that there are three factors that significantly affect the MSSD (ignore the control loop-updating interval, chamber pressure build up time delay, and so on):

- 1). The time delay caused by the direction control valve in responding the turning off control signal ( $t_{off}$ );
- 2). The transient velocity during the direction control valve is in “on” state;
- 3). The system frictional forces which stop the load motion (stopping stage motion).

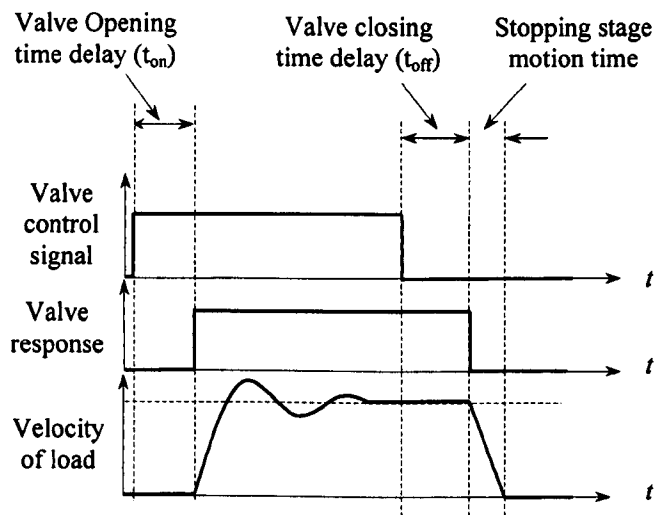


Figure 4-12 Relationship between the valve control signal, the valve response and the load velocity



#### 4.4.2 Approaches for increasing positioning accuracy

From the discussion in the above section it is known that, to increase positioning accuracy of CIPDs, the following approaches can be considered:

- Using relatively high-bandwidth valves for the direction control, so that the time delays ( $t_{on}$  and  $t_{off}$ ) can be kept as small as possible.
- Using low transient velocity for the load motion around the target position. This approach also has the effect of reducing the stopping stage motion time because the load dynamic is relatively small. Mathematical analysis shows that the amplitude of the transient velocity profile of CIPDs is determined by Velocity Gain  $K_v$ . The Velocity Gain  $K_v$  is largely determined by the effective area ratio of exhaust orifice and the piston in exhaust chamber, that is (details are presented in Section 6.9),

$$K_v = (R\sqrt{T_s}C_0C_d)\frac{A_e}{A_b} \quad (4-4)$$

where:  $K_v$ : CIPD Velocity Gain

$A_e$ : exhaust orifice area ( $m^2$ )

$A_b$ : driving chamber piston area ( $m^2$ )

$R$ : gas constant ( $\frac{J}{Kg}$ )

$T_s$ : supply gas temperature ( $K$ )

$C_d$ : discharge coefficient

$C_0$ : constant ( $C_0 = 0.04$ )

In practice, relatively high-bandwidth pneumatic valves are normally more expensive than low-bandwidth pneumatic valves. Therefore, using low transient velocity for the load motion around the target position is a cost-effective approach to increase the positioning accuracy of CIPDs.

### 4.4.3 Acceleration and deceleration control of CIPDs

The acceleration and deceleration of load make huge contribution to the operating cycle times while the dynamics of the load at its target position normally also affects the positioning accuracy and amplitude of the overshoot. The ideal process for a high-speed point-to-point motion should be that: starting with the highest possible acceleration and stopping with a deceleration caused by a force which reduces the load dynamic to zero at the target position in the shortest time.

For CIPDs, a high acceleration rate can be easily achieved by applying a large size of the exhaust orifice during accelerating motion stage. However, reducing the dynamics of the load to zero at its target position as efficient as possible is a more difficult task.

A deceleration control strategy has been developed in this research for the control of high-speed CIPDs. The basic theory of the strategy is that using some of 2-port on-off valves, referred as Speed Control Valves (SVs), to control the effective area of exhaust orifice during the deceleration phase of motion. The SVs are parallel in connection, and each SV controls the application of a fixed-size exhaust orifice. The smallest exhaust orifice provides the lowest load motion speed, and higher motion speed can be achieved by opening more SVs at some time, which means that a number of fixed-size orifices are applied to get a equivalent larger exhaust orifice. Figure 4-13 graphically illustrates the deceleration control strategy. It also presents the relationship between velocity profile of load, the state of SVs, and the positioning profile.

Figure 4-14 shows the corresponding hardware setup with four SVs. The airflow rate regulator  $FR_0$  sets up a area of exhaust orifice for the lowest motion speed while other airflow rate regulators ( $FR_1 - FR_4$ ) set up different exhaust orifice areas for higher motion speed by opening different number of airflow rate regulators.

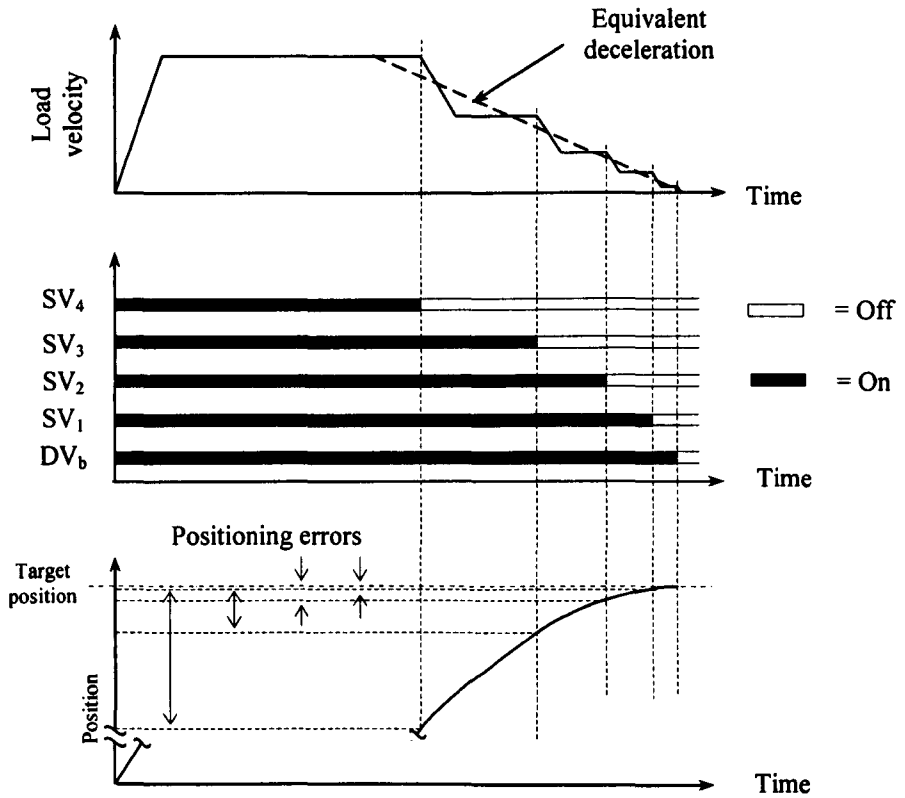


Figure 4-13 Deceleration control strategy of CIPDs

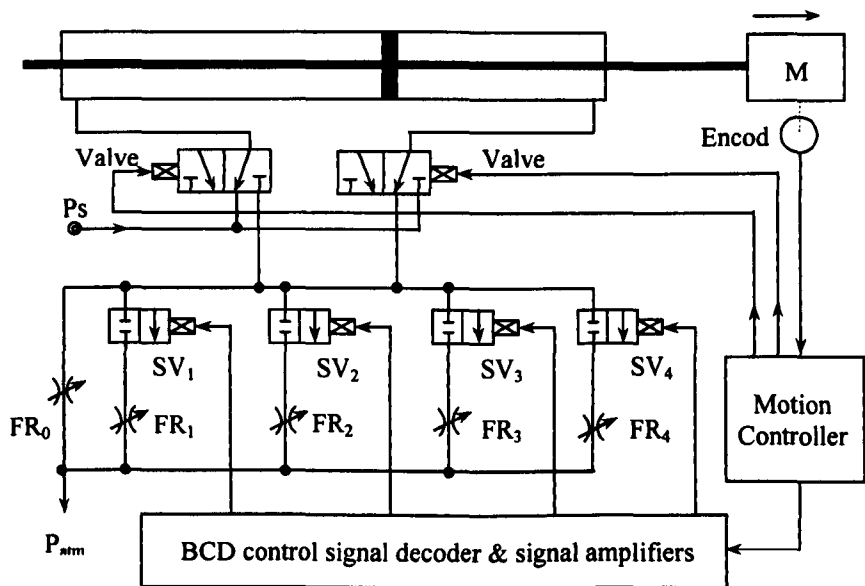


Figure 4-14 Pneumatic circuit of high-speed CIPDs with four speed valves

During acceleration phase of motion, all SVs are opened so that the load can start at the highest acceleration. However, during deceleration phase of motion the SVs will be closed one by one according to transient positioning error between the measured position and the target position. There is a look up table, referred as Speed Valve Control Criteria Table (SVCCT), must be defined in the motion controller program. The SVCCT contains a list for the relationship between the transient positioning error and the state of the SVs (open or closed).

The motion controller compares the positioning error at each sampling time with the predefined SVCCT, and generates cooperative control signals to the SVs. As the positioning error is getting smaller, all SVs will be closed finally. The PD-based three-state control algorithm will be invoked, only after all SVs are closed, to generate control signals to the direction control valves. Table 4-1 shows an example of SVCCT for the deceleration control strategy. The positioning errors listed in the table are the program developer definable.

Table 4-1 An example of user definable Speed Valve Control Criteria Table used in the deceleration control strategy

Positioning error	Opened speed control valves
> 30 mm	SV <sub>1</sub> , SV <sub>2</sub> , SV <sub>3</sub> , SV <sub>4</sub>
> 20mm	SV <sub>1</sub> , SV <sub>2</sub> , SV <sub>3</sub>
> 10 mm	SV <sub>1</sub> , SV <sub>2</sub>
> 5 mm	SV <sub>1</sub>

One of the features of employing the deceleration control strategy is that the number of speed control valves installed in a CIPD at user stage does not affect the application program pre-installed in the motion controller. In other words, for different application specifications, users are allowed to install different numbers of speed control valves and set different exhaust orifice size without concerning any changes for the motion controller, e.g. modifying application program.

# Chapter 5 Network Service of Components-Based Integrated Pneumatic Drives

## 5.1 Introduction

During last two decades, the world of telecommunications has been rapidly developed. One of the major paradigm shifts is the rapid expansion of Internet. Internet is used now not only for electronic mail, but also as a means of instantly exchange a wide range of information around the world. Electronic commerce transactions via Internet are also moving toward full-scale application. At the same time, the shift toward super high-volume optic-fiber trunk line networks is also advancing on a global scale, in order to accommodate the rapid increases in data traffic.

Presently, one of the areas most sensitive to these changes may be the area of network service provision, especially among those international firms that provide these services through Internet. It has been noted that forward-looking companies have attempted to make their distribution channels more flexible and adaptive. That is, firms must link manufacturing, services, and distribution functions to meet customer needs, and the “winners” will be those firms that develop innovative solutions to providing those links that best satisfy their customers’ needs. Hence, it is not enough to sell just a product; the real impact on profitability comes from exploiting downstream opportunities, by providing the customers with products such as financing, maintenance, spare parts and consumables (Knecht and Leszinski et al, 1993; Wise and Baumgartner, 1999). Nowadays, the majority of manufacturing companies (with industrial customers) not only deliver a tangible product, but also serve a network service market.

## **5.2 Connectivity of Components-based Integrated Pneumatic Drives Network with Business networks**

Business networks and device control networks are very different. Control and monitoring applications have many requirements that differ greatly from those of business applications. There are also some common requirements between control and business applications, for example security, reliability, and flexible wide-area. Device network developers can take advantage of these capabilities by properly interconnecting the device network with business network components.

The manufacturer of a product also should, in taking extended producer responsibility, have data available on all stages of the product life cycle. This calls for an integrated information system, with databases and management tools under the control of the manufacturer but open to access by other parties such as those involved in supply of components, the maintenance and the recycling of the product. The rapidly changing nature of information technologies means that network services systems must be robust and flexible, if well designed they can exploit emerging technologies to bring the manufacture, component supplier, user and recycler together as a unit.

Furthermore, future consumer products will potentially require systems that record data to monitor environmental parameters such as time, temperature, shock or vibration. This environmental data can be combined with static information (e.g. composition of product's materials) and possibly the service life of valuable components. The choice of data not only have potential impact in environmental issues regarding to recycling and reuse, it could avoid expensive product diagnostics in repair or/and maintenance activities. The data must be communicated to the relevant stakeholder for action; all actors in the supply chain must share data.

The CIPDs control network has been designed to support the connectivity with Internet. The CIPDs control network is connected to Internet through a gateway device. Figure 5-1 shows the proposed architecture of CIPDs control network connected with Internet.

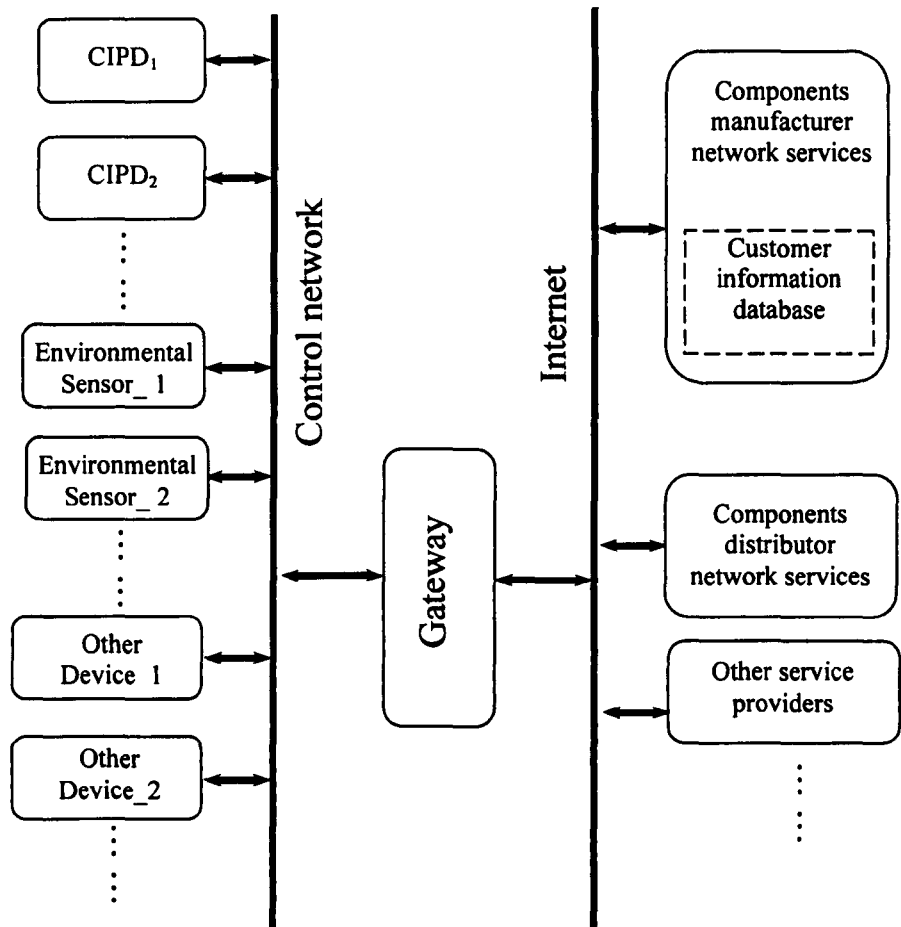


Figure 5-1 Proposed architecture of CIPDs network services.

### 5.3 Composition of Gateway device

Figure 5-2 illustrates the proposed composition of the gateway device. This device provides all necessary mechanisms for the control network design including the I/O function database and gateway device image for the

design in the virtual environment. Meanwhile, this device also has mechanisms for the Internet self-configuration and auto-registration processes. Through these processes, not only the gateway device gets an Internet IP address, but also automatically adds the content of the Control System Information Database into Customer Information Database, which is accessible by other service providers.

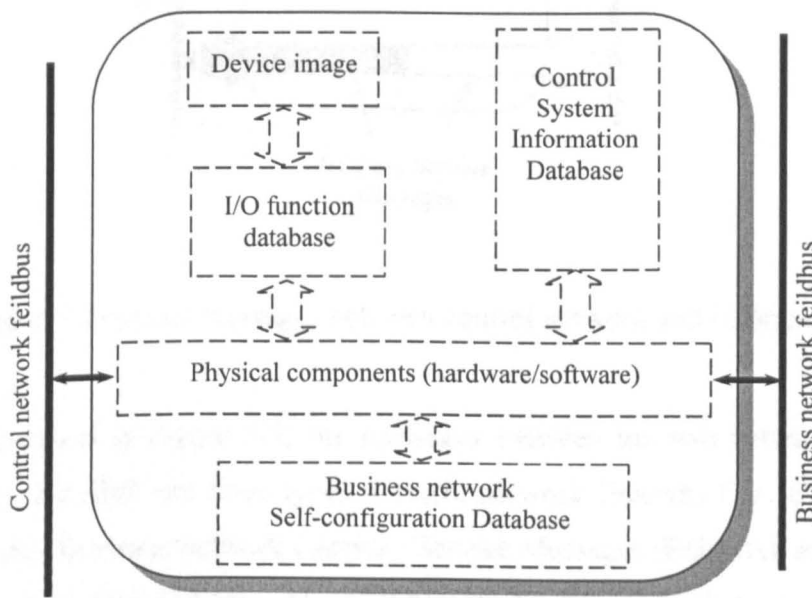


Figure 5-2 Composition of gateway device

#### 5.4 An example of Gateway Device

An example of gateway device has been developed for this research. The main purpose of the example gateway device is establishing communication path between the LON control network and Internet business network.



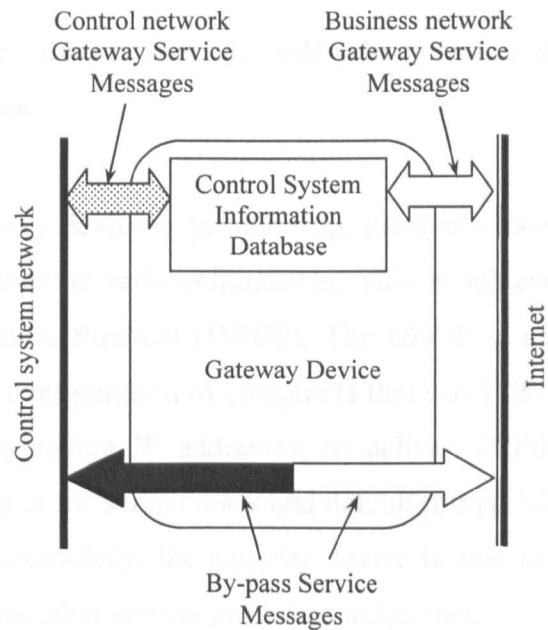


Figure 5-3 Types of messages between control network and business network

As illustrated in Figure 5-3, the messages between the two networks can be largely classified into three types: Control network Gateway Service Messages (CGSMs), Business network Gateway Service Messages (BGSMs), and By-pass Service Messages (BSMs). The CGSMs are the messages that are transmitted between the gateway device and other nodes within the control network for updating the Control System Information Database in the gateway device; The BGSMs are the messages that transmitted between the gateway device and the service providers over Internet for providing control system information to service providers. These messages also include the information from service provider, for example, service history record update message. The BSMs are the messages for the communication between the business service providers and the individual node within the control system. The gateway device only translates the messages for communication over two different networks.

Through this communication strategy, not only the service providers are able to acquire the information regarding to the control system and individual

node in the control system, but also able to test the individual node as well.

#### **5.4.1 Gateway device Internet self-configuration and auto-registration processes**

When the gateway device is powered up, the first process the gateway device carried out is Internet self-configuration. This is achieved using the Dynamic Host Configuration Protocol (DHCP). The DHCP is an Internet protocol for automating the configuration of computers that use TCP/IP. DHCP can be used to automatically assign IP addresses, to deliver TCP/IP stack configuration parameters such as the subnet mask and default router. When the DHCP process is completed successfully, the gateway device is able to communicate with its manufacturer and other service provider via Internet.

The next process carried out by the gateway device is auto-registration. Firstly the gateway device set up a connection with its manufacturer. The TCP/IP information about its manufacturer, such as IP address, listening port number, are held in the Self-configuration Database within the gateway device. When the connection is established, the gateway device sends out the TCP/IP information of itself to the Customer Information Database held by the manufacturer. Sequentially the manufacturer and other service providers can communicate with the gateway device.

#### **5.4.2 Hardware composition of the example gateway device**

The gateway device implemented in this research consists of a TP/FT-10 Control Module, an 8052 architecture microcontroller (AT89C52ED2), a WIZnet IIM7010A network module, and other electronic components. Figure 5-4 is a block diagram of the gateway device employed in this research.

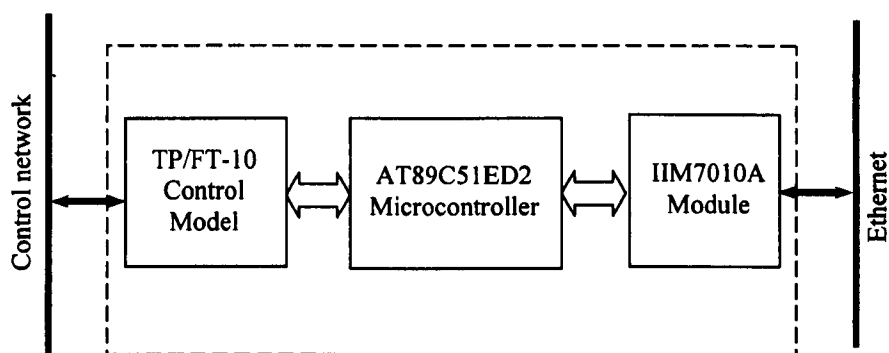


Figure 5-4 Block diagram of Gateway device used in the research

The IIM7010A is a network module that includes a W3100A, Ethernet PHY (RTL8201BL), MAG-JACK (RJ45 with X'FMR) with other glue logics. The W3100 is an LSI of hardware protocol stack that provides an easy, low-cost solution for high-speed Internet connectivity for digital devices by allowing simple installation of TCP/IP stack in the hardware. The W3100 contains TCP/IP Protocol Stacks such as TCP, UDP, IP, ARP and ICMP protocols, as well as Ethernet protocols such as Data Link Control and MAC protocol. Therefore, the IIM7010A is an ideal option for users who want to develop their Internet enabling systems rapidly.

The TP/FT-10 Control Module is responsible for interfacing the gateway device with the control network, and parsing out (or packing up) the information that transmitted over the control network messages.

The AT89C51ED2 microcontroller is responsible for control of the IIM7010A Ethernet module including setting up the related control registers of the W3100 chip. Before a message sending out, for example, the microcontroller sets up the destination IP address, destination port number, and transfer the data for the message into Send Data Buffer of IIM7010A. When a message is received, the microcontroller read out the date held in the Received Data Buffer of IIM7010A, the IP address and port number of the sender. The

microcontroller is also responsible for the communication between the TP/FT-10 Control Module and the IIM7010A module, and management of the Control System Information Database.

# Chapter 6 Mathematical Analysis of the Pneumatic System of Components-based Integrated Pneumatic Drives

## 6.1 Introduction

Mathematical analyses play an important role in modern control system engineering. Mathematical analyses are the understanding of how the process operates. With the analyses in hand, designer can proceed to use the analyses to predict the impact of various design choices. The major objectives of mathematical analyses of control systems are producing the desired transient response, reducing steady-state error, achieving stability, and some other design concerns, such as cost and the sensitivity of the system performance to changes in parameters. Through the analysis of existing transient response, for example, we could know the effect of system parameters adjustment on yielding a desired transient response.

This chapter presents the mathematical analyses of the CIPDs. The analyses start from system modelling which is developed in both frequency domain and time main. The effect of system parameters on the transient response, the system steady-state error, and system stability are discussed according to the system modelling. The analyses also include the estimation of load steady speed and hardware selection considerations.

## 6.2 Basic Assumptions

To perform rational mathematical analyses, a number of basic assumptions are made about the valve, actuator, and system operating conditions as follows:

- Supply pressure  $P_s$  and supply temperature  $T_s$  are constants.
- Heat transfer between working gas (air was used in this research) and its environment is negligible. Temperature of the gas flowing between the valve and the actuator is at all times equal to supply temperature,  $T_s$ . That means that the inherent effect of temperature variation on system dynamics is considered to be negligible when compared with the effect of changes of various other state variables.
- The working fluid is assumed to be an ideal gas so that the general gas laws can be applied.
- Each port of the control valves is assumed to act like a standard orifice, so that standard orifice theory can be applied.
- The leakage between the valve and the actuator, and among other sources is neglected. (In practical situations internal or external leakage in the system should be minimized or avoided).
- Control valve constants  $C_d$  and  $C_o$  do not vary with valve opening.
- Steady state motion of the drive is attainable, e.g. a constant terminal velocity can be reached.
- When a steady state motion occurs, it is assumed that negligible variation occurs in actuator chamber pressures.
- Other additional assumptions stated locally in each section.

## 6.3 Basic governing equations and their linearization

The analysis of pneumatic system usually requires individual mathematical descriptions of the three component dynamics, namely: (1) the flow relationships of the control valves; (2) the dynamic flow relationships within the actuator control chambers; and (3) the load dynamics. They are individually

presented as follows.

### 6.3.1 The flow relationships of the control valves

The diagram of a linear pneumatic actuator is depicted in Figure 6-1, in which the flow paths are shown. According to the standard orifice theory, the mass flow rate across the two control ports of the control valve can be regarded as a function of the valve spool displacement and the chamber pressures, which can be expressed as Equations (6-1), (6-2), and (6-3).

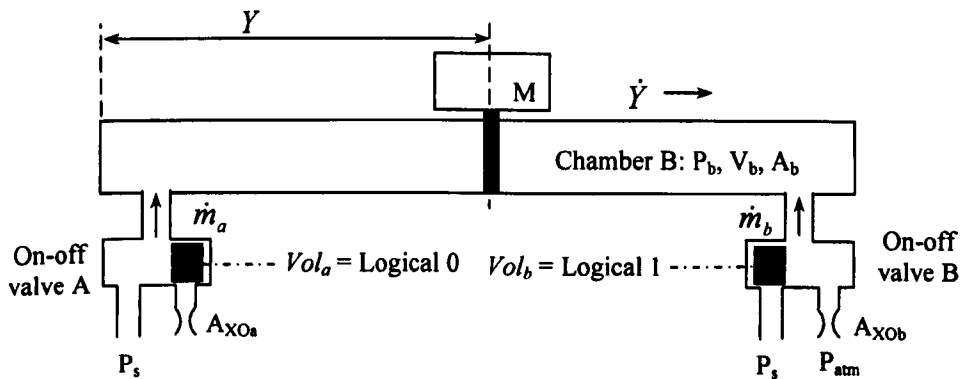


Figure 6-1 Schematic diagram of the system when the Chamber B is driving chamber

$$\dot{m}_a = \begin{cases} C_d C_0 w X f_{ps}(P_r) & Vol_a = Logical 0 \\ C_d C_0 A_{XOa} f_{pa}(P_r) & Vol_a = Logical 1 \end{cases} \quad (6-1)$$

$$-\dot{m}_b = \begin{cases} C_d C_0 w X f_{ps}(P_r) & Vol_b = Logical 0 \\ C_d C_0 A_{XOb} f_{pb}(P_r) & Vol_b = Logical 1 \end{cases} \quad (6-2)$$

where

$$f_{ps,pa,pb}(P_r) = \frac{P_u}{\sqrt{T_s}} \begin{cases} 1, & \frac{P_{atm}}{P_u} \leq P_r \leq C_r \\ C_k [P_r^{2/r} - P_r^{(r+1)/r}]^{\frac{1}{2}}, & C_r < P_r < 1 \end{cases} \quad (6-3)$$

with

$$P_r = P_d / P_u$$

For air:

$$r = 1.4,$$

$$C_d = 0.82,$$

$$C_k = \sqrt{\frac{2}{r-1} \left(\frac{r+1}{2}\right)^{\frac{r+1}{r-1}}} = 3.864,$$

$$C_r = \left(\frac{2}{r+1}\right)^{\frac{r}{r-1}} = 0.528$$

$$C_0 = \sqrt{\frac{r}{R((r+1)/2)^{(r+1)/(r-1)}}} = 0.04$$

Where

$a, b$ : subscripts for Chamber A and Chamber B respectively

$A_{xOa,b}$ : exhaust orifice area of Chamber A and Chamber B ( $m^2$ )

$C_d$ : orifice-discharge coefficient

$m$ : mass of gas (g)

$\dot{m}_{a,b}$ : air flow rate of Chamber A and Chamber B (g/s)

$P_d$ : down stream pressure (bar)

$P_u$ : up stream pressure (bar)

$r$ : ratio of specific heats

$R$ : universal gas constant ( $\frac{J}{Kg \cdot K}$ )

$T_s$ : gas supply temperature (K)



$Vol_{a,b}$ : logical on-off valve control signal (Logical 0 is the voltage for “off” state, Logical 1 is the voltage for “on” state)

$w$ : port width (m)

$X$ : spool displacement of on-off valve (m)

$\dot{Y}$ : load velocity (m/s)

For CIDPs, the motion control of the load is achieved by releasing the compressed air to atmosphere; hence the condition that  $\frac{P_{atm}}{P_u} \leq P_r \leq C_r$  in Equation 6-3 is always true. Therefore, if the Chamber B is the driving chamber, the Equation (6-2) becomes:

$$-\dot{m}_b = C_d C_o A_{xOb} \frac{P_s}{\sqrt{T_s}} \quad (6-4)$$

According to the relationship between on-off valve state and control signal voltage, the following equation exist because that the exhaust air is controlled by the state of the control valve (“on” state or “off” state):

$$A_{xO} = \begin{cases} C_{ov} Vol, & t > 0 \\ 0, & t \leq 0 \end{cases} \quad (6-5)$$

where:

$C_{ov}$ : exhaust orifice area/control signal voltage coefficient

$Vol$ : valve control signal voltage (V)

Substitute Equation (6-5) into Equation (6-4), the following equation can be obtained supposing the Chamber B is the driving chamber:

$$-\dot{m}_b = \frac{C_d C_0 C_{ov} P_s}{\sqrt{T_s}} Vol_b \quad (6-6)$$

### 6.3.2 Dynamic flow relationship within the actuator chambers

When the changes in each chamber occur adiabatically (e.g. the rate of heat exchange through the system boundary is negligible), the relationship between the flow rates and the change of both pressure and volume in the actuator chambers have the following forms (Shearer, 1956; Zhang, 1999).

$$\dot{m}_a = \frac{A_a P_a}{RT_s} \dot{Y} + \frac{V_a}{rRT_s} \dot{P}_a \quad (6-7)$$

$$\dot{m}_b = -\frac{A_b P_b}{RT_s} \dot{Y} + \frac{V_b}{rRT_s} \dot{P}_b \quad (6-8)$$

with  $V_a = A_a Y$ ,  $V_b = A_b (l - Y)$

where

$A_{a,b}$ : piston area of Chamber A and B ( $m^2$ )

$l$ : length of stroke (m)

$\dot{m}_{a,b}$ : air flow rate of Chamber A and Chamber B (g/s)

$P_{a,b}$ : chamber pressure of Chamber A and B (bar)

$r$ : ratio of specific heats

$R$ : universal gas constant ( $\frac{J}{Kg K}$ )

$T_s$ : supply temperature

$V_{a,b}$ : volume of Chamber A and B ( $m^3$ )

$Y$ : load position (m)

$\dot{Y}$ : load velocity (m/s)

When only small perturbations from some initial equilibrium points are considered. Equations (6-7) and (6-8) can be written in linearized form as:

$$\Delta \dot{m}_a = \frac{A_a P_{ai}}{RT_s} \Delta \dot{Y} + \frac{V_{ai}}{rRT_s} \Delta \dot{P}_a \quad (6-9)$$

$$\Delta \dot{m}_b = -\frac{A_b P_{bi}}{RT_s} \Delta \dot{Y} + \frac{V_{bi}}{rRT_s} \Delta \dot{P}_b \quad (6-10)$$

### 6.3.3 Piston and payload dynamics

The piston and payload (slider mass) dynamics are modelled by using Newton's second law; i.e. the total applied force on the piston is equal to the inertia force of the sliding body plus the frictional force.

The total applied force is equivalent to the chambers' differential pressure times the cross sectional area of the pneumatic cylinder. The frictional force is perhaps the most important nonlinearity that is found on any mechanical system with moving parts. For pneumatic system, the friction mainly arises in the contacts of the piston with the cylinder walls as well as in the linear slide-way and other minor rubbing elements. It is commonly described as linear viscous damping, Coulomb friction and stiction or some combination of them and they are represented by a discontinuity at zero velocity, therefore, attempts are made to linearize significant Coulomb friction or stiction may lead to erroneous predictions of a system's behaviour (Zhang, 1999).

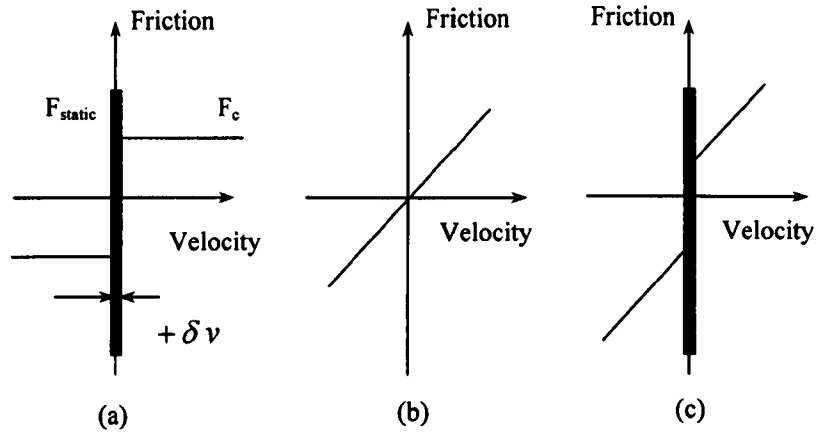


Figure 6-2 Friction model: (a) nonlinear Coulomb friction and stiction; (b) linear viscous friction; (c) combination friction model

By using a linear viscous damping, Coulomb friction and stiction combination friction model (refer to Figure 6-2), Equation (6-11) described the dynamic behaviour of the system:

$$(A_a P_a - A_b P_b) - F_f \text{sign}(\dot{Y}) - c_f \dot{Y} = M\ddot{Y} \quad (6-11)$$

$$\text{with } F_f = \begin{cases} F_c & |\dot{Y}| > \delta v \\ F_{static} & |\dot{Y}| \leq \delta v \end{cases} \quad (6-12)$$

where

$c_f$  : viscous damping coefficient ( $\frac{Ns}{m}$ )

$F_f$  : frictional force (N)

$F_{Static}$  : static friction (N)

$\dot{Y}$  : load velocity (m/s)

$\ddot{Y}$  : load acceleration ( $m^2/s$ )

When only small perturbations from some initial equilibrium points are considered. Equation (6-11) can be linearized as:

$$(A_a \Delta P_a - A_b \Delta P_b) - c_f \Delta \dot{Y} = M \Delta \ddot{Y} \quad (6-13)$$

## **6.4 Modelling of open-loop system**

As discussed in Section 4.3.1, there are three motion states in a complete motion process. The three motion states are: moving state of motion, stopping state of motion, and stand by state of motion. For the system modelling purpose, the moving state and the stopping state have different initial conditions. The moving state motion is a motion with zero initial conditions; hence both modelling in frequency domain and in time domain will be carried out in the next sections. However, the stopping state motion is a motion with nonzero initial conditions. For example, the initial position and initial velocity are those remained by the moving state of motion. Therefore, the system modelling for the stopping state will be carried out in the time domain in the next sections.

### **6.4.1 The open-loop transfer function of moving state of motion**

In control theory, transfer functions are commonly used to characterize the input-output relationships of components of system. The applicability of the concept of the transfer function is limited to linear, time-invariant systems. A control system designer can often make a linear approximation to a nonlinear system. Linearization technique is applicable to many nonlinear systems. The process of linearizing nonlinear systems is important, for by linearizing nonlinear equations, it is possible to apply numerous linear analysis methods that will produce information on the behaviour of nonlinear systems.

Pneumatic drives are considered to be highly nonlinear. With an increasing of the nonlinearity or when the operating point gets further away from the

linearization point, the deviation between the linear model's behaviour and the system's behaviour increases significantly and these deviations may invalidate the linearization approach. However, linearization analysis of pneumatic systems are still used by many researchers because the linearization analysis is effective in investigating the stability of control system and valid for dynamic characteristics analysis near the operating point.

Assume that Chamber B is drive chamber (refer to Figure 6-1). According to the structure of the system and initial conditions ( $\dot{m}_{ai} = \dot{m}_{bi} = 0$ ,  $P_{ai} = P_{bi} = P_s$ ,  $\dot{Y}_i = 0$ ), it is known that:

$$P_a = P_s = C_{PS} \quad (6-14)$$

$$\Delta P_a = \Delta P_s = \Delta C_{PS} = 0 \quad (6-15)$$

where  $C_{PS}$  is the pressure of compressed air supply that is a constant.

Substitute Equation (6-15) into Equation (6-13), then the following equation can be obtained:

$$-A_b \Delta P_b - c_f \Delta \dot{Y} = M \Delta \ddot{Y} \quad (6-16)$$

By Laplace Transformation, Equation (6-6) becomes

$$-s m_b(s) = \frac{C_d C_0 C_{ov} P_s}{\sqrt{T_s}} Vol_b(s) \quad (6-17)$$

By Laplace Transformation, Equation (6-10) becomes

$$s^2 m_b(s) = -\frac{A_b P_{bi}}{RT_s} s^2 Y(s) + \frac{V_{bi}}{rRT_s} s^2 P_b(s) \quad (6-18)$$

Combining the Equations (6-17) and (6-18), gives

$$-\frac{C_{ov} C_d C_0 P_s}{\sqrt{T_s}} Vol_b(s) = -\frac{A_b P_s}{RT_s} s Y(s) + \frac{V_{bi}}{rRT_s} s P_b(s) \quad (6-19)$$

which can be rewritten as

$$s P_b(s) = -\frac{rRT_s C_{ov} C_d C_0 P_s}{V_{bi} \sqrt{T_s}} Vol_b(s) + \frac{rA_b P_s}{V_{bi}} s Y(s) \quad (6-20)$$

with  $V_{bi} = A_b Y_i$

By Laplace Transformation, Equation (6-16) becomes

$$-A_b s P_b(s) - c_f s^2 Y(s) = Ms^3 Y(s) \quad (6-21)$$

Substitute Equation (6-20) into Equation (6-21), the open-loop transfer function is obtained as the following:

$$\frac{sY(s)}{Vol_b(s)} = \frac{b_0}{s^2 + 2\zeta\omega_n s + \omega_n^2} \quad (6-22)$$

with

$$2\zeta\omega_n = \frac{c_f}{M} \quad (6-23)$$

$$\omega_n^2 = \frac{rA_b^2 P_s}{MV_{bi}} = \frac{rA_b^2 P_s}{MA_b Y_i} = \frac{rA_b P_s}{MY_i} \quad (6-24)$$

$$b_0 = \frac{rRT_s C_{ov} C_d C_o A_b P_s}{MV_{bi} \sqrt{T_s}} = \frac{rRT_s C_{ov} C_d C_o P_s}{MY_i \sqrt{T_s}} \quad (6-25)$$

where

$\zeta$ : damping ratio

$\omega_n$ : natural frequency

$a, b$ : subscripts for Chamber A and Chamber B respectively

$C_d$ : orifice-discharge coefficient

$M$ : mass of gas (g)

$r$ : ratio of specific heats

$R$ : universal gas constant ( $\frac{J}{Kg \cdot K}$ )

$T_s$ : gas supply temperature (K)

$Vol_b$ : logical on-off valve control signal (Logical 0 is the voltage for “off” state, Logical 1 is the voltage for “on” state)

$Y_i$ : initial position (m)

Based on the linearized model derived above, it is seen that a pneumatic drives with the structure shown in Figure 6-1 can be modelled as a second-order system for velocity regulation.

#### 6.4.2 The state-space representation of moving state of motion

Assume that chamber B is the drive chamber (refer to Figure 6-1), according to the piston control method and Equations (6-6) and (6-8), the following equations can be derived:



$$\dot{P}_a = \dot{P}_s = 0 \quad (6-26)$$

$$\dot{P}_b = \frac{rP_b}{Y} \dot{Y} - \frac{rR\sqrt{T_s}C_dC_0C_{ov}P_b}{A_bY} Vol_b \quad (6-27)$$

Let  $x_1 = Y, x_2 = \dot{Y}, x_3 = P_b$ , from Equations (6-11), (6-12), and (6-27), the dynamics of the cylinder described in state-space presentation are as follows:

$$\dot{x}_1 = x_2 \quad (6-28)$$

$$\dot{x}_2 = \frac{A_a P_s}{M} - \frac{F_f}{M} \text{sign}(x_2) - \frac{c_f}{M} x_2 - \frac{A_b}{M} x_3 \quad (6-29)$$

$$\dot{x}_3 = \frac{rx_3}{x_1} x_2 - \frac{rR\sqrt{T_s}C_dC_0C_{ov}x_3}{A_b x_1} Vol_b \quad (6-30)$$

$$\text{with } F_f = \begin{cases} F_f & x_2 > 0 \\ -F_f & x_2 < 0 \end{cases}$$

### 6.4.3 State-space presentation of the stopping state of motion

For stopping state motion, the system initial conditions are not all zeros (i.e.  $\dot{Y} \neq 0$ ), the initial velocity, for example, is the velocity remained by moving state. Therefore, the dynamics of the cylinder at stopping state motion is only described in the time domain.

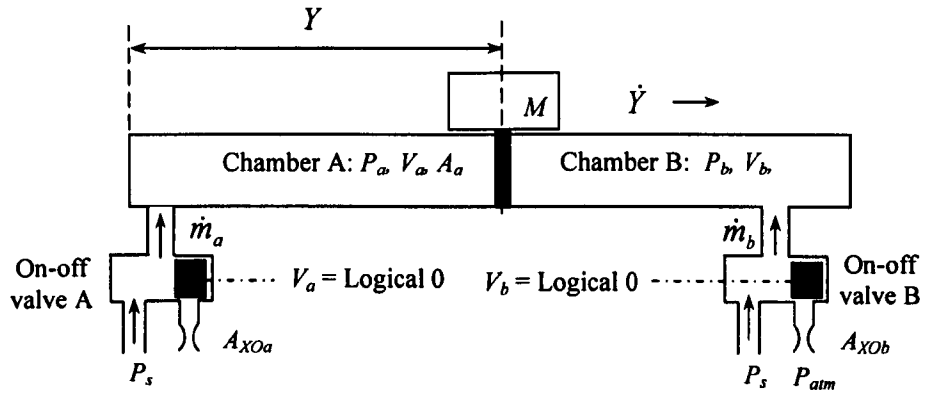


Figure 6-3 Schematic diagram of the system at stopping state of motion

According to Equations (6-2), (6-7) and (6-8), when the control valve (Valve B) is turned from the “On” state to the “Off” state, the following equations can be obtained (Chamber B is driving chamber):

$$\dot{P}_a = \dot{P}_s = 0 \quad (6-31)$$

$$\dot{P}_b = \frac{rRT_s C_d C_0 w X f_{ps} \left( \frac{P_b}{P_s} \right)}{A_b Y} + \frac{r P_b}{Y} \dot{Y} \quad (6-32)$$

Let  $x_1 = Y$ ,  $x_2 = \dot{Y}$ ,  $x_3 = P_b$ , from Equations (6-11), (6-12), (6-32), the state-space presentation of the piston (load) at stopping state motion are as follows:

$$\dot{x}_1 = x_2 \quad (6-33)$$

$$\dot{x}_2 = \frac{A_a P_s}{M} - \frac{F_f}{M} \text{sign}(x_2) - \frac{c_f}{M} x_2 - \frac{A_b}{M} x_3 \quad (6-34)$$

$$\dot{x}_3 = \frac{rRT_s C_d C_0 w X f\left(\frac{x_3}{P_s}\right)}{A_b x_1} + \frac{r x_3}{x_1} x_2 \quad (6-35)$$

#### 6.4.4 State-space presentation of a complete motion process

From Figure 4-5 it can be seen that a complete motion process consists of a moving state of motion and a stopping state of motion. Therefore, state-space presentation of a complete motion process can be obtained using Equations (6-28), (6-29), (6-30), (6-33), (6-34), and (6-35), as follows:

$$\dot{x}_1 = x_2 \quad (6-36)$$

$$\dot{x}_2 = \frac{A_d P_s}{M} - \frac{F_f}{M} \text{sign}(x_2) - \frac{c_f}{M} x_2 - \frac{A_b}{M} x_3 \quad (6-37)$$

$$\dot{x}_3 = \begin{cases} \frac{r x_3}{x_1} x_2 - \frac{r R \sqrt{T_s} C_d C_0 A_{XOb} x_3}{A_b x_1} & \text{When valve is open} \\ \frac{r x_3}{x_1} x_2 + \frac{r R T_s C_d C_0 w X f\left(\frac{x_3}{P_s}\right)}{A_b x_1} & \text{When valve is closed} \end{cases} \quad (6-38)$$

$$\text{with } f\left(\frac{x_3}{P_s}\right) = \frac{P_s C_k}{\sqrt{T}} \left[ \left(\frac{x_3}{P_s}\right)^{2/r} - \left(\frac{x_3}{P_s}\right)^{(r+1)/r} \right]^{\frac{1}{2}}, \quad (\text{for air } r = 1.4)$$

$$\text{and } F_f = \begin{cases} F_f & x_2 > 0 \\ -F_f & x_2 < 0 \end{cases}$$

### 6.5 The system transient-response specifications

Frequently, the performance characteristics of a control system are specified on terms of the transient response to a unit-step input since it is easy to generate and is sufficiently drastic. The transient response of a system to a unit-step input depends on the initial conditions. For convenience in comparing transient responses of various systems, it is a common practice to use the standard initial condition that the system is at rest initially with output and all time derivatives thereof zero. Then the response characteristics can be easily compared.

The damping ratio  $\zeta$  and natural frequency  $\omega_n$  of control systems are two important specifications associated with second-order systems. Other common specifications associated with the system response are Percent overshoot, %OS; Peak time,  $T_p$ ; Settling time,  $T_s$ ; and Rise time,  $T_r$ .

From Equations (6-23) and (6-24), the following two equations can be derived:

$$\omega_n = \sqrt{\frac{rA_b P_s}{MY_i}} \quad (6-39)$$

$$\zeta = \frac{c_f \sqrt{Y_i}}{2\sqrt{rMA_b P_s}} \quad (6-40)$$

From Equations (6-39) and (6-40) it can be seen that the damping ratio  $\zeta$  and natural frequency  $\omega_n$  changes with geometric parameters, load's mass and initial position, and air supply pressure.

## 6.6 Stability analysis of open-loop controlled integrated pneumatic drives

Stability is the most important specification for a system. If a system is unstable, transient response is moot points. A simple criterion, known as Routh-Hurwitz Criterion, is applied to analyse the stability of the CIPDs.

As discussed in Section 4.3, the input signal of the system is a three-states control signal. During the control of the state “10” or “01”, the system is in moving state of motion, thus the stability analysis of the system can be carried out by using the system transfer function of the moving state of motion. During the control of the state “00”, the system can be either on stopping state of motion or in steady state. Thus, the stability of the system at this state is specified by the stopping state of motion. In this section, the stability analysis of the system is separated into two parts. The first part is stability analysis of open-loop system, while second part is stability analysis of closed-loop system.

### 6.6.1 Stability analysis of open-loop system at the moving state of motion

According to the system transfer function presented in Equation (6-22) to Equation (6-25), a Routh table can be generated as one shown in Table 6-1.

Table 6-1 The Routh table of the system at moving state of motion

$S^2$	1	$\frac{rA_b P_s}{MY_i}$
$S^1$	$\frac{c_f}{M}$	0
$S^0$	$\frac{rA_b P_s}{MY_i}$	0

From Table 6-1 it can be seen that there is no sign changes in the first column. According to the Routh-Hurwitz Criterion it is known that there are no roots of the polynomial in the right half-plane. Therefore, the open-loop system at moving state of motion is a stable system for velocity regulation. According to Equation (6-22), it also can be seen that the open-loop system has a pole which is zero, hence the open-loop system at moving state of motion is unstable for positioning regulation.

### 6.6.2 Stability analysis of the stopping state of motion

To simplify the simulation process, one more assumption here is made that when the valve control signal is turned from logical 1 to logical 0 (that means the driving chamber is directly connected to the air supply  $P_s$ ), the pressure in driving chamber can immediately increases to the value of air supply pressure  $P_s$ , in other words, during stopping stage of motion  $\dot{P}_a = \dot{P}_b = 0$ .

Under the assumptions, and according to Equations (6-33), (6-34), and (6-35), the state-space presentation of the stopping state of motion can be re-written as Equations (6-41) and (6-42):

$$\dot{X} = AX + Bu = \begin{bmatrix} 0 & 1 \\ 0 & -\frac{c_f}{M} \end{bmatrix} X + \begin{bmatrix} 0 \\ -1 \end{bmatrix} \left( \frac{F_f}{M} \text{sign}(x_2) \right) \quad (6-41)$$

$$y = CX + Du = [1 \quad 0]X \quad (6-42)$$

Since a system poles and the eigenvalues of a system are the same, the stability requirement of a system represented in state-space dictates that the eigenvalues cannot be in the right half of the s-plane nor be multiple on the  $j\omega$ -axis. We can obtain the eigenvalues from the state-space presentation equations; Equation (6-43) yields the eigenvalues of a system directly.

$$\det (s\mathbf{I} - \mathbf{A}) = 0 \quad (6-43)$$

From Equation (6-41), it is known that:

$$(s\mathbf{I} - \mathbf{A}) = \begin{bmatrix} s & 0 \\ 0 & s \end{bmatrix} - \begin{bmatrix} 0 & 1 \\ 0 & -\frac{c_f}{M} \end{bmatrix} = \begin{bmatrix} s & -1 \\ 0 & s + \frac{c_f}{M} \end{bmatrix} = s^2 + \frac{c_f}{M}s = s \left( s + \frac{c_f}{M} \right) = 0 \quad (6-44)$$

it can be seen that the system at stopping state of motion has two poles: 0 and  $-\frac{c_f}{M}$ , hence, the system at stopping state of motion is stable for velocity regulation, and is unstable for position regulation.

### 6.7 Stability analysis of PD-based three-state closed-loop controlled integrated pneumatic drives

The CIPDs employ a three-state control algorithm that is based on a PD control analogue control algorithm. As discussed in the Section 4.3.3, and shown in Figure 4-11, the PD-based three-state control strategy converts an analogue control signal to a three-state control signal which controls the control valves. The result of the conversion is a control signal either for moving state motion of a direction (“01” or “10”), or for stopping state and stand by state of motion (“00”).

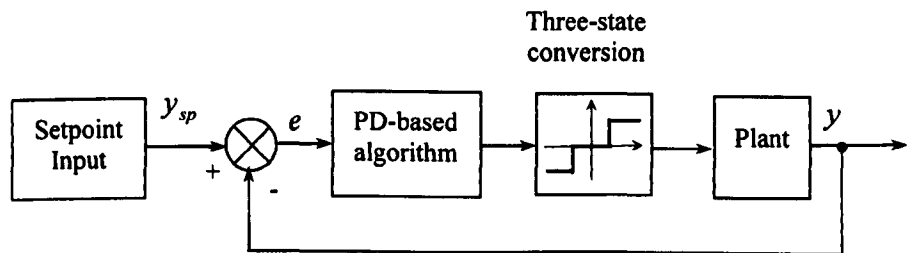


Figure 6-4 Simplified block diagram of CIPD's servo control loop

Figure 6-4 shows a simplified block diagram of servo control loop within a CIPD. It is seen that a closed-loop controlled CIPD is a nonlinear system that has a dead zone.

Lyapunov's direct method is a useful and general approach for studying the stability of nonlinear control systems. The basic philosophy of Lyapunov's direct method is the mathematical extension of a fundamental physical observation: if the total energy of a mechanical system is continuously dissipated, then the system, whether linear or nonlinear, must eventually settle down to an equilibrium point (J. E. Slotine and W. Li, 1991). The total mechanical energy of a system is the sum of its kinetic energy and its potential energy. The kinetic energy exists whenever an object which has mass is in motion with some velocity. The potential energy exists whenever an object which has mass has a position within a force field.

### 6.7.1 Energy variation within a complete motion process

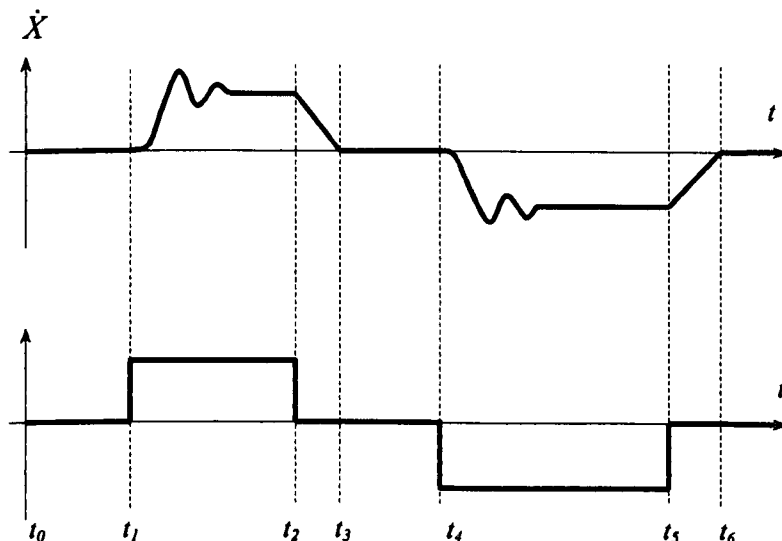


Figure 6-5 The relationship between valve control signal and the load velocity



Figure 6-5 schematically illustrates the relationship between valve control signal and the load velocity. A load positioning control action consists of one or more completed motion processes. Each completed motion process includes a moving state of motion (e.g. from  $t_1$  to  $t_2$ ) and a subsequent stopping state of motion (e.g. from  $t_2$  to  $t_3$ ).

During moving state of motion, the load is continuously receiving energy, due to the continuously discharge of compressed air from the driving chamber. However, when the motion process turned to stopping state of motion, the driving chamber is recharged to the compressed air supply pressure, and the energy of the load is continuously dissipated by the system fractional force. Hence, the energy of load after a complete motion process is:

$$E = E_{MK} - E_{SK} + E_p \quad (6-45)$$

where

$E$  : total load energy of CIPD

$E_{MK}$  : kinetic energy received during moving state of motion

$E_{SK}$  : kinetic energy dissipated during stopping state of motion

$E_p$  : potential energy.

#### **6.7.1.1 The kinetic energy during moving state of motion**

According to the relationship between the valve control signal and the load velocity illustrated in Figure 6-5, the kinetic energy the load obtained during moving state of motion is:

$$\begin{aligned}
 E_{MK} &= \int_{t_{on}}^{t_{off}} F \cdot dx = m \int_{t_{on}}^{t_{off}} d \frac{\dot{X}}{dt} \cdot \dot{X} dt = \frac{1}{2} m \int_{t_{on}}^{t_{off}} \frac{d}{dt} (\dot{X}^2) dt \\
 &= \frac{1}{2} m [\dot{X}(t_{off})^2 - \dot{X}(t_{on})^2]
 \end{aligned}
 \tag{6-46}$$

where

$F$  : force across piston (N)

$E_{MK}$  : kinetic energy obtained during moving state of motion (J)

$m$  : total load mass (Kg)

$t_{on}$  : time of opening control valve for a moving state of motion

$t_{off}$  : time of closing control valve for stopping state of motion

$X$  : load displacement (m)

$\dot{X}$  : load velocity (m/s)

From Equation (6-46), it is known that the growth of kinetic energy during the motion state is dependent to the motion velocity at the time of the control valve turning “on” and turning “off”, respectively. When assuming that the CIPD is a second-order system as described by Equation (6-22), it is known that there exists a maximum kinetic energy ( $E_{MK \max}$ ) that can be obtained during the moving state of motion, due to the velocity property of a second order system that has a maximum value.

### 6.7.1.2 The maximum dissipation of load kinetic energy during the stopping state of motion

The maximum dissipation of the load kinetic energy during stopping state of motion can be described as the following:

$$E_{SK \max} = \int_{t_{off}}^{t_{on}} F dx = \int_{t_{off}}^{t_{on}} F \dot{X} dt = \int_{t_{off}}^{t_{on}} m \ddot{X} \dot{X} dt
 \tag{6-47}$$

where

$E_{SK \max}$  : maximum kinetic energy dissipation during stopping state of motion (J)

$F$  : force difference across the piston (N)

$\dot{X}$  : load velocity (m/s)

$\ddot{X}$  : load acceleration (m<sup>2</sup>/s)

$t_{on}$  : time of opening control valve after stopping state of motion

$t_{off}$  : time of closing control valve after moving state of motion

According to the state-space presentation in Equation (6-35), the Equation (6-47) can be written as Equation (6-48), assuming that when stopping state of motion started, the driving chamber pressure is re-charged to the supply pressure ( $P_s$ ) immediately.

$$\begin{aligned}
 E_{SK \max} &= \int_{t_{off}}^{t_{on}} (F_f \text{sign}(\dot{X}) + c_f \dot{X}) \dot{X} dt \\
 &= F_f \int_{t_{off}}^{t_{on}} \dot{X} dt + c_f \int_{t_{off}}^{t_{on}} \dot{X}^2 dt
 \end{aligned}
 \tag{6-48}$$

It can be seen that the maximum kinetic energy dissipation during the stopping state of motion is dependent to the period of the control valve staying at the “closed” state ( $t_{on} - t_{off}$ ).

### 6.7.1.3 Potential energy

An object can store energy as the result of its position within a force field. For most application, CIPDs are only associated with gravitational potential energy. Gravitational potential energy is the energy stored in an object as the result of its vertical position.

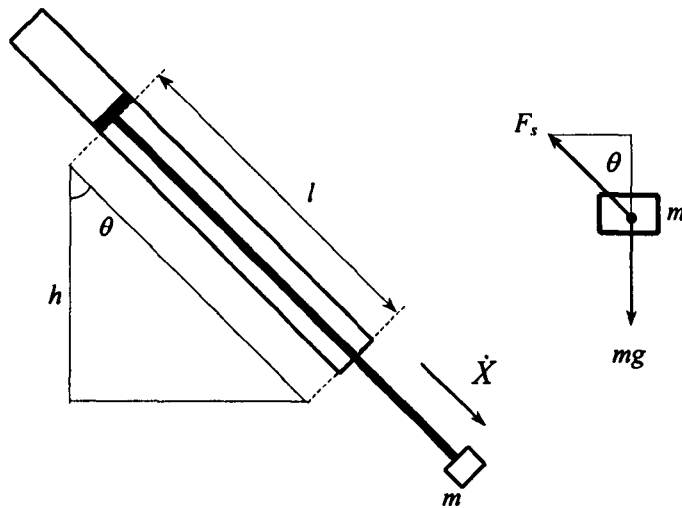


Figure 6-6 Illustration of potential energy of CIPD

According to Figure 6-6, the potential energy for a CIPD's load can be described as the following:

$$E_p = mgh = mgl \cos \theta \quad (6-49)$$

where

$E_p$  : potential energy (J)

$l$  : distance of piston to the end of cylinder (m)

$\theta$  : angle of the cylinder to its vertical position

$m$  : total mass of load (including rod mass) (Kg)

$g$  : gravitation acceleration

Theoretically, when a CIPD is horizontally installed, the potential energy does not make contribution to the system. In practice, when gravity of load cannot overcome the static friction of system, that is  $mg \leq F_s \cos \theta$ , then the potential energy can be ignored.

### 6.7.2 Stability analysis and Simulink verification

From above discussion, the variation of kinetic energy is dependent to the periods of control valves staying at “on” state and “off” state. According to PD analogue control algorithm and the three-state control signal generation theory, it can be seen that after a CIPD is physically setup, there are factors that significantly affect the output state of the three-state control signal. These two factors are:

- The gains of proportion and derivative action of PD control algorithm;
- The Region of Acceptable Error (RAE).

#### 6.7.2.1 Simulink model composition of closed-loop control system

To verify the stability analysis result presented in the next subsections, Simulink simulations have been conducted.

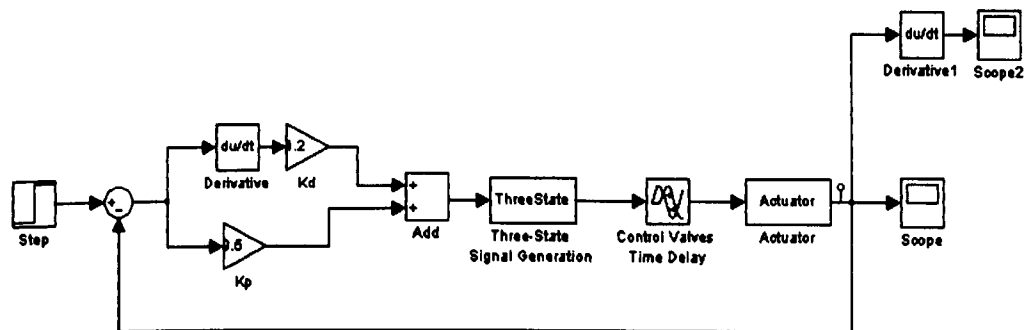


Figure 6-7 Composition of closed-loop control system Simulink model

Figure 6-7 shows the composition of closed-loop control system Simulink model which involved two S-Functions written in C language. The first S-Function is ThreeState which convert the PD control algorithm result to a three-state control signal. The second S-Function is Actuator which simulate the performance of a pneumatic cylinder using the mathematical models obtained in Section 6.4.4. A time delay block has been inserted between the two S-

Functions tow simulate the control valves time delay.

### 6.7.2.2 Stability analysis

The analysis stability analysis can be carried out according to the following different situations:

- 1). When  $E_{MK} - E_{SK_{max}} \leq 0$ , and  $E_p = 0$  or can be ignored:

This means that the motion controller will generates a long period for “00” control signal due to low PD gains and a large RAE. Meanwhile, the energy of load can be dissipated during the first stopping state of motion. Therefore, the system is a Lyapunov stable system. Under this situation, the load can be moved to the target with an acceptable error by opening the corresponding control valve only once. Figure 6-8 and Figure 6-9 illustrate the simulation results of velocity profile and positioning profile, respectively, when the closed-loop control CIPD is a stable system.

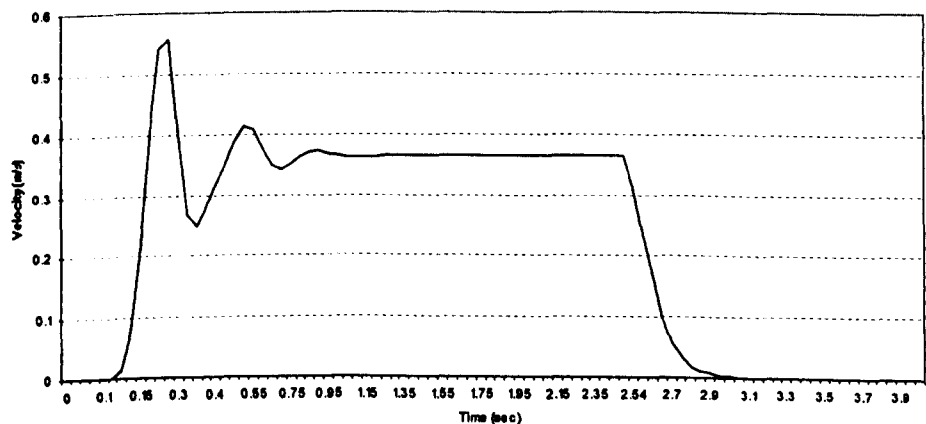


Figure 6-8 Simulation result: velocity profile when the closed-loop control CIPD is a stable system

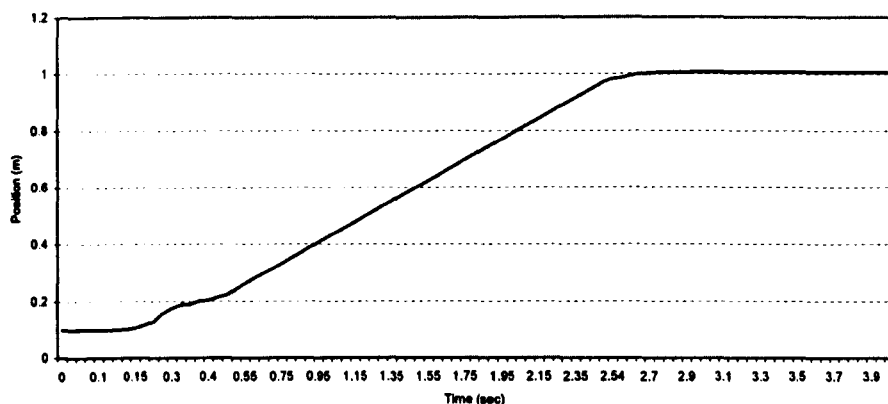


Figure 6-9 Simulation result: Positioning profile when the closed-loop control CIPD is a stable system

2). When  $E_{MK} - E_{SK\max} > 0$  in first complete motion process,

$$\frac{d(E_{MK} - E_{SK\max})}{dt} < 0 \text{ in subsequent motion processes, and } E_p = 0 \text{ or can be}$$

ignored:

This means that, due to relative high PD gains or relative small RAE, the motion controller generates a “00” with a period which is too sort to dissipate the load energy in first stopping state of motion, and a positioning overshoot occurred. Hence the controller will generate a control signal for moving state of motion to opposite direction. The motion controller will repeat the generation of opposite direction of motion if overshoot occurred again. However, the load energy can be dissipated eventually after a number of stopping state of motion between the opposite direction of motion. Therefore, under this situation the system is a Lyapunov asymptotically stable system. Figure 6-10 and Figure 6-11 illustrate the simulation results of velocity profile and positioning profile,

respectively, when the closed-loop control CIPD is an asymptotically stable system.

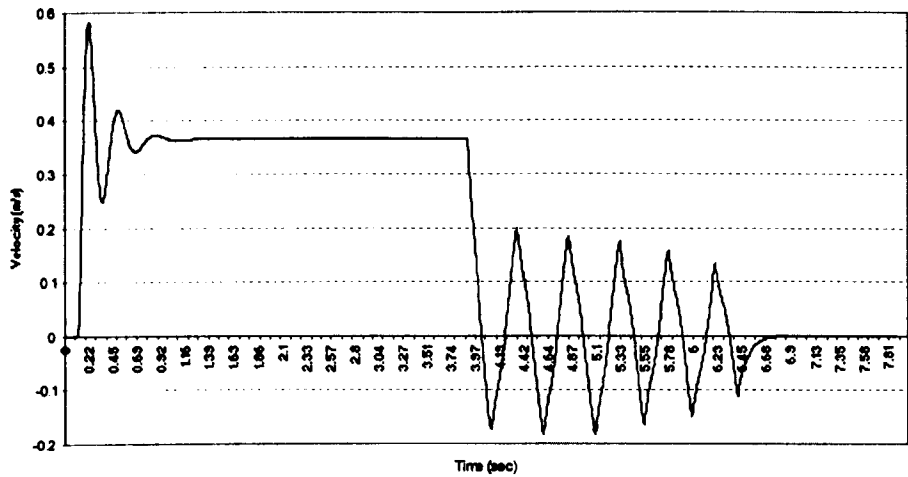


Figure 6-10 Simulation result: velocity profile when the closed-loop control CIPD is an asymptotically stable system

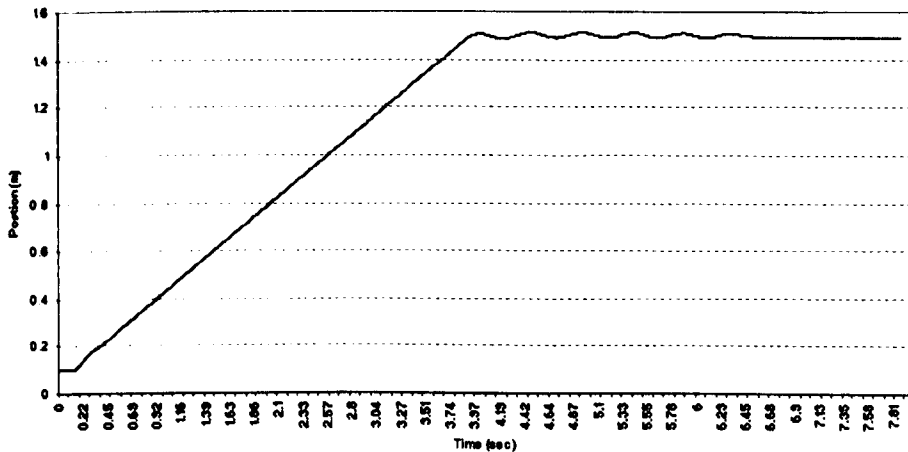


Figure 6-11 Simulation result: positioning profile when the closed-loop control CIPD is an asymptotically stable system



- 3). When  $E_{MK} - E_{SK_{max}} > 0$  in first complete motion process,  
 $\frac{d(E_{MK} - E_{SK_{max}})}{dt} \geq 0$  in subsequent motion processes, or when  $E_p \neq 0$ :

This means that, due to high PD gains and a small RAE, the motion controller generates a “00” with a period which is too sort to dissipate the load energy in stopping state of motion between repeated opposite direction of motion, and positioning overshoot always occurred. Hence the controller will repeatedly generate a control signal of for an opposite direction motion. However, due to the existence of  $E_{MK_{max}}$  and  $E_{SK_{max}}$ , the term  $\frac{d(E_{MK} - E_{SK_{max}})}{dt}$  will be zero after a time. Hence, the load will be oscillating around the target position with bounded positioning overshoot. Figure 6-12 and Figure 6-13 illustrate the simulation results of velocity profile and positioning profile, respectively, when the closed-loop control CIPD is an unstable system.

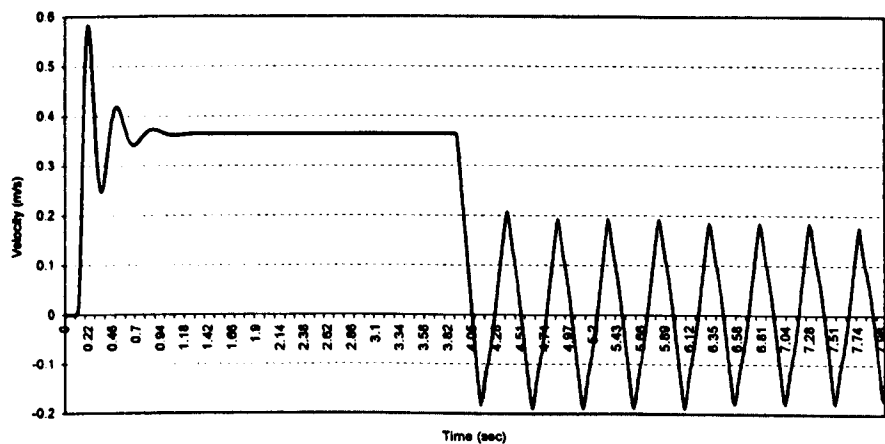


Figure 6-12 Simulation result: velocity profile when the closed-loop control CIPD is an unstable system

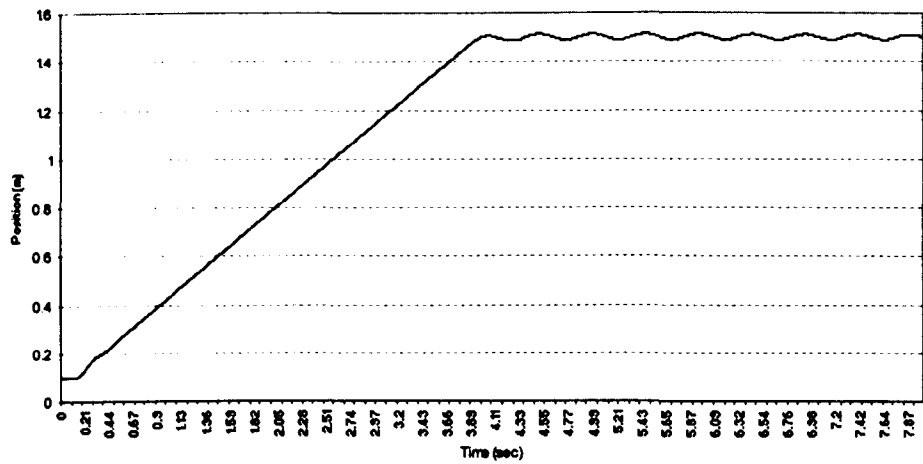


Figure 6-13 Simulation result: positioning profile when the closed-loop control CIPD is an unstable system

### 6.8 Determination of the non-driving chamber pressure

According to the motion control strategy of CIPDs described in Section 4.2, the driving pressure should be close to the supply pressure as much as possible. If subsonic flow occurs at the entry port, then Equation (6-50) can be applied for estimating the steady state pressure of the driving chamber ( $P_u$  and Weston, 1990) assuming that Chamber B is driving chamber.

$$P_o = P_s \left[ \frac{2}{\left(1 + 4 / N_o^2\right)^{1/2} + 1} \right]^{k/(k-1)} \quad (6-50)$$

with

$$N_a = C_k \frac{A_b C_{da} w_a X_a}{A_a C_{db} w_b X_b} \sqrt{\frac{T_a^2}{T_b T_s}} \quad (6-51)$$

where

$$C_k : \text{Constant } C_k = \sqrt{\frac{2}{k-1} \left( \frac{k+1}{2} \right)^{(k+1)/(k-1)}} = 3.864$$

To simplify the analysis, assume that the effect area of piston is equal, and then Equation (6-51) becomes:

$$N_a = C_k \frac{C_{da} w_a X_a}{C_{db} w_b X_b} \quad (6-52)$$

According to the Equations (6-50), (6-51) and (6-52), to achieve the condition that the non-driving chamber pressure ( $P_a$ ) close to the supply pressure ( $P_s$ ) as much as possible,  $N_a$  should approach infinitely large. That means the area of entry port ( $w_a X_a$ ) should infinitely larger than the area of exhaust port ( $w_b X_b$ ).

Figure 6-14 shows the relationship between the ratio of inlet-outlet port area and the ratio of chamber pressure-supply pressure. It can be seen that when the inlet orifice is four times larger than the outlet orifice, the pressure of driving chamber reaches 99.9% of supply pressure. This means that all of orifices of pneumatic equipment / parts in air supply line should be four times or more larger than the orifice of air-flow rate regulator at outlet port (e.g. FR<sub>B</sub>).

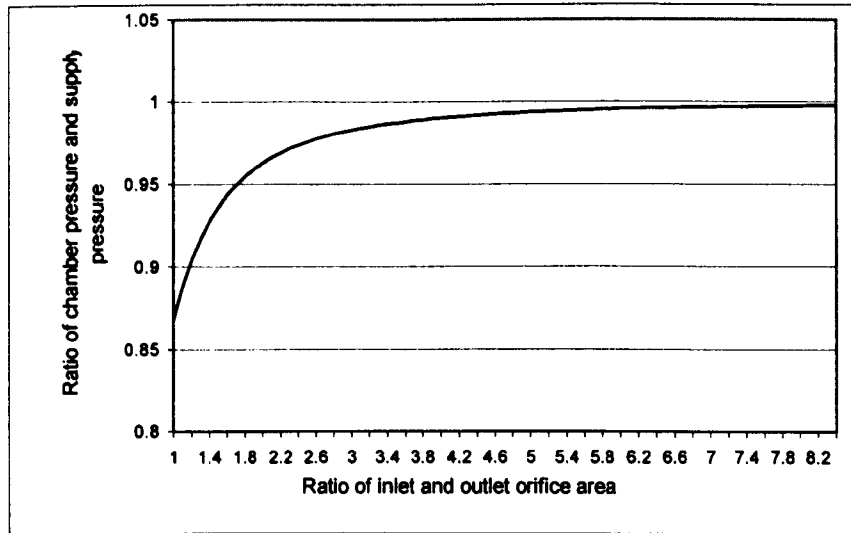


Figure 6-14 The relationship between ratio of chamber pressure-supply pressures and ratio of inlet-outlet orifice area

### 6.9 Effect of the exhaust orifice size on load velocity response

The mathematical analysis in Section 6.4.1 shows that the pneumatic manipulating system of CIPDs can be simulated as a second order system for velocity regulation. The transfer function described in Equation (6-22) can be re-written as:

$$\frac{sY(s)}{Vol_b(s)} = K_v \left( \frac{\omega_n^2}{s^2 + 2\zeta\omega_n s + \omega_n^2} \right) \quad (6-53)$$

with

$$2\zeta\omega_n = \frac{c_f}{M} \quad (6-54)$$

$$\omega_n^2 = \frac{rA_b^2 P_s}{MV_{b_i}} = \frac{rA_b^2 P_s}{MA_b Y_i} = \frac{rA_b P_s}{MY_i} \quad (6-55)$$

$$K_v = (R\sqrt{T_s} C_0 C_d) \frac{C_{ov}}{A_b} \quad (6-56)$$

$$C_{ov} = \frac{A_e}{Vol_b} \quad (6-57)$$

where

$A_b$  piston area of Chamber B

$A_e$ : exhaust orifice area

$C_d$ : orifice-discharge coefficient

$M$ : mass of gas (g)

$r$ : ratio of specific heats

$R$ : universal gas constant ( $\frac{J/Kg}{K}$ )

$T_s$ : gas supply temperature (K)

$Vol_b$ : logical on-off valve control signal (Logical 0 is the voltage for “off” state, Logical 1 is the voltage for “on” state)

$Y_i$ : initial position (m)

If use logic “1” to present the valve control signal voltage  $Vol_b$ , then the value of  $C_{ov}$  equals to the area of the exhaust orifice  $A_e$ . Hence,

$$K_v = (R\sqrt{T_s} C_0 C_d) \frac{A_e}{A_b} \quad (6-58)$$

From Equation (6-56) it can be seen that, the amplitude of velocity profile of the CIPDs is determined by  $K_v$ , which is defined as Velocity Gain in this research. The Velocity Gain  $K_v$  is largely determined by the effective area ratio of exhaust orifice and the piston in exhaust chamber.

# Chapter 7 Experimental System Setup

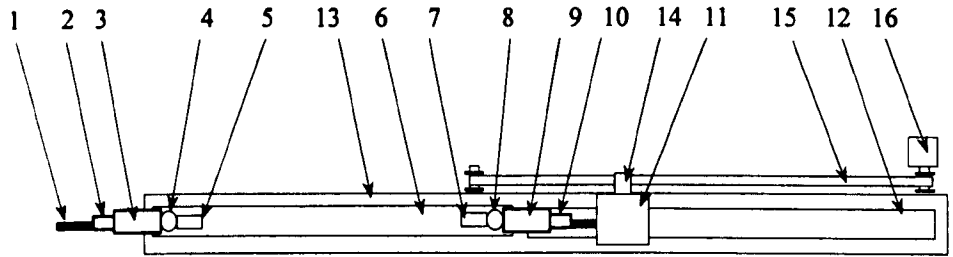
## 7.1 Introduction

Three experimental systems have been constructed during the research for different experimental study purposes. The first experimental system, referred as ES-I, is the experimental study system for verifying mathematical modelling of the CIPDs; The second experimental study system, referred as ES-II, has been employed for evaluation of high-speed motion control of the CIPDs; The third experimental study system, referred as ES-III, has been employed for demonstration of distributed control system employing two CIPDs. This chapter presents details of the three experimental study systems setup.

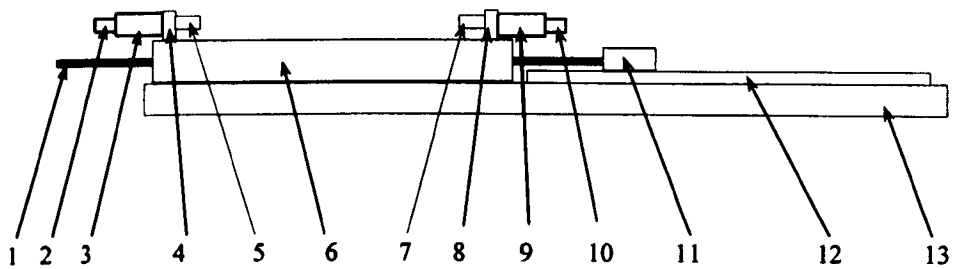
## 7.2 Setup of ES-I (Mathematical Analysis Verification System)

### 7.2.1 Structure of the ES-I

For convenience of verifying mathematical analysis of the CIPDs presented in Chapter 6, a conventional symmetric pneumatic cylinder has been employed to set up this experimental system. The cylinder was chosen because of its hardware properties, such as static friction, viscous damping coefficient, and weight of the rod, could generate an identifiable velocity profile within the motion region of the cylinder. Also the equivalent piston areas make the mathematical analysis verification easier. The details of some properties measurements are presented in Section 8.2.



Top view



Front

- |                          |                                 |
|--------------------------|---------------------------------|
| 1. Rod of cylinder       | 2. Flow regulator A             |
| 3. On-off valve A        | 4. Two-way port A               |
| 5. Pressure transducer A | 6. Cylinder                     |
| 7. Pressure transducer B | 8. Two-way port B               |
| 9. On-off valve B        | 10. Flow regulator B            |
| 11. Load                 | 12. Slide guide                 |
| 13. Rack of system       | 14. Connector for load and belt |
| 15. Tooth belt           | 16. Encoder                     |

Figure 7-1 Simplified construction views of the EP-I



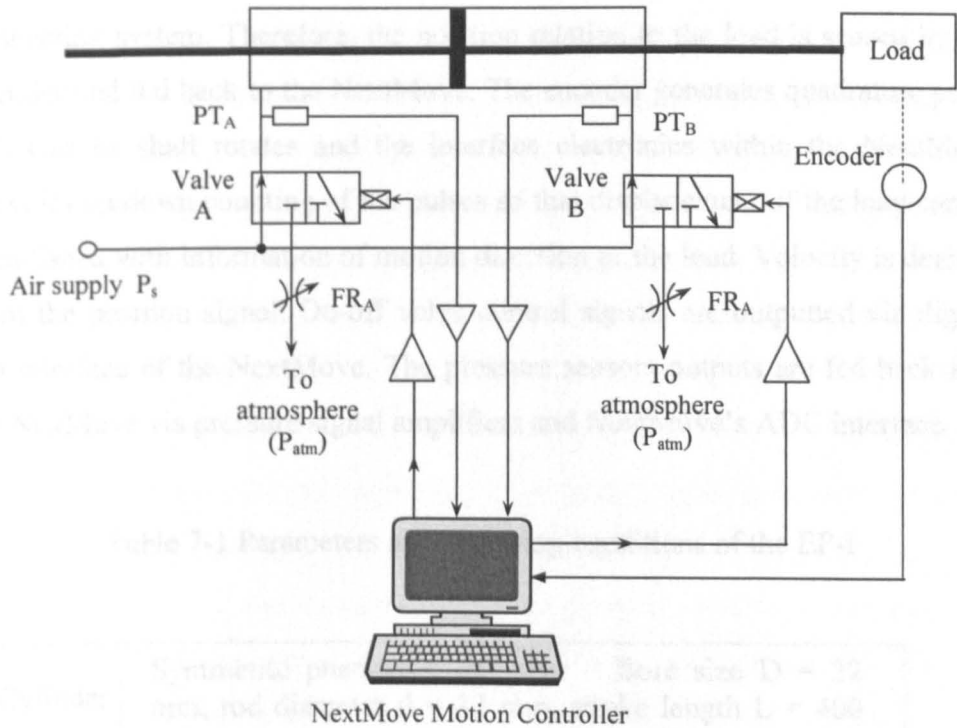


Figure 7-2 The block diagram of the closed loop control system

Simplified construction diagram of the ES-I are depicted in Figure 7-1. Other components the system employs are:

- Two pressure transducers ( $PT_A$ ,  $PT_B$ ) with amplifiers;
- An incremental/decremental encoder;
- Two pneumatic valves ( $V_A$ ,  $V_B$ ) and their amplifiers;
- Two airflow rate regulators ( $FR_A$ ,  $FR_B$ );
- A computer with a NextMove Digital Motion Controller;
- Other mechanisms such as: payload, slide guide, system rack.

A block diagram of the closed loop control system is shown in Figure 7-2.

In the ES-I, the signal processing and control algorithm implementation are accomplished by the NextMove Digital Motion Controller (it is

referred as NextMove through rest of this thesis). Linear displacement of the load is converted to rotational motion of the encoder shaft via the tooth belt connecting system. Therefore, the position relating to the load is sensed by the encoder and fed back to the NextMove. The encoder generates quadrature pulse trains as its shaft rotates and the interface electronics within the NextMove provides up/down counting of the pulses so that displacement of the load can be established with information of motion direction of the load. Velocity is derived from the position signal. On-off valve control signals are outputted via digital I/O interface of the NextMove. The pressure sensors outputs are fed back into the NextMove via pressure signal amplifiers and NextMove's ADC interface.

Table 7-1 Parameters and operating conditions of the EP-I

Cylinder	Symmetric pneumatic cylinder: Bore size $D = 32$ mm, rod diameter $d = 12$ mm, stroke length $L = 400$ mm
Control valves (1)	SMC <sup>®</sup> VF3150 5-Port Pilot on-off valves; Response time: 20ms or less (at 0.5MPa); Max. operating cycle: 10 Hz; On voltage: 24V DC; Off voltage: 0V DC. Power consumption: 1.8W.
Control valves (2)	FESTO <sup>®</sup> MPYE-5-1/8HF-010B Proportional valves; Part number: 151693; Standard nominal flow rate: 700 liter/min ( $\pm 10\%$ ); Bandwidth: 100 Hz; Operating voltage: 24V DC; Setpoint voltage: 0 – 10 V DC, Mid position at 5V; Connector: 1/8".
Pressure sensors	RS 256-736; Maximum operating pressure: 10 Bar; Operating voltage 10 V; Output: 0 – 100 mV.
Encoder	BRITISH ENCODER; Type 755A; No.6A0428; PPR = 1500; Operating voltage: 5V.
Supply pressure	7 Bar
Load	4.5 Kg (including the rod)

The computer is used to record experimental data established by the NextMove. More details about the NextMove are presented in next section. The main parameters and characteristics of other components, and the operating

conditions of the ES-I are listed in Table 7-1.

To verify the effect of the bandwidth of the control valves on the positioning accuracy, two pairs of different pneumatic valves are used during the experimental study. The first pair of valves is SMC<sup>®</sup> VF3150 5-Port on-off valves, while the second pair of valves is FESTO<sup>®</sup> MPYE-5-1/8HF-010B Proportional Valves. Both sets of valves are configured as 3-Port on-off valves. The difference to be concerned between these two sets of valves is their bandwidth which can be found in Table 7-1.

The symbol of the FESTO<sup>®</sup> MPYE-5-1/8HF-010B valve is shown in Figure 7-3. Figure 7-4 schematically shows the flow characteristic of FESTO<sup>®</sup> MPYE-5-1/8HF-010B valve. For common use, when input signal voltage rises from 0V to 5V, the flow rate reduces at outlet 2. When input signal voltage rises from 5V to 10V, the flow rate rises at outlet 4, but there exists a dead zone around the centre position.

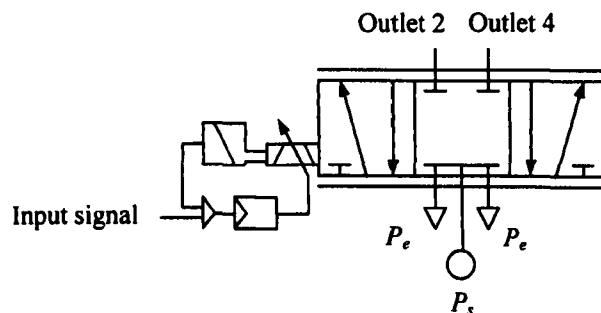


Figure 7-3 The symbol of FESTO<sup>®</sup> MPYE-5-1/8HF-010B valve

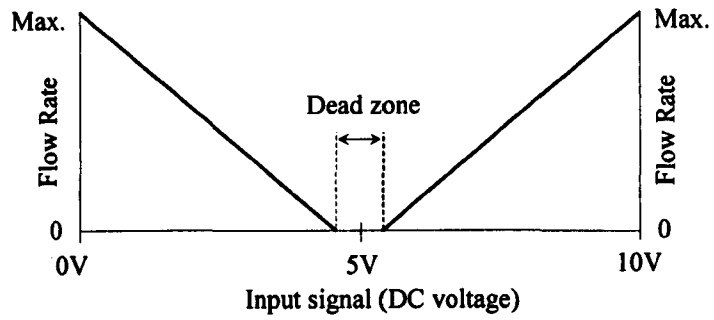


Figure 7-4 The flow characteristic of FESTO® MPYE-5-1/8HF-010B valve

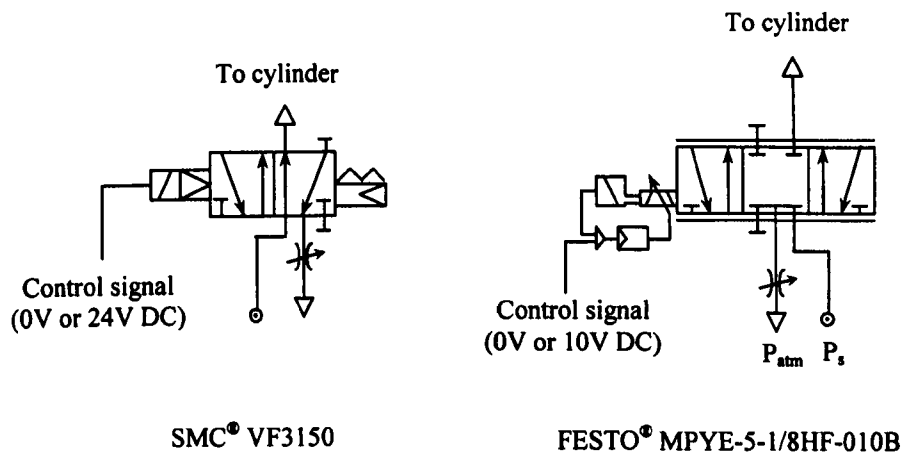


Figure 7-5 Configuration of pneumatic control valves for EP-I

The configurations of the control valves used in the ES-I are illustrated in Figure 7-5

## 7.2.2 Specifications and characteristics of the ES-I

The specifications and characteristics of some components employed by the ES-I are briefly discussed in the follows:

### 7.2.2.1 *NextMove Digital Motion Controller*

The NextMove Digital Motion Controller is an advanced multi-axis motion controller developed by Optimised Control Ltd. and aiming at demanding motion control applications for both open loop and closed loop system. The NextMove provides high speed floating point digital signal processing ability. It has four axes of servo control with 12 bit analogue outputs and incremental encoder feedback (250, 500 or 1000  $\mu$ s servo loop update rate), four axes of stepper motor control. 16-bit ISA bus interface via 2K byte DPR (Dual Port RAM) for high-speed communications with host computer. 512K byte static RAM, 12 M baud serial port for high speed card to card data transfer and four 12 bit analogue differential inputs.

The NextMove uses a Texas Instruments TMS320c31 $\mu$  controller as it's processing unit. There are several levels of interrupt and background tasks which normally calls the standard function in NextMove. These functions control the profiler and setting parameters used in the control algorithm. The user supplies demands to the profiler in User Units (UU) which are floating point values. There is a standard format for the function which the user can call to set and get parameters.

The programming language could be nmMint (NextMove motion interpreter), HPGL or C. nmMint is a structured form of BASIC, specially designed for motion control applications, and has been written to allow users to run a wide range of applications, such as profile generation, servo loop PID motion control and open loop control. C application programs can be downloaded into NextMove Controller to accomplish more complex applications. Figure 7-6 shows a block diagram of NextMove Digital Motion Controller configuration and how it is interfaced to the ES-I and data analysing host.

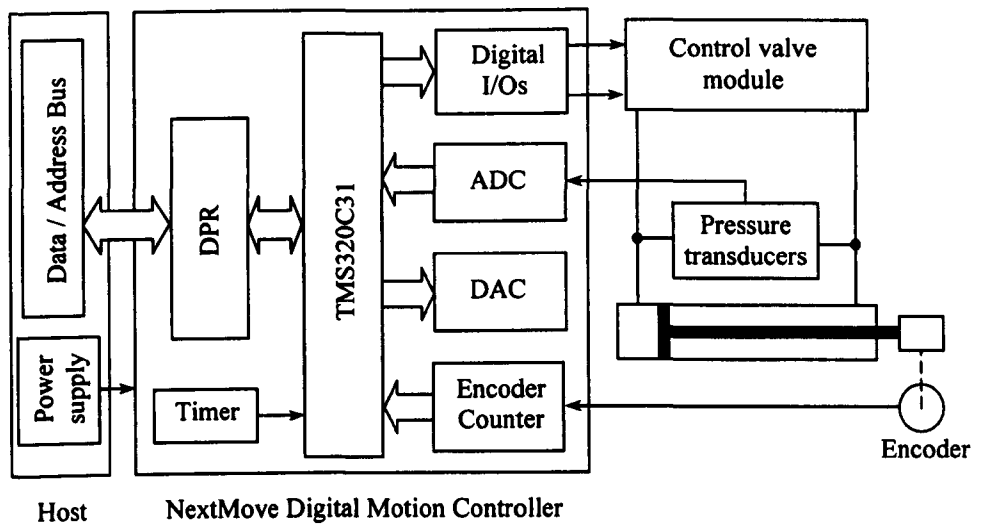


Figure 7-6 Block diagram of NextMove Digital Motion Controller configuration with EP-I and data analysing host.

### 7.2.2.2 Airflow rate regulator

The orifice sizes of the airflow rate regulators are an important parameter for verifying the mathematical modelling. However, from market it is difficult to find an airflow rate regulator that has a known orifice size after the orifice adjustment; therefore, two mechanical parts have been designed to build a special airflow rate regulator that the orifice size is certain.

These two parts are named Connector and Orifice Regulation Plate, respectively in this research. Figure 7-7 shows dimensions of the two parts. A set of Orifice Regulation Plate with different sizes of inner orifice is made for the experiment. A standard pneumatic silencer is also used to build the airflow rate regulators. Figure 7-8 schematically shows setup of the airflow rate regulator. An Orifice Regulation Plate with some sealing material on the outer edge is fixed into the connector by screwing the pneumatic silencer into the connector.

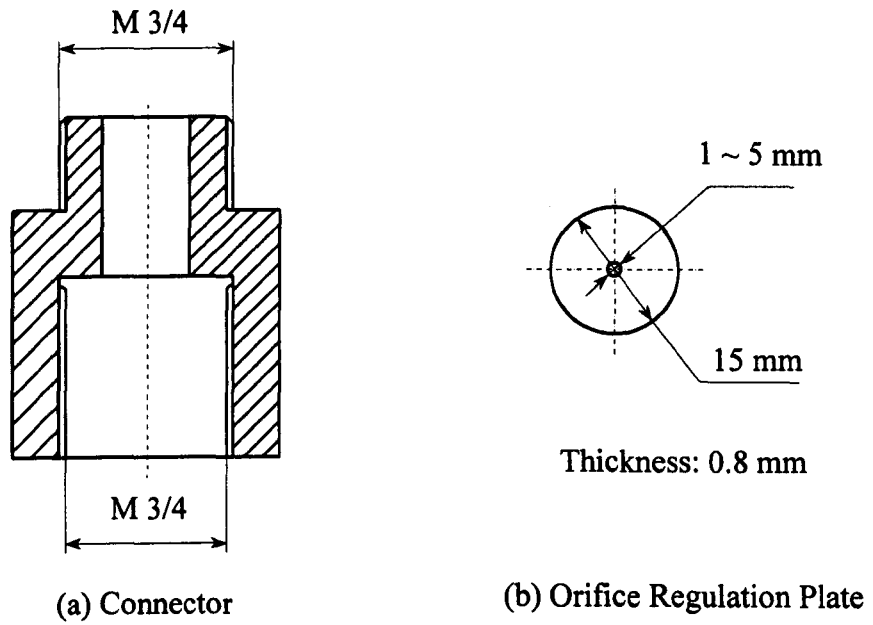


Figure 7-7 Dimensions of the Connector and the Orifice Regulation Plate

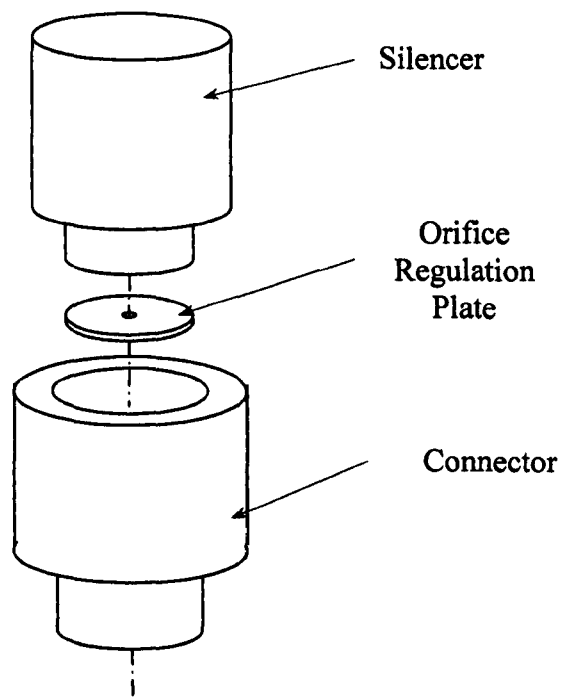


Figure 7-8 Setup of the airflow rate regulator

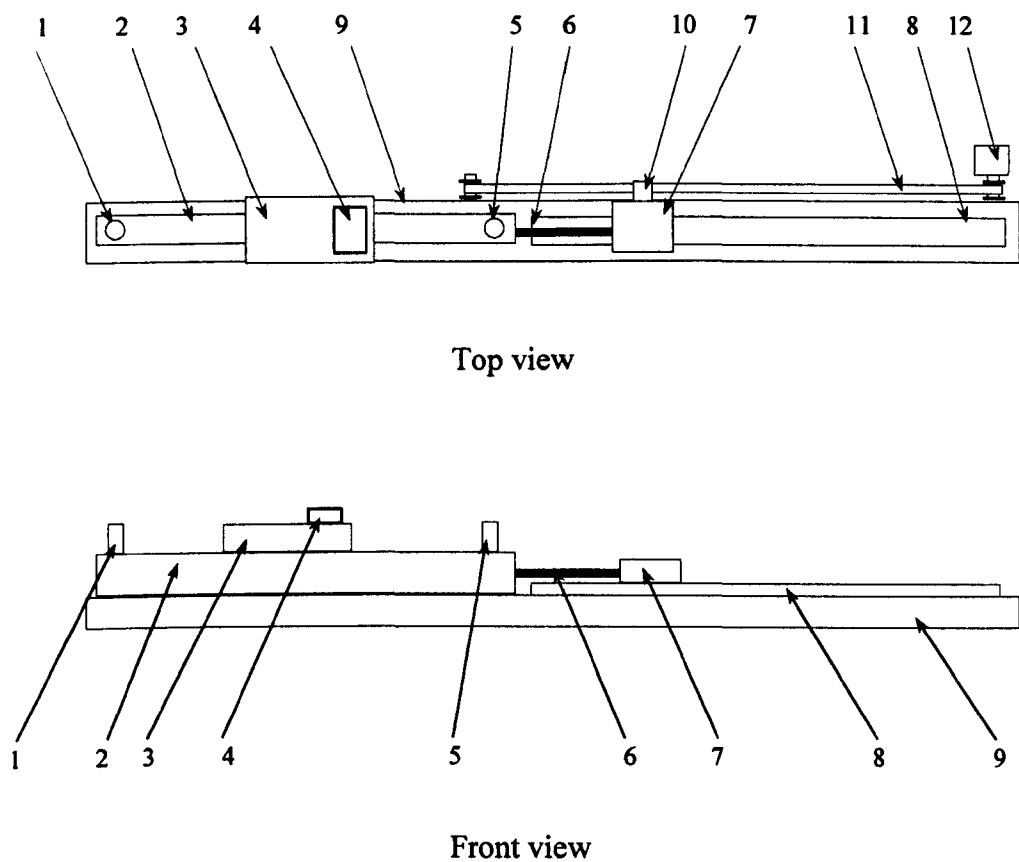
### **7.3 Setup of ES-II (System For High-speed Motion Control of CIPDs )**

Simplified construction views of ES-II, which is employed for the experimental studies of high-speed motion control of CIPDs, are depicted in Figure 7-9. Figure 7-10 shows a block diagram of the closed loop control of ES-II. In Figure 7-10, the components connected by dash-dot lines are used for data processing purpose; it does not have any contribution on the control loop of the system.

ES-II is constructed based on the theory presented in Section 4.4. Main components included in the system are:

- One asymmetric pneumatic cylinder.
- Four pneumatic valves, two of which are 3-port, 2-position on-off valve (Valve A and B) used for the motion direction control of the load and. Other two are 2-port, 2-position on-off valves (Valve C and D) used for the motion speed control of the load.
- A motion controller built based on Echelon TP/FT-10F control module.
- An increamental/decremental encoder. The information about the position of the load is sensed by the encoder and fed back to the controller.
- A pressure regulator, it is used to reduce the pressure in the chamber associated with the large area of piston, so that the load is stable at the Stand-by state.
- Three adjustable airflow rate regulators.
- A computer. This computer is used for LonWork network management and monitoring some network variables. It is also used to send some control commands, e.g. target position, to the main controller. This computer dose not makes any effect on the closed loop control of the system.





1. Tow-way port A
3. Control valves
5. Two-way port B
7. Load
9. System rack
11. Tooth belt

2. Cylinder
4. Controller
6. Cylinder Rod
8. Slide guide
10. Coupler for load and belt
12. Encoder

Figure 7-9 Simplified construction views of the Experimental Study System

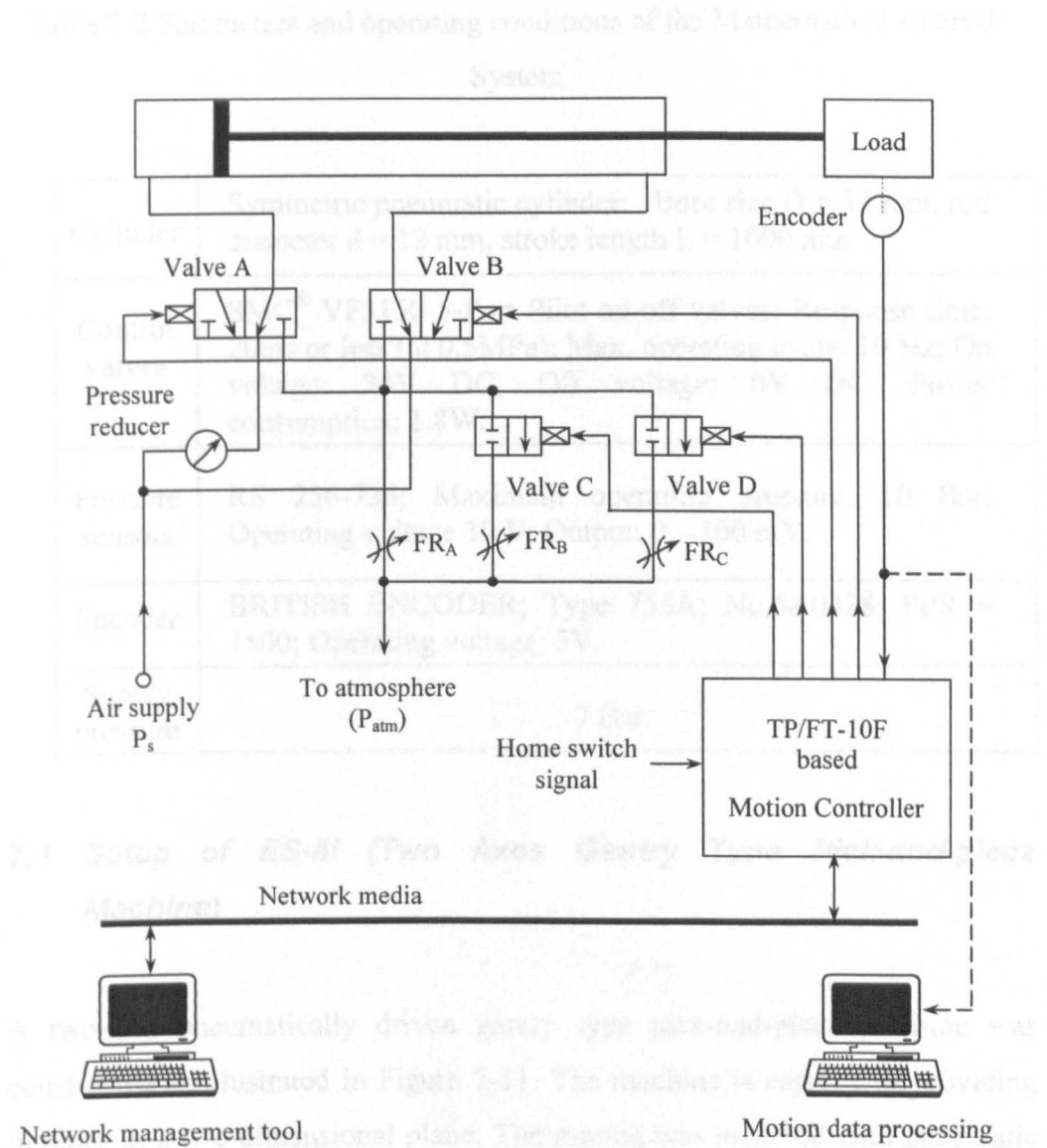


Figure 7-10 The block diagram of the closed loop control system

The main parameters and characteristics of other parts and operating conditions of the ESS are listed in Table 7-2.

Table 7-2 Parameters and operating conditions of the Mathematical Analysis System

Cylinder	Symmetric pneumatic cylinder: Bore size $D = 32$ mm, rod diameter $d = 12$ mm, stroke length $L = 1000$ mm
Control valves	SMC® VF3150 5-Port Pilot on-off valves; Response time: 20ms or less (at 0.5MPa); Max. operating cycle: 10 Hz; On voltage: 24V DC; Off voltage: 0V DC. Power consumption: 1.8W.
Pressure sensors	RS 256-736; Maximum operating pressure: 10 Bar; Operating voltage 10 V; Output: 0 – 100 mV.
Encoder	BRITISH ENCODER; Type 755A; No.6A0428; PPR = 1500; Operating voltage: 5V.
Supply pressure	7 Bar

#### 7.4 Setup of ES-III (Two Axes Gantry Type Pick-and-place Machine)

A two-axis pneumatically driven gantry type pick-and-place machine was constructed as illustrated in Figure 7-11. The machine is capable of providing motions in a two-dimensional plane. The motion was powered with pneumatic cylinders. The motion in the plane can be described with an X-axis and a Y-axis.

**The X-axis drive** – It provided the swing action. This was powered by a cylinder called X-axis cylinder (X-Cylinder) in this study. The swing angle caused by the rod movement of the X-axis cylinder is measured by an encoder referred to as the X-Encoder. In this study, the X-axis was presented using the displacements of the cylinder rod that drove the swing motion.

**The Y-axis drive** – It provides vertical motion along the rod of a cylinder called Y-Cylinder in this study. The rod displacement of Y-Cylinder is measured by an

encoder referred as Y-Encoder.

### 7.5 Construction of Two Axes Gantry Type Pick-and-place Machine

The simplified constructional diagram of the two axes gantry type pick-and-place machine is given in Figure 7-12. The motion generated by this system can be demonstrated in a simplified way in Figure 7-13.

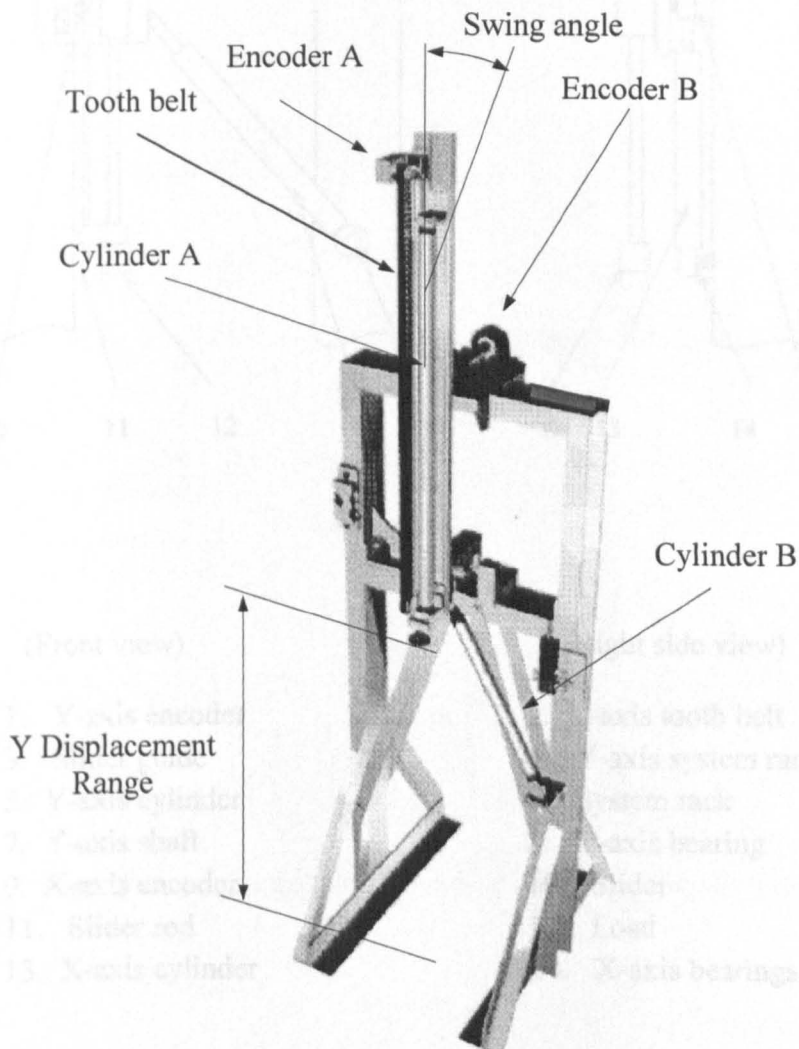
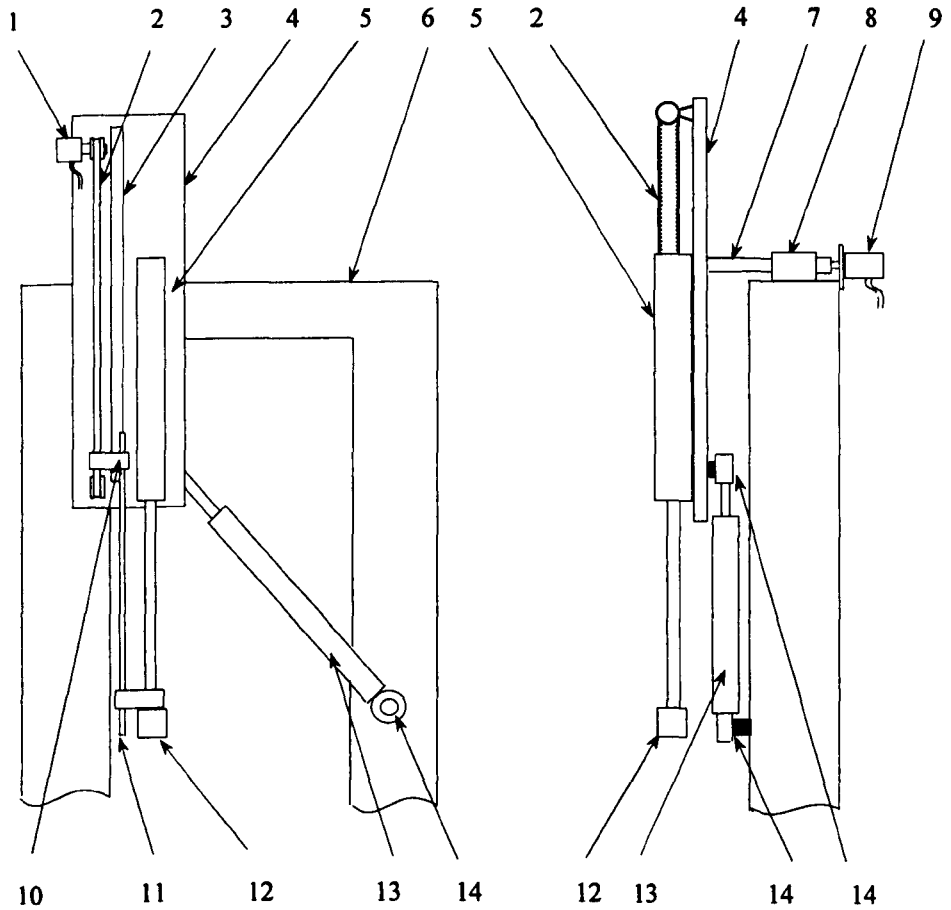


Figure 7-12 Simplified constructional views of pick-and-place machine

Figure 7-11 3-D view of pneumatically driven pick-and-place machine



(Front view)

1. Y-axis encoder
3. Slider guide
5. Y-axis cylinder
7. Y-axis shaft
9. X-axis encoder
11. Slider rod
13. X-axis cylinder

(Right side view)

2. Y-axis tooth belt
4. Y-axis system rack
6. System rack
8. Y-axis bearing
10. Slider
12. Load
14. X-axis bearings

Figure 7-12 Simplified construction views of pick-and-place machine

## 7.8 TPF1-10 Control Module Based Servo Motion Controller

General servo motion controllers based on TPF1-10 Control Module have been designed and built up for the control of pick-and-place machine. The design and development of this controller is based on the development of the servo motion controller. Such development tools provide an easy way for the implementation of distributed control system. LanWorks Technology is a complete platform for implementing motion network system and supports a wide variety of motion control modules. More information about LanWorks Technology is provided in Appendix.

This chapter presents some examples of motion transfer including pick-and-place machine. The motion transfer is controlled by the motion controller.

As shown in Figure 7-13, the Control Module contains core elements for a device design in a pick-and-place machine. However, to build a completed motion controller, some assistant circuits are normally required.

Some of electronic circuit has been designed to associate the TPF1-10 control module to perform the GPCDs motion control processing. This motion control processing mainly includes the following tasks:

Figure 7-13 Schematic diagram of motion for the pick-and- place machine

- Sampling load position;
- System initialization;
- PD control algorithm processing and three-state control signal conversion;
- Control loop updating;
- Driving control valves.

## **7.6 TP/FT-10 Control Module Based Servo Motion Controller**

Several servo motion controllers based on TP/FT-10 Control Module have been design and built up for the control of CIPDs. A set of development tool for employment of LonWorks Technology are used for the development of the servo motion controller. Such development tools provide an easy way for the implementation of distributed control system. LonWorks Technology is a complete platform for implementing control network systems and supports a wide variety of communications media including twist pair, power-line communication. More information about LonWorks Technology is presented in Appendix.

This chapter presents some details of the motion controller including assistant circuitry of TP/FT-10 control module, motion control strategy programming.

### **7.6.1 Assistant circuits of the TP/FT-10 Control Module**

An Echelon's TP/FT-10F Control Module contains core elements for a device designs using LonWorks technology. However, to build a completed motion controller, some assistant circuits are normally required.

Some of electronic circuit has been designed to associate the TP/FT-10 control module to perform the CIPDs motion control processing. This motion control processing mainly includes the following tasks:

- Network control variable processing;
- Sampling load position;
- System initialisation;
- PD control algorithm processing and three-state control signal conversion;
- Control loop updating;
- Driving control valves.

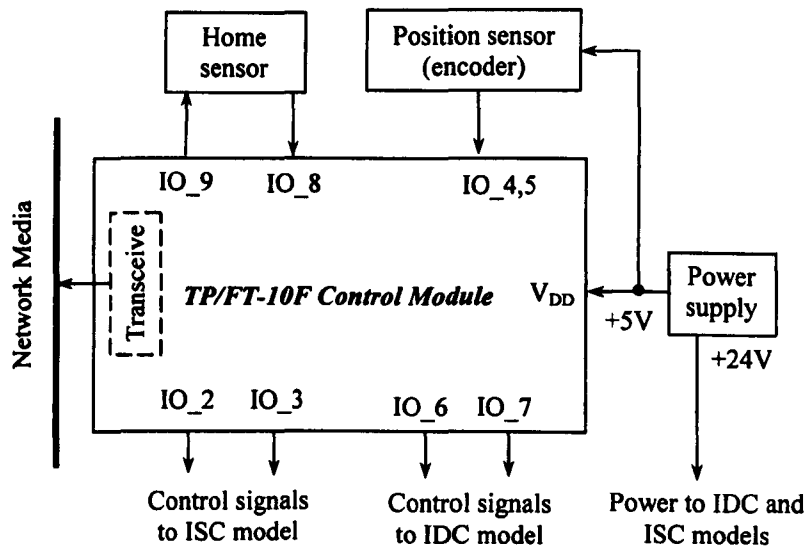


Figure 7-14 Block diagram of CIPD motion controller

The assistant circuit can be divided into 3 functioning blocks:

- Power supply;
- Position measurement;
- Home position sensor.

Figure 7-14 is block diagram of the CIPD motion controller. It also shows relationship between the assistant circuits and the TP/FT-10F Control Module. Detailed circuit diagrams of Assistant circuits are given in the follows.

#### 7.6.1.1 Power supply:

The power supply unit supplies +5V power source to the TP/FT-10F Control Module and the encoder, and +24V power source to the ISC module and the IDC module, respectively.



### 7.6.1.2 Position measurement:

Two of incremental/decremental type encoders with quadrature output signals are employed in this experimental study system. The Neuron Chip quadrature input function provides a simple means to process external data encoded in quadrature format. The function can be invoked by using a few statements in a Neuron C application program. Either IO\_4 or IO\_6 of TP/FT-10 Control Module may be used to define two I/Os as quadrature inputs pins. The second pin needed for the two quadrature inputs is assumed to be the next higher pin number (IO\_5 or IO\_7). Figure 7-15 shows the encoder connection to the Neuron Chip. For this application, IO\_4 and IO\_5 are used as quadrature input pins.

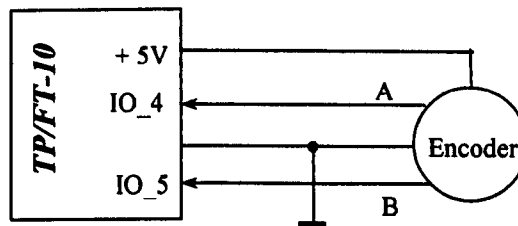


Figure 7-15 Encoder connection to the Neuron Chip

### 7.6.1.3 Home position sensor block:

A home position is a reference to a servo control system to initialise the system. Figure 7-16 is the circuit diagram of home position sensor block. This block consists of a normal-closed switch and a diode. The switch is allocated at a position so that it can only be closed by the system when the system is at home position. When the home switch is triggered (opened), a Logical 1 signal is input to the IO\_8. This signal executes a sub-program which sets the IO\_9 to low level. Thereafter, the low level of IO\_9 will hold the IO\_8 at low level forever

via the diode. Therefore, any further changes of home switch's state (open or closed) will have no effect to the system.

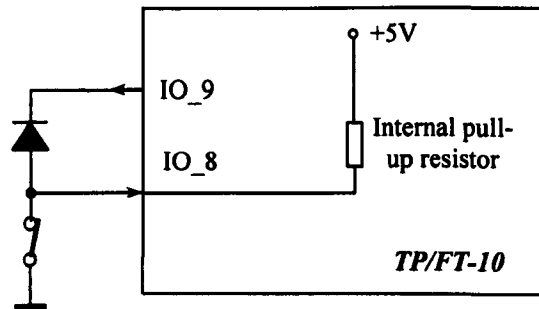


Figure 7-16 Circuit diagram of home position sensor block

## 7.7 Programming of the servo motion controller

Programming of the servo motion controller was carried out using the NodeBuilder development tool to write the application source code, compile, build and load the application program into the controller.

### 7.7.1 Closed loop control update timer

One of the three timers within the Neuron Chip is employed as closed loop control processing update timer. The timer is set up to 4 ms. Every time the timer expires, the program for closed loop control algorithm will be triggered. Hence, the motion controller outputs are updated every 4 ms according the load position fed back by the encoder.

### 7.7.2 Use of *Integer* in control algorithm programming

The performance of a fast real time control system is heavily related on the structure of the control algorithm program. A reasonable good structure can save the calculating time which is important for the fast real time control.

A motion control algorithm of feedback control system includes some mathematical calculations, for example, working out positioning error between the setpoint (normally floating-point number) and process variables, proportional, derivative, integral feedback loop, and other terms of calculations. The load motion process information (e.g. position, velocity, acceleration) is also calculated according to a pulse train signal from the position sensor. In such case, an element named "Scale" is normally used to set all encoder driven variables to user defined units, for example, Position (mm) = Total pulses received / Scale (pulse/mm).

In practice, the value of the scale is not only depending on the user defined unite for control variables, but also depending on the mechanical structure of the plant. Hence, the scale normally is a floating-point number, which makes the control variable to be a floating-point number. The control variable will be used through out the control algorithm calculation, hence such control algorithm calculation are floating-point number based calculation. Figure 5-10 shows the general processing procedure of deriving a control command by the control algorithm sub-routine.

The Neuron C compiler does not directly support the use of the ANSI C arithmetic and comparison operators with floating-point values. There is a complete library of functions for floating-point math. All of floating-point math processes are achieved by calling the function.

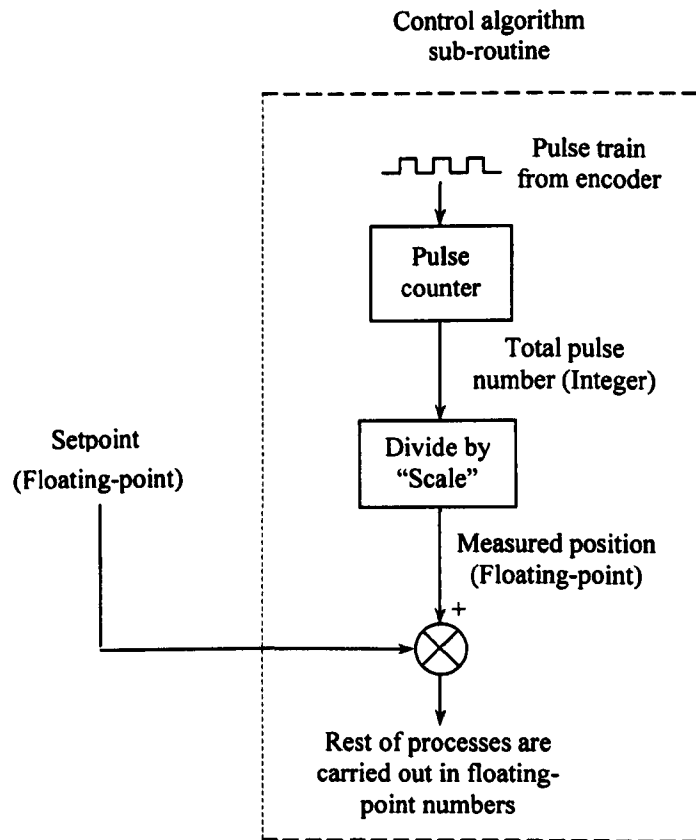


Figure 7-17 General processing procedure of control algorithm calculation

However, calling functions for floating-point maths is time consuming. Table 7-3 lists the performance of some basic floating-point math normally involved in control algorithms. They were measured using a Neuron Chip with a 10 MHz input clock.

Table 7-3 Floating-point math performance (ms.)

Function	Maximum (ms)	Average (ms)
Add	0.56	0.36
Divide	2.43	2.08
Multiply	1.61	1.33
Conversion to 16-bit integer	2.84	0.75

In this research, the closed-loop update period is designed for 2 ms.. This time is not enough for involving floating-point maths within control algorithm. Therefore, the control algorithm processing has been designed using integers through out the algorithm sub-routine. This is achieved by converting the setpoint (floating-point number) to be pulse number (target pulse number) which is a integer, and use the pulse number for rest calculations.

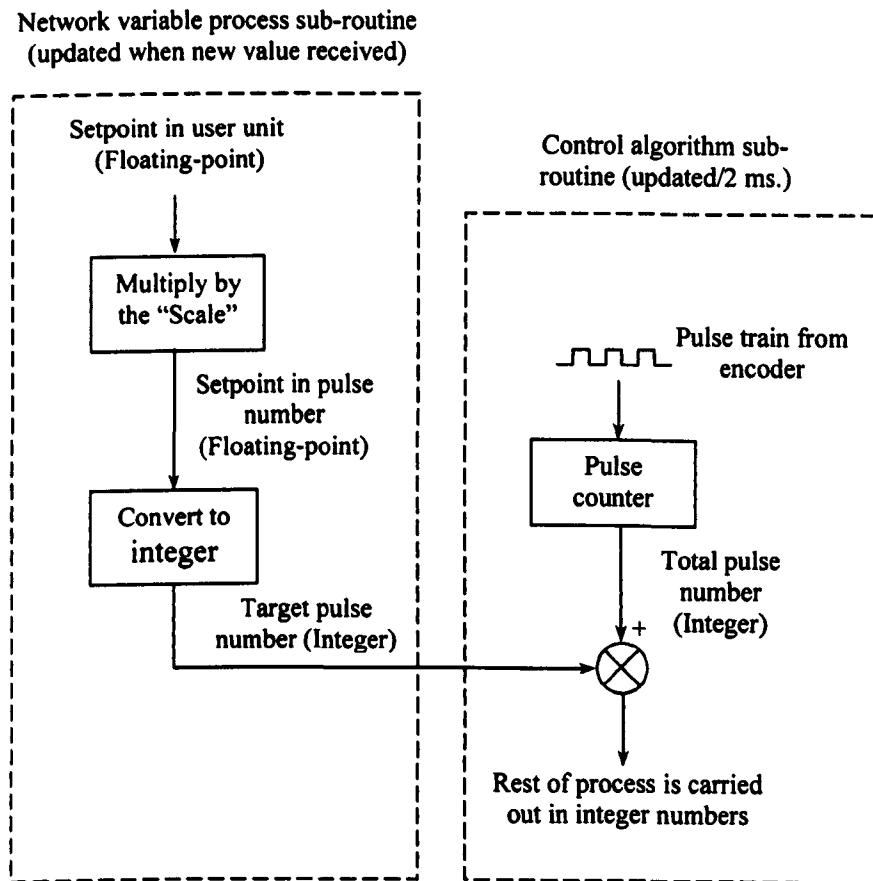


Figure 7-18 Processing procedure of variable calculation of CIPDs

Figure 7-18 shows the processing procedure of variable calculation employed within CIPDs. The setpoint (target position) is network variable and sent by other devices. When a new value of setpoint is received, it will be multiplied by the scale, and then converted to an integer value in number of pulse number (target pulse number). Truncation of the converting a floating point

number to a Neuron C signed integer is towards zero, e.g.  $-567.6745$  will be converted to be  $-567$ , and  $398.578$  will be converted to be  $398$ . This process will be carried out by a subroutine for network variable process, which is out side of the control algorithm process. By using this arrangement, whole control algorithm process will be carried out in integers.

## Chapter 8 Experimental Studies

### **8.1 Introduction**

The structure of the three experimental systems and pneumatic system mathematical modelling of CIPDs are presented in Chapter 1 and Chapter 6, respectively. This chapter introduces a set of experimental studies carried out using the three experimental systems during this research. The main purposes of the experimental studies are to verify the theoretical analysis and evaluate performance of CIPDs control strategies developed in the research. The verification of the mathematical modelling was carried out on the ES-I. The experimental studies were started by testing some characteristics of the experimental system, such as: static friction, viscous friction and Coulomb friction. These characteristics are the key factors in mathematical modelling process. The performance evaluations were carried out on the ES-II and ES-III.

### **8.2 Friction characteristics of the ES-I (Mathematical Analysis System)**

Friction is perhaps the most important nonlinearity that is found in many mechanical systems with moving parts. It is commonly described as linear viscous damping, Coulomb friction and stiction or some combination of them. In linear control theory, either it is assumed that the friction is linear viscous, or attempts are made to linearize the friction about some operation point in order to make a linear analysis possible. Unfortunately, attempts to ignore or linearize significant Coulomb friction or stiction, both of which are represented by a discontinuity at zero velocity, may lead to erroneous predictions of a system's behaviour.

Such friction also plays an important role in the positioning control of pneumatic drives. The friction within pneumatic drives mainly arises in the contacts of the piston with the cylinder walls as well as in the linear slide-way and other minor rubbing elements. In this section, the experimental studies are carried out to measure the static friction and its distribution along the cylinder stroke, and to determine the viscous friction as well.

### 8.2.1 Static friction of the ES-I

The total system static friction is determined by the force difference between the two sides of the piston when the load velocity  $\dot{Y}$  is zero. In control engineering, the calculation of maximum static friction is more important because that system changes from static state to dynamic state when the maximum static friction is overcome.

By applying Newton's second law, the dynamic behaviour of the system can be described by the following equation (assume  $A_a = A_b = A$ ):

$$A(P_a - P_b) - F_f \text{sign}(\dot{Y}) - c_f \dot{Y} = M\ddot{Y} \quad (8-1)$$

At static state,  $\dot{Y} = 0$  and  $\ddot{Y} = 0$ . Therefore the total system static friction is

$$F_{static} = A(P_a - P_b) \quad (8-2)$$

Thus the chamber pressures just before the load moving are measured to derive the force difference. The measurements have been carried out for different piston position and motion direction, the definition of measured piston positions and motion directions are shown in Figure 8-1.



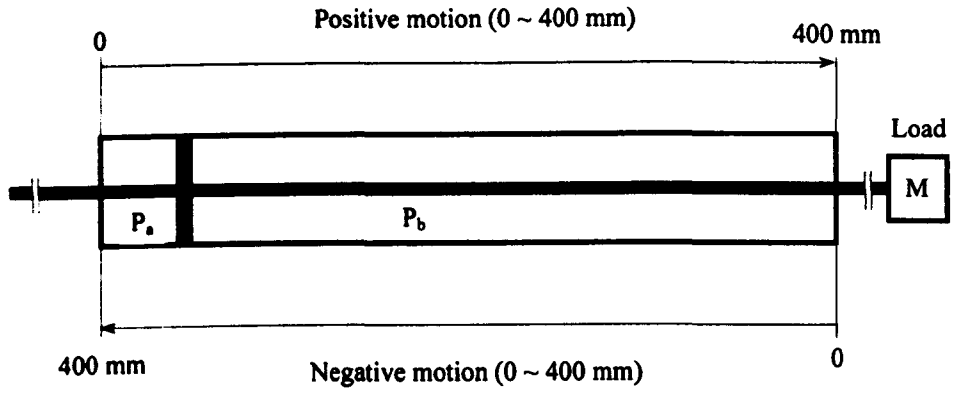


Figure 8-1 The definitions for the piston positions and motion direction

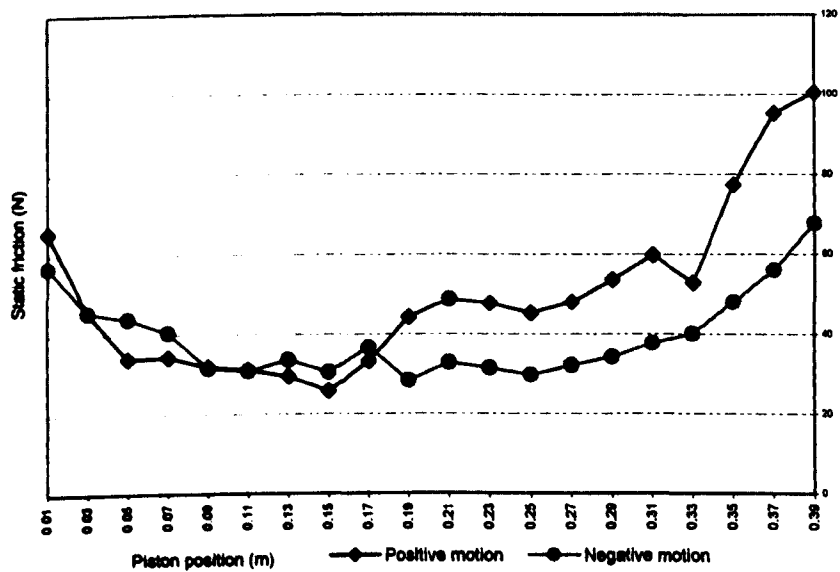


Figure 8-2 Static friction distribution of the experimental system

### 8.2.2 The system viscous friction and Coulomb friction

At steady moving state ( $\dot{Y} \neq 0, \ddot{Y} = 0$ ), the static friction becomes dynamic friction. From Equation (8-1), one obtains

$$F_{dynamic} = A(P_a - P_b) = F_C \text{sign}(\dot{Y}) + c_f \dot{Y} \quad (8-3)$$

If two sets of the chamber pressures at two different steady state velocities are measured, the viscous friction coefficient  $c_f$  and Coulomb friction  $F_C$  can then be obtained by putting them into Equation (8-3) and resolving the simultaneous equations (this method has also been applied by previous researcher Z. Zhang, 1999).

The experimental test for measuring the viscous friction coefficient  $c_f$  and Coulomb friction  $F_C$  was run for three times to ensure test repeatability. Table 8-1 lists the experimental results, the data in the two columns in each test are from different directions.

Table 8-1 Experimental results of testing  $C_f$  and  $F_C$

	Test 1		Test 2		Test 3	
$P_a$ (Bar)	7.77	7.37	7.77	8.00	7.88	7.37
$P_b$ (Bar)	7.50	7.01	7.50	7.67	7.60	7.01
$\dot{Y}$ (m/s)	0.14	0.30	0.14	0.263	0.15	0.30
$C_f$	38.8		36.6		36.8	
$F_C$	13.2		13.14		13.8	
Average $C_f$	36.7		Average $F_C$		13.47	

### 8.3 Verification of mathematical modelling of CIPDs

The verifications of the mathematical modelling, derived in both the transfer function and the state-space presentation in Chapter 6, have been conducted with the experimental system ES-I. The structure and system parameters are presented in Section 7.2. MatLab simulation tool is also used in these verifications. The parameters used in the MatLab simulation are listed in Table 8-2. Some of the parameters are calculated out for experiment results.

Table 8-2 Parameters used in MatLab simulation

Parameter	Symbol	Value
Piston area of Chamber A, B	$A_{a,b}$	0.00069 m <sup>2</sup>
Size of exhaust orifice	$A_{XOb}$	11×10 <sup>-7</sup>
Discharge coefficient	$C_d$	0.82
Viscous damping coefficient	$C_f$	36.7
Stroke length of cylinder	$l$	0.45m
Load mass	$M$	4.5Kg
Initial pressure of Chamber B	$P_{bi}$	7.5 Bars
Gas constant	$R$	287/K
Temperature of air supply	$T_s$	300K
Initial position of the piston	$Y_i$	0.05 m

### 8.3.1 Verification of open loop system transfer function of the CIPDs

The verification of open loop system transfer function of CIPDs, presented as Equation (6-25) in Section 6.4.1, were carried out by comparison of the MatLab simulation result and experimental result.

Figure 8-3 graphically shows the comparison. It can be seen that the transfer function is largely indicative of the likely behaviour for the system considered.

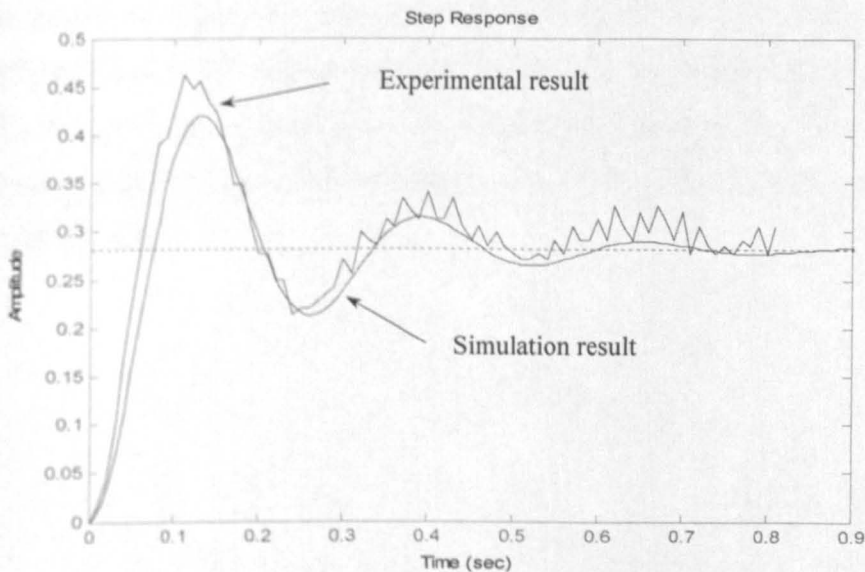


Figure 8-3 Comparison of simulation and experimental results of transfer function of the CIPDs

### 8.3.2 Verification of the Velocity Gain $K_v$ of the CIPDs

The previous discussion in Section 6.9 shows that the amplitude of the velocity profile of CIPDs is determined by the Velocity Gain  $K_v$ . The Velocity Gain  $K_v$  is largely determined by the effective area ratio of exhaust orifice and the piston in exhaust chamber as described in Equation (6-59) that:

$$K_v = (R\sqrt{T_s}C_0C_d) \frac{C_{ov}}{A_b}$$

To verify this equation, some simulation and experimental studies have been carried out. In the simulation studies, three of different sizes of exhaust orifice have been applied to the transfer function. The results of the simulation are shown in Figure 8-4. The experimental studies have been carried out by applying different exhaust orifice size (by changing the Orifice Regulation Plate, refer to Figure 7-7 and Figure 7-8). The results of experimental studies are shown in Figure 8-5 (one of data are also presented in Figure 8-3). From both simulation and experimental results, and together with Figure 8-3, it can be seen that the size of exhaust orifice affects the amplitude of the load transient velocity profile, and the steady moving velocity can be estimated using the Velocity Gain  $K_v$ .

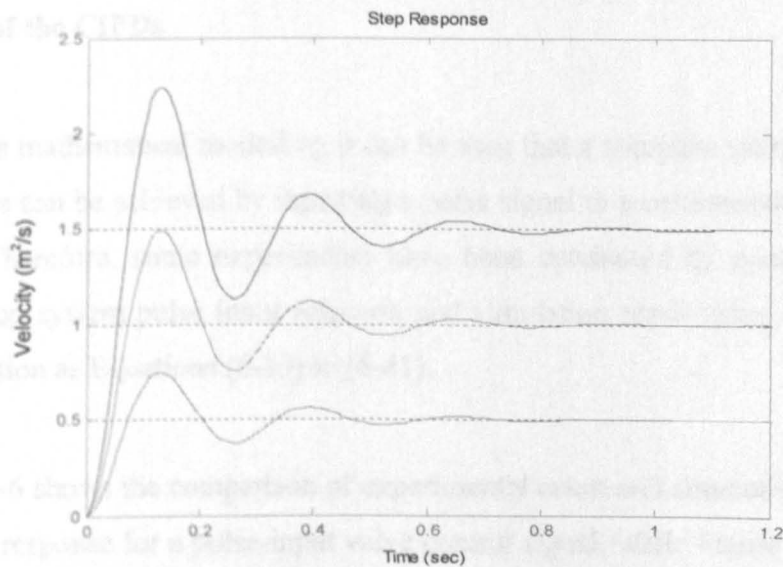


Figure 8-4 Simulation results of velocity profile with different sizes of exhaust orifice

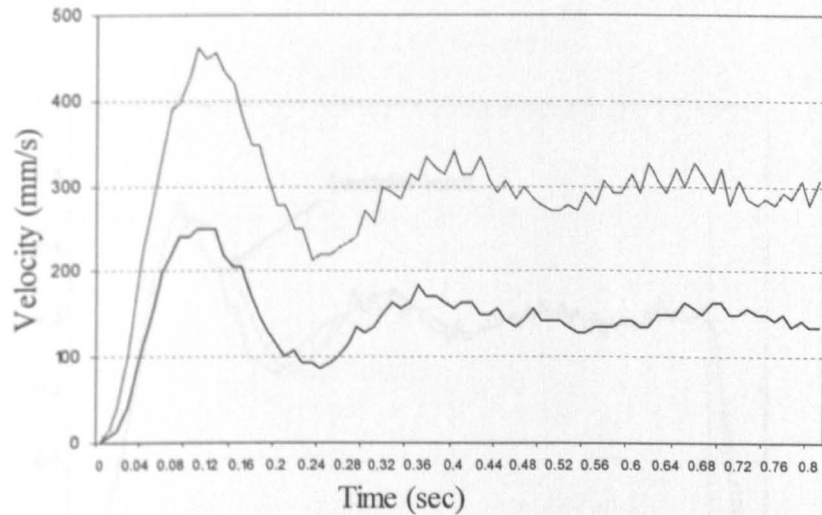


Figure 8-5 Experimental results of velocity profile with different sizes of exhaust orifice

### 8.3.3 Verification of pulse-input response using state-space presentation of the CIPDs

From the mathematical modelling it can be seen that a complete motion process of CIPDs can be achieved by inputting a pulse signal to a corresponding control valve. Therefore, some experiments have been conducted by comparing the open-loop system pulse input response and simulation result using state-space presentation as Equations (6-39) to (6-41).

Figure 8-6 shows the comparison of experimental result and simulation result of velocity response for a pulse-input valve control signal, while Figure 8-7 shows the comparison of the experimental and simulation results of the pressure response in driving chamber.

Figure 8-8 shows the difference of the transfer function and state-space presentation of step-input response.

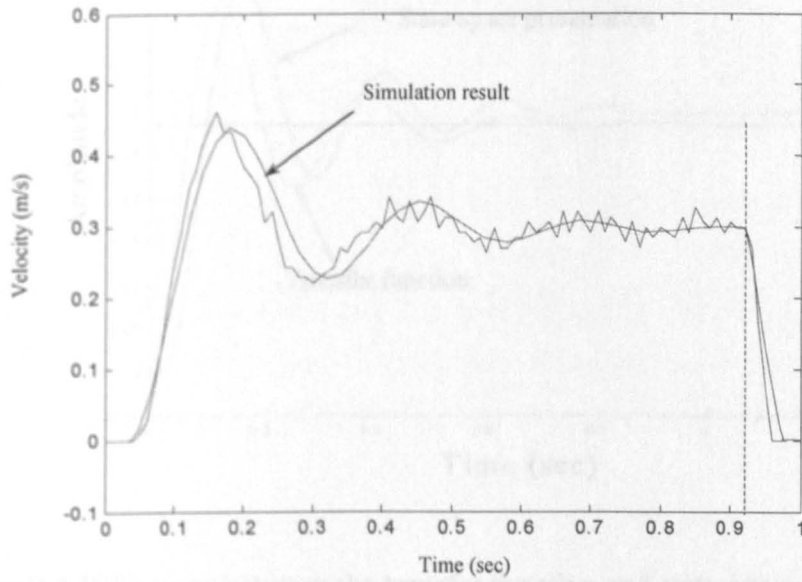


Figure 8-6 Comparison of experimental and simulation results of pulse-input velocity response

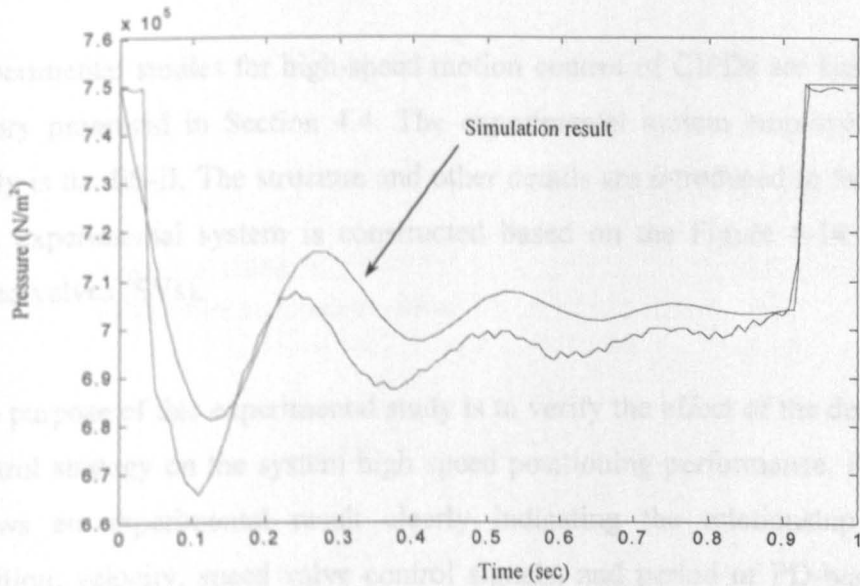


Figure 8-7 Comparison of experimental and simulation results of pulse-input driving chamber pressure response

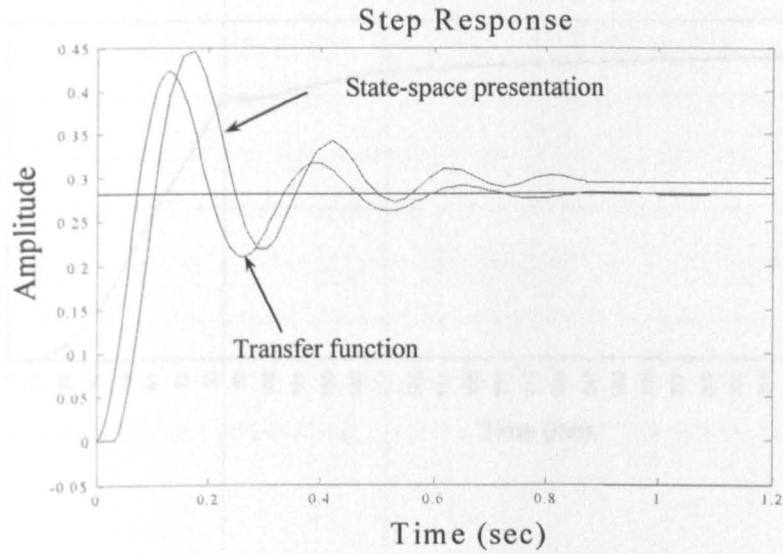


Figure 8-8 Difference between the transfer function and state-space presentation for simulation of step-input response

#### 8.4 Experimental Studies of High-speed Motion Control of CIPDs

Experimental studies for high-speed motion control of CIPDs are based on the theory presented in Section 4.4. The experimental system employed for this study is the ES-II. The structure and other details are introduced in Section 7.3. The experimental system is constructed based on the Figure 4-14 with two speed valves (SVs).

The purpose of this experimental study is to verify the effect of the deceleration control strategy on the system high speed positioning performance. Figure 8-9 shows an experimental result clearly indicating the relationship between position, velocity, speed valve control signals, and period of PD-based three-state control strategy of high-speed CIPDs.



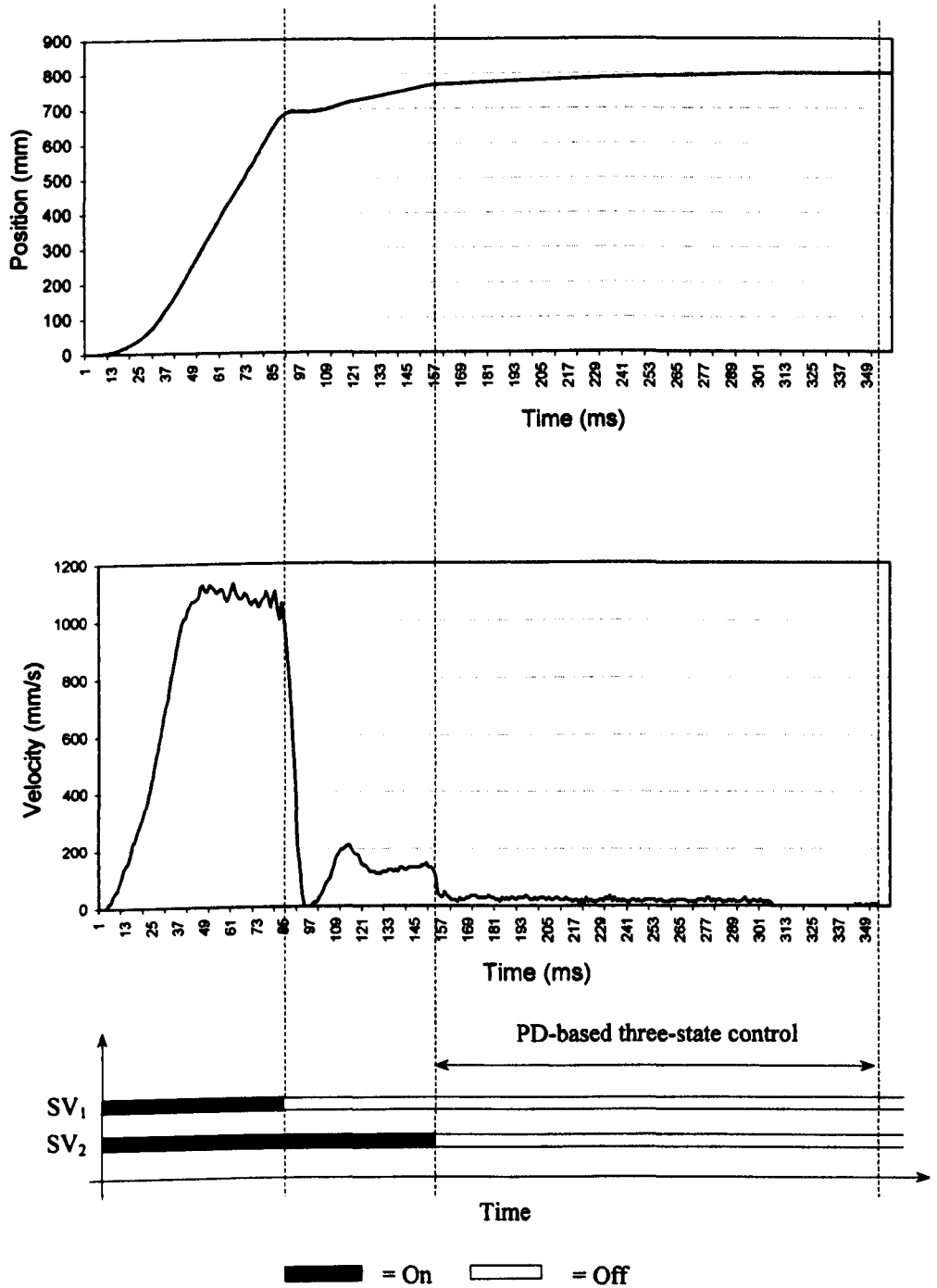


Figure 8-9 Experimental results showing the relationship between position, velocity, and speed valve control signals of high-speed CIPDs

Figure 8-10 shows the experimental result of the velocity profile from two experimental studies (Experimental A and B). The difference in experimental conditions of these two experiments is the size of the exhaust orifices controlled by  $SV_1$  and  $SV_2$ . From the experimental results it can be seen that, by carefully adjusting the size of the exhaust orifices in the Experiment B, the load can be decelerated efficiently when it is approaching its target position, with very small velocity overshoot. Therefore, the deceleration control strategy can be an effective method in improving the behaviour of high speed CIPDs. Figure 8-11 shows the corresponding positioning profile of the Experimental A and B.

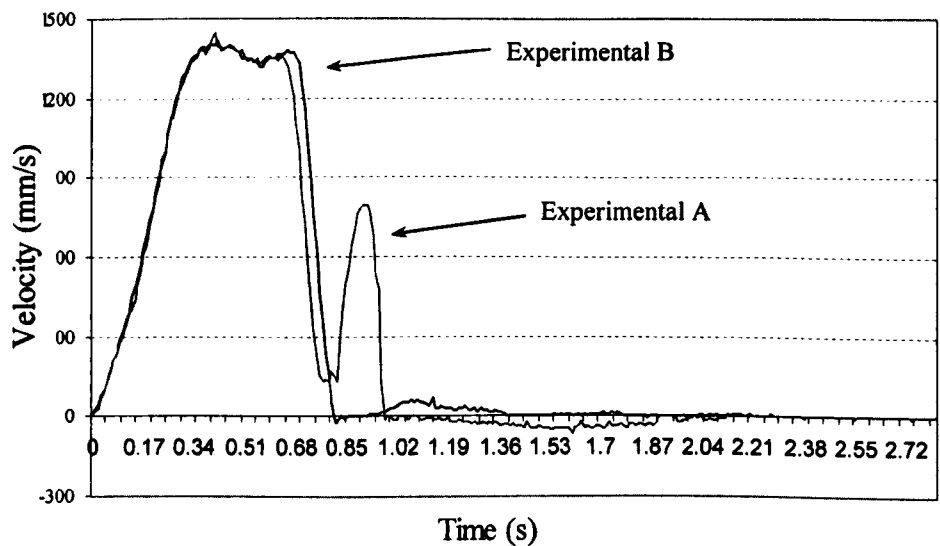


Figure 8-10 Effect of speed valves controlled exhaust orifice size on the deceleration regulation

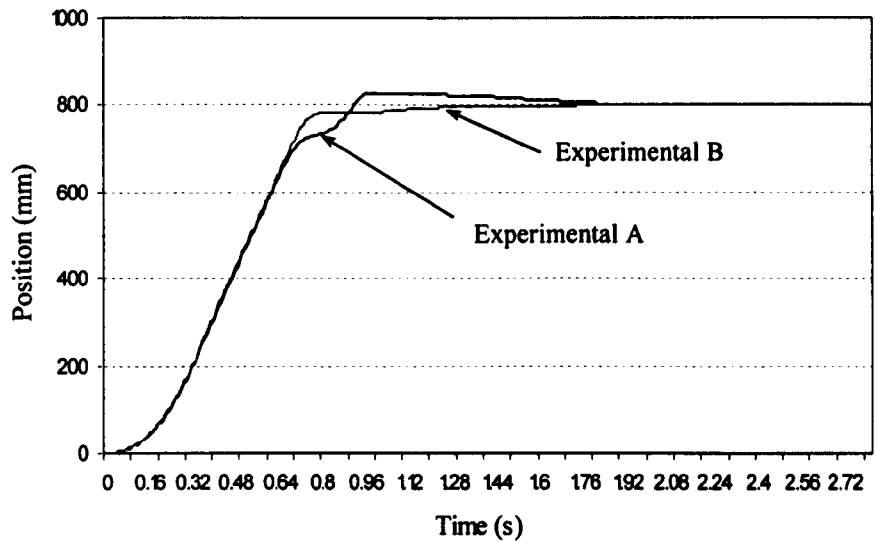


Figure 8-11 Positioning profile of two experiments with different size of exhaust orifices

## 8.5 Experimental Studies on the Two Axes Gantry Type Pick-and-place Machine (ES-III)

### 8.5.1 Nodes within the two axes gantry type pick-and-place machine network

The two-axis gantry type pick-and-place machine (ES-III) has been described in Section 7.4. Figure 8-12 illustrates the construction of the experimental control system for the pick-and-place machine.

There are five nodes within the local control system. Two of them are CIPDs used as X-axis controller and Y-axis controller that are built based on the structure shown in Figure 4-14, with two speed control valves are used in each drives. A Gateway node creates a connection between the local control network and Internet, hence the remote services access strategy presented in Section 5.2

can be verified. A source control node is also installed in the local control network for demonstration purpose. In the experiments, this node can respond the remote service commands, which are sent from somewhere in the world via Internet, that to turn on (or turn off) the power sources of Y-axis Drive. The last node is called Commander in this research; the details about the Commander will be introduced in Section 8.5.3.

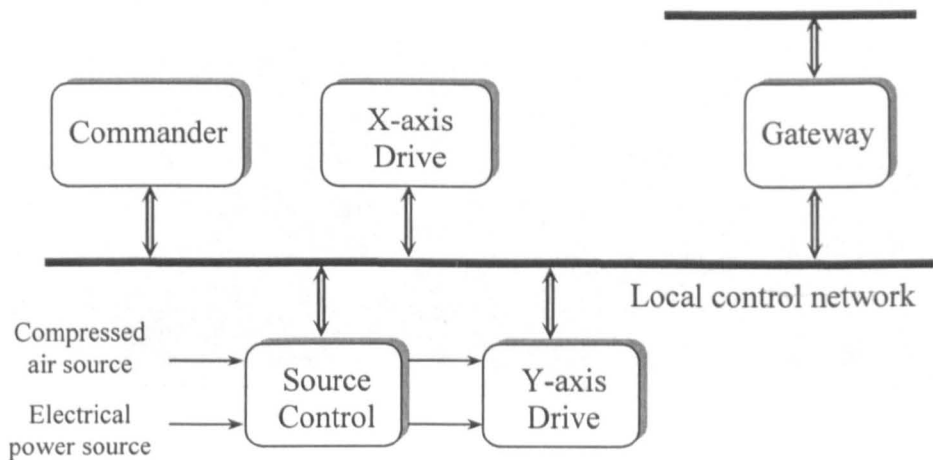


Figure 8-12 Network of the two axes gantry type pick-and-place machine

When the system is powered up, the Gateway will firstly obtain an IP address and other TCP/IP network information using DHCP protocol, and then the Gateway will be trying to register the local control network with its manufacturer by sending out registration message. Once the registration is successful, the Gateway can be accessed from anywhere in the world using an Internet exploring tool with Gateway's IP address. In response, the Gateway will send out a web page to display the information of local control network, and services that the manufacturer allowed to use. Figure 8-13 illustrates an example of web page that stored in the Gateway and displayed by Microsoft Internet Explorer. Through this web page, users are able to control the supply state of power sources, and to send new target positions to the X-axis and the Y-

axis mention controllers, respectively.

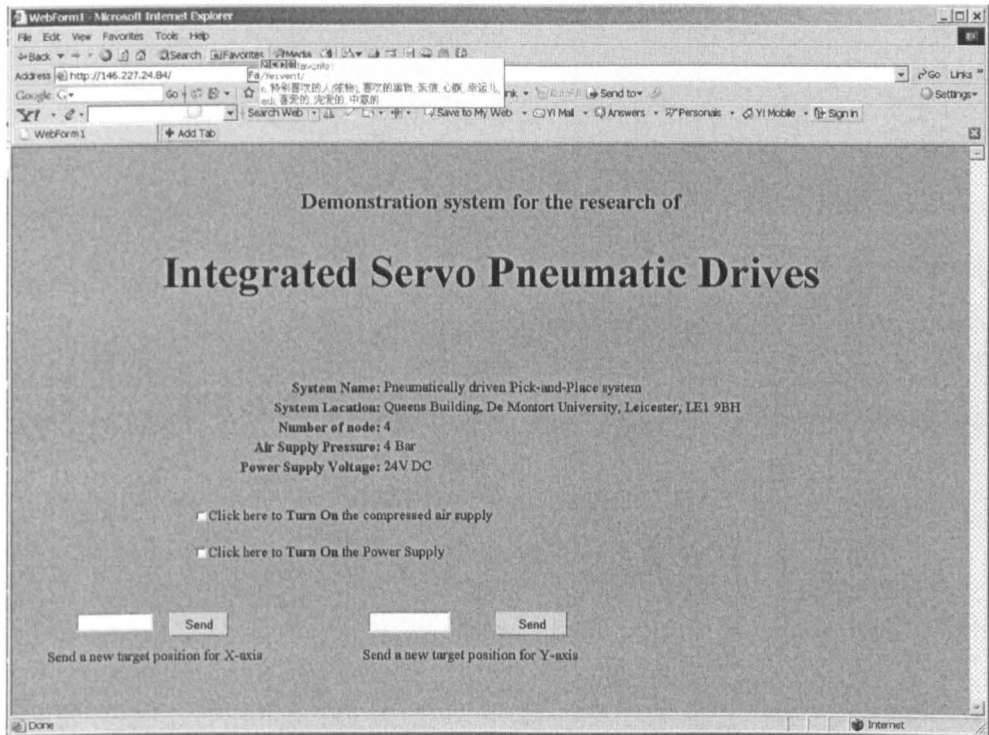


Figure 8-13 An example web page stored in the Gateway and displayed by Microsoft Internet Explorer

### 8.5.2 Test of the motion controller performance

As discussed in Section 7.7, the performance for the motion controller is significantly affected by the structure of control algorithm sub-routine and the frequency of the control loop update timer. Higher frequency of control loop update rate can normally leads to more effective control performance. However, if the frequency is too high, then the controller may not be able to complete the control algorithm process in each control loop update interval. This can cause controller to generate incorrect outputs. Therefore, it is very important to test the performance of the motion controller before carrying on the experimental studies.

A program, which simulates the control algorithm process in real application, has been written for testing of the controller performance.

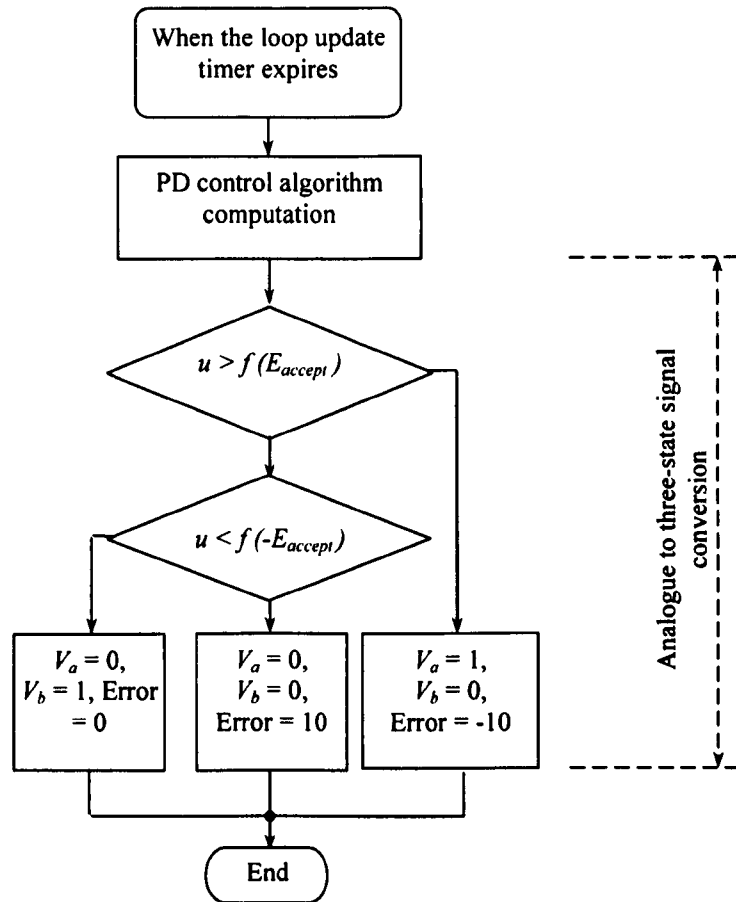


Figure 8-14 Flowchart of closed-loop control computation simulation program

Figure 8-14 is the flowchart of the simulation program. In the program, an initial value of 0 is setup as positioning error for the PD control algorithm computation, this value will cause the controller to output a “00” control signal after the analogue to three-state signal conversion. Subsequently, the position error will be setup to 10, which will causes the controller to output a “10” signal after second execution. The positioning error will be to –10 for third execution.

The third execution will output a “01” control signal and set the position error to be 0 for next execution which is same as the first execution, and so on. In this method, following the execution of the program triggered by the control loop update timer expiration, the position error will be changed in the cycle of “0 → 10 → -10 → (return to 0)”, and the output of the controller will be in the cycle of “00 → 10 → 01 → (return to 00)”.

The tests were carried out by setting up the timer for different time, and then the outputs of the motion controller for the direction control valves are monitored. Figure 8-15 shows the experimental result when the trigger interval is 4 ms. The experimental results show that the controller required about 3 ms time to complete the computation, and when the execution interval is less than 3 ms, it cannot be guaranteed to complete the control algorithm process.

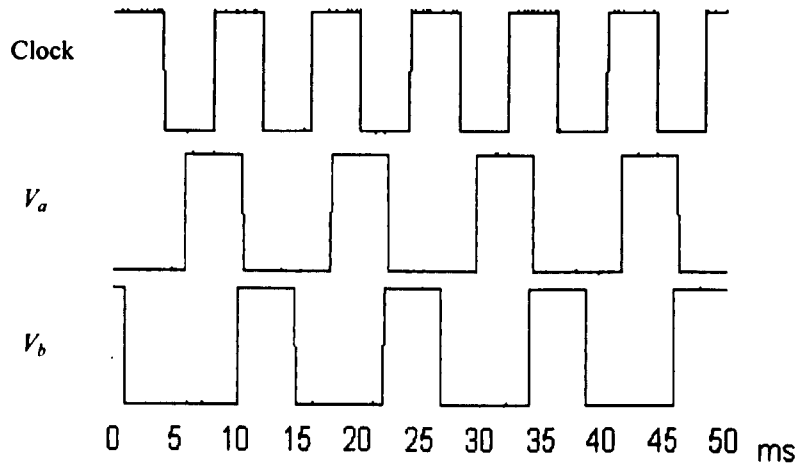


Figure 8-15 Performance of simulation program with 4 ms execution interval

### 8.5.3 The Commander

The Commander is designed only for this experimental study purpose, and is built based on TP/FT-10 model. It plays a role as a sensor or other node generating LonWorks network variables as target positions to the X, Y-axis controllers. Hence, the pick-and-place actions of the machine can be completed by the Commander node sending out a series of target positions to the X and Y-axis drives. The Commander has a control panel with setting switch and four control buttons. It can be set to either AUTO or MANUAL by the setting switch. When the Commander is set to AUTO, it will send out target position network variables automatically in a sequence for completing pick-and-place actions; When the Commander is set to MANUAL, sending out variables (target positions) can be controlled by users, alternative, user could control the pick-and-place machine to do an individual action using one of the four buttons. Figure 8-16 shows the control panel of the Commander, while Figure 8-17 shows the sequence of automatically sending out the target positions by the Commander, Figure 8-18 illustrates the corresponding actions of the pick-and-place machine for the AUTO setting. Each action can also be achieved individually using the MANUAL setting and the four control buttons.

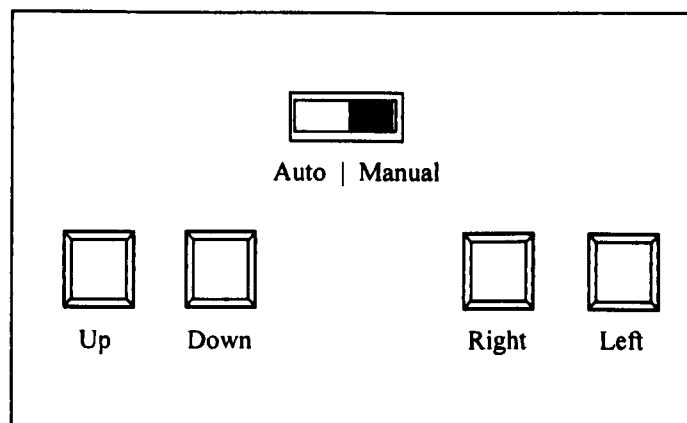


Figure 8-16 Control panel of the Commander



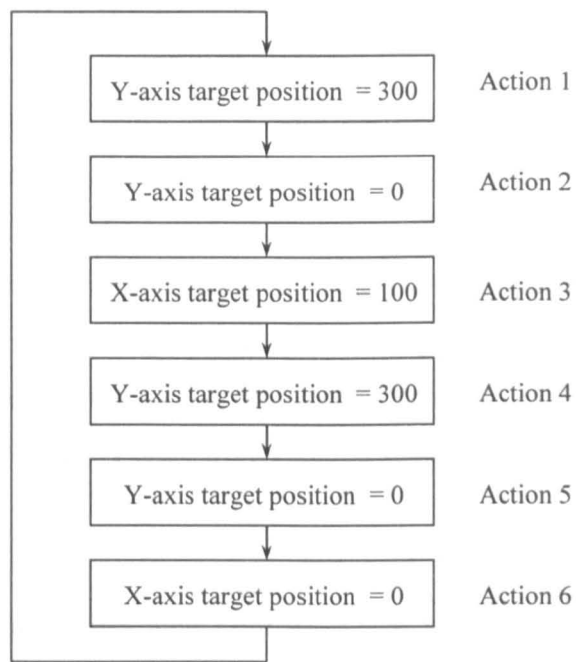


Figure 8-17 Sequence of sending out the target position by the Commander

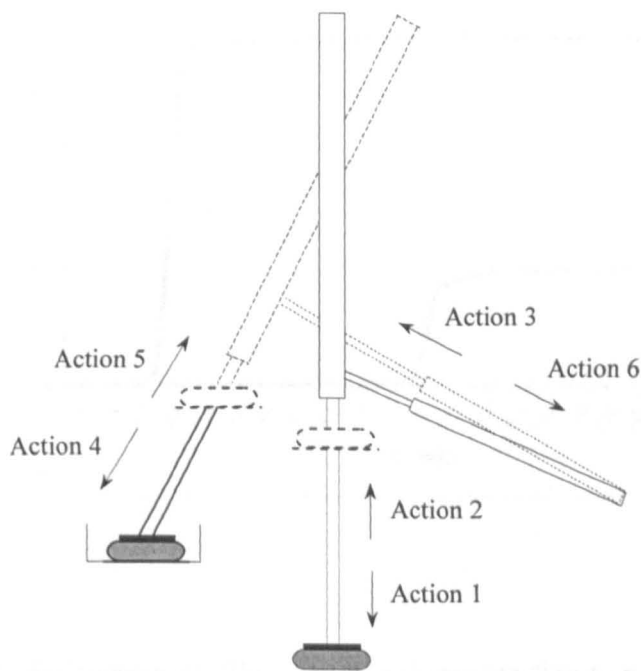


Figure 8-18 Corresponding actions of the pick-and-place machine

### 8.5.4 Experimental results of control of the Pick-and-place Machine

Some experimental studies have been carried out to verify the distributed control and strategy of remote service access via Internet of the pick-and-place machine. Figure 8-19 shows the positioning profile when the Commander sends individual target positions of 300 mm to the X-axis drive, and 100 mm to the y-axis drive, respectively. Figure 8-20 shows the positioning profile of the X-axis, Y-axis when the Commander is set to automatically send out target positions. The circled numbers in Figure 8-20 indicate the corresponding actions shown in Figure 8-18.

The experimental studies have confirmed that by using the CIPDs, the system setup, including wiring, tuning, and further developing, can be achieved easily. Hence, the CIPDs provide potentials for building high flexible, cost effective manufacturing systems.

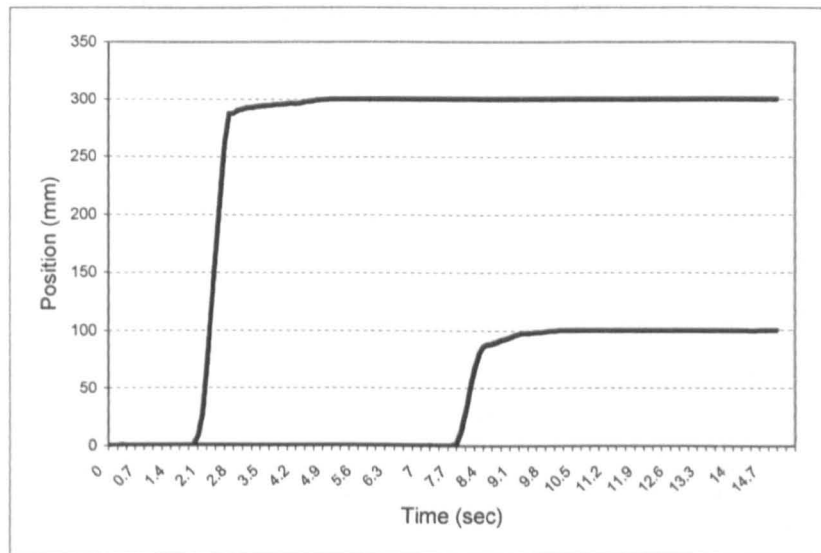


Figure 8-19 Positioning profile of X, Y-axis responding to network variables of target positions

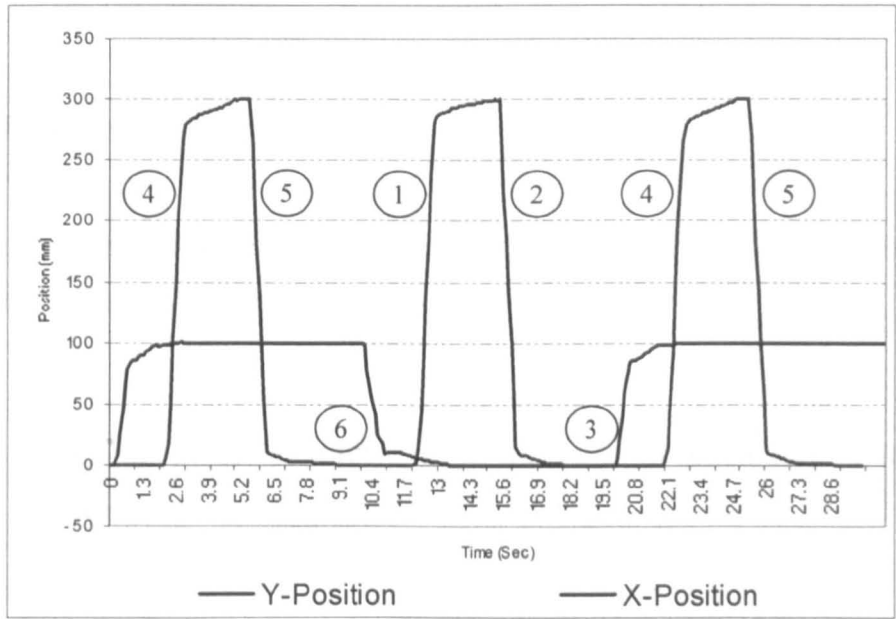


Figure 8-20 Positioning profile of distributed controlled the X, Y-axis

# Chapter 9 Conclusions

## **9.1 Research Contributions**

The research contributions to the knowledge of servo pneumatic drives control are summarised in the following sections.

### **9.1.1 Development of “on-off” control strategy for pneumatic cylinder motion**

Most of previous researches on the control of servo pneumatic drives are based on the traditional motion control strategy. In such strategy, a movement control is achieved by controlling the compressed air that being charged into both of the pneumatic actuator chambers. The pressures in the chambers are equal to the atmospheric pressure or lower than the air supply pressure when the drive is in the standby state. To achieve a good control performance, one or several cooperative high-bandwidth proportional or on-off control valves are placed between the compressed air source and the pneumatic actuator. However, from the manufacturing point of view, the cost of high bandwidth proportional and on-off valves is expensive. This deters the manufacturer from applying this kind of system, thus making them less favourable.

A new pneumatic cylinder motion control strategy has been developed in this research. In this new control strategy, chambers of the pneumatic actuator are directly connected to the compressed air source when the drive is in standby state. The motion control of the actuator is achieved by controlling the release air. Thus, for a complete motion process, air pressure in only one of the chamber is being controlled (the other remains constant). By using this method, not only the air in the chambers is more controllable but also low-

bandwidth pneumatic valves can be employed, hence providing a lower cost pneumatic system.

### **9.1.2 Development of PD-based three-state control algorithm for the “on-off” control strategy**

The new motion control strategy employs two on-off valves as direction control valves. A full motion process can be implemented by controlling only one of the direction valves. There are three motion states within a full motion process. By using logical state of valve control signals of the two direction control valves, the three motion states can be denoted as: “01” motion state (extending motion state), “10” motion state (retracting motion state), and “00” motion state (deceleration and standby state).

A three-state control algorithm is developed for point-to-point motion control of pneumatic system with the new motion control strategy. The algorithm is based on an analogue based control algorithm, for example, PID-based control algorithm. In this algorithm, a function block referred as Interpreting Block converts an analogue control signal to a three-state signal, and outputs cooperated valve control signals the two direction control valves. The three-state control algorithm provides an easy way in control of on-off valves using some traditional control algorithm. It can be implemented by either programming or hardware, or their combination.

### **9.1.3 Development of components-based architecture of integrated pneumatic drives**

The CIPDs designed in this research are oriented by components-based methodology. This architecture provides some significant features.

Initially, a CIPD can be built up using three CIPD components: Integrated Pneumatic Actuator (IPA), Integrated Direction Control Module (IDC), and Integrated Speed Control Module (ISCV). The motion controller inside IPA is integrated with LonWorks Technology with pre-loaded application image. With the special designed cylinder motion control strategy and motion control algorithm, the application image is independent to the characteristics of the other components. Compared with traditional pneumatic drives, main features provided by the architecture are:

- *Flexibility in building up pneumatic drives for different application specifications.* For pneumatic drives providing point-to-point motion force, the specifications that are more concerned in real application mainly are the motion distance, the driving force capability, the motion speed, the positioning accuracy, and so on. These specifications can be met by choosing different combinations of the three components as such specifications are mechanically determined, except the positioning accuracy which is pre-fixed by the application image and independent to the components used. Hence, users can build up different pneumatic drives using different standard CIPD components to meet different application specifications, without concern of modifying the application image.
- *Easy in system tuning.* CIPDs employ a special motion control strategy. The motion speed of load can be adjusted mechanically by a normal user rather than programming the motion controller by a specialist. Furthermore, the application image of a CIPD is independent to characteristics of other components.
- *Multiple-media communication ability.* A CIPD can also be regarded as a component in a large-scale distributed control system. The CIPDs employ the LonWorks Technology which support Multiple-media communication ability; As the design of CIPDs is oriented by distributed control technology, the CIPDs

support the design in both “real” world and “virtual” world. Hence provide a great flexibility for large scale manufacturing system design.

#### **9.1.4 Mathematical analyses of pneumatic system with the new cylinder motion control approach and the “on-off” control strategy**

Mathematical analyses of pneumatic system with the new cylinder motion control approach have been carried out in this research, regarding to the system modelling, system stability, and other system characteristic issues.

The modelling is based on the standard orifice theory and gas laws, and developed in both frequency domain and time domain. The model verifications have been conducted by comparing open-loop system dynamical response obtained through simulation and experiments. Both theory and experimental studies show that pneumatic drives with the new motion control strategy can be largely represented as a second order system for velocity regulation.

Stability is the most important specification for a control system. According to the system transfer function, it is known that, at moving state of motion, there are no roots of the polynomial in the right half-plane. Therefore, the open-loop system is a stable system at moving state of motion. According to the state-space presentation of stopping stage of motion, one conclusion can be made that, at stopping state of motion, the system has two poles, and both poles are real values and not in the right half of the s-plan. Therefore, the system at stopping state of motion is stable. According to the Lyapunov’s direct method, the analyses also showed that a closed-loop controlled CIPD can be a stable system, an asymptotically stable system, or an unstable system, largely depends on the RAE once the system has been setup.

### **9.1.5 Discovery of the Velocity Gain of pneumatic system with the new motion control strategy**

The mathematical analyses carried out during the research have also revealed a relationship that can be applied to estimate the load velocity for the system employing the new motion control strategy. In this research, the relationship is referred Velocity Gain  $K_v$ . The Velocity Gain  $K_v$  is largely determined by the effective area ratio of exhaust orifice and the piston in exhaust chamber. The relationship has been verified by both the experimental results and simulation results.

### **9.1.6 Application considerations of Neuron Chip 3150 for distributed control of pneumatic drives**

LonWorks technology is a complete platform for implementing control network systems. It includes all of the elements required to design, deploy and support control networks. In order to employ the application processor of the Neuron Chip for implementation of distributed controlled pneumatic drive, several solutions have been developed in this research. A set of assistant circuits have been designed working with the Neuron Chip to gain the benefits of efficiently use of the processor. The control algorithm computation update trigger timer, for example, outputs a pulse train signal to meet the scheduler of the Neuron Chip. Each time the change in the state of the signal will cause the control algorithm to be updated; the use of integer in the control algorithm programming could speed up the computation process. Such solutions can be guidance of Neuron Chips applications in other areas requiring fast real-time control system.

### **9.1.7 Research of high-speed motion control of pneumatic drives**

For high-speed point-to-point machinery, fast operating cycle times and good



positioning accuracy with very small or without overshoot is often a prerequisite.

A deceleration control strategy for high-speed motion control of pneumatic drives has been developed in this research. The basic theory of the control strategy is based on control of the Velocity Gain  $K_v$ , which is largely determined by the effective area ratio of exhaust orifice and the piston in exhaust chamber. The application program pre-installed in the motion controller is independent to the hardware. Therefore, to build a cost-effective pneumatic drive, users are allowed to install different numbers of speed control valves and set different exhaust orifice size without changing any programming for the motion controller.

## **9.2 Recommendations for Further Research Work**

### **9.2.1 Further research on performance of pneumatic drives with the new motion control strategy using other control algorithm**

This research has only focused on performance of CIPDs based on PID-based control algorithm. Further research works on the performance of CIPDs with other control algorithm or approach, e.g. Fuzzy logic control, are recommended to understand the CIPDs in a wide aspect.

### **9.2.2 Research on velocity profile control of pneumatic drives with the new motion control strategy**

This research has only focused on point-to-point motion control of CIPDs. For some special applications, velocity profile control may be required. Therefore, further research work on such topic is also recommended. From the mathematical analysis it is known that the amplitude of transient velocity profile of CIPDs is determined by the Velocity Gain  $K_v$ , which is largely

determined by the effective area ratio of exhaust orifice and the piston in exhaust chamber. Hence, for velocity profile control of CIPDs, use of proportional valve may be required to achieve proportional change between the control command signals and the ratio of exhaust orifice and the piston in exhaust chamber.

### **9.2.3 Research on the application of other network technology in the CIPDs**

This research employed the Lonworks Technology as the technology for the distributed control of CIPDs. The data transmitting rate of the control module used in the research is maximum 1.25Mbps, which is much lower than some other network communication protocols and technologies, such as, CPT/IP, Fireware 1394, Bluetooth, IEEE802.11b, Zigbee, and so on. Some of those technologies are for wireless communication which provide more flexibility. Therefore, it will be beneficial to do some further research on application of other network communication technologies with high network communication rate, or wireless communication, in the design of CIPDs.

## Appendix LonWorks Technology

LonWorks technology is a complete platform for implementing control network systems. These networks consist of intelligent devices that interact with their environment, and communicate with one another over a variety of communications media using a common, message-based control protocol. Today, thousands of intelligent devices and appliances are equipped with LonWorks networks. You can find them in every aspect of the device networking environment. LonWorks networks simplify system management, conserve energy, improve operations, and reduce costs.

In a LonWorks network, no central control or master-slave architecture is needed. Control devices communicate with each other using a common protocol. Each device in the network contains embedded intelligence that implements the protocol and performs control functions. In addition, each device includes a physical interface that couples the device with the communications medium.

LonWorks technology includes all of the elements required to design, deploy, and support control networks, specifically the following components:

- MC143150 and MC 143120 Neuron Chips
- LonTalk Protocol
- LonWorks transceivers
- LonBuilder and NodeBuilder Development Tools

LonWorks technology supports distributed, peer-to-peer communications. A typical device (called node) in a LonWorks control network performs a simple task. General devices such as sensors, switched, relays motor drives, and

instruments can normally be developed as nodes on a LonWorks control network. The overall network performs a complex control application, such as running a manufacturing line or automating a building.

LonWorks Technology supports a wide variety of communications media. The most common used are twisted-pair and power-line network. Power line has for long been seen as a potential communication medium due to its widespread availability. Applications targeted at home, building, industrial, transport and utility automation are ideally suited to power line communication. This is due to the conveniently situated power line infrastructure. Advances in high density digital integrated circuits have paved the way for power line communication to become a viable communication option. Traditionally, power line communication equated to unreliability. Nowadays this is certainly not the case.

A LonWork network device consists of a transceiver, a Neuron chip, an I/O circuitry and sense / control devices. Figure A-0-1 shows the typical composing of a LonWorks node.

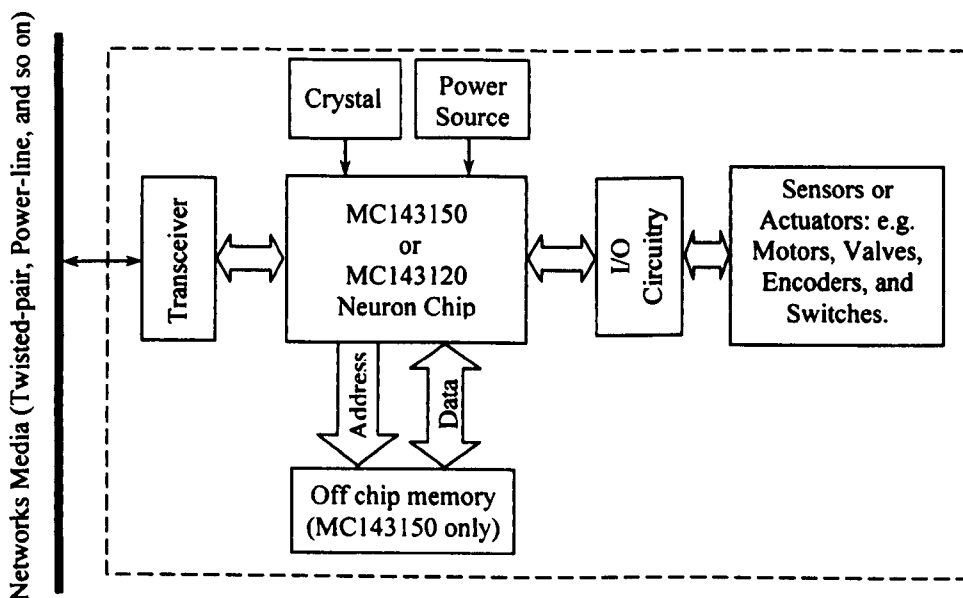


Figure A-0-1 Typical composing of a LonWorks node

The Motorola MC143150 and MC143120 Neuron Chips are sophisticated VLSI devices that make it possible to implement low-cost local operating network applications. Through a unique combination of hardware and firmware, they provide all the key functions necessary to process inputs from sensors and control devices intelligently, and propagate control information across a variety of network media. The Motorola MC143150 and MC143120 Neuron Chips, with the LonBuilder and NodeBuilder Development Tools, provides the system designer many benefits, such as: easy implementation of distributed sense and control networks, flexible reconfiguration capability after network installation, management of LonTalk protocol messages on the network, and an object-oriented high level environment for system development.

Neuron C is the programming language designed for Neuron Chips and based on ANSI C. It includes extension to ANSI C that directly support the Neuron Chip firmware, which make it a very powerful tool for the development of LonWorks application.

### **A.1 Motorola MC143150 Neuron Chip**

The MC143150 is designed for sense and control systems that require large application programs. The MC 143150 has an external memory interface that allows the system designer to use 42K of the available 64k of address space for application program storage. Figure A-0-2 illustrates a simplified block diagram of a MC143150 Neuron Chip.

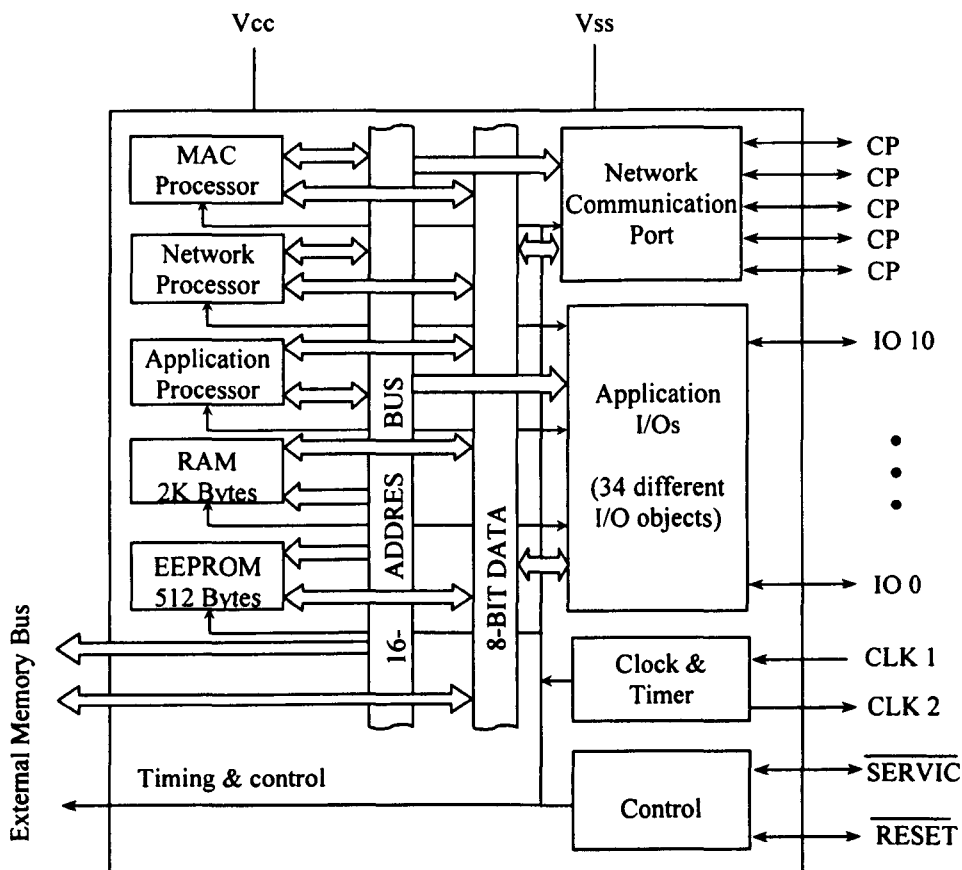


Figure A-0-2 Simplified block diagram of an MC143150 Neuron Chip

An MC143150 Neuron Chip has three 8-bit pipelined processors, one of which is application processor and other two interact with a communication subsystem to make the transfer of information in distributed control system. There are three modes of operation for Neuron Chip's 5-pin communication port. They are single-ended, differential, and special-purpose. Single-ended and differential modes use differential Manchester encoding which is a widely used reliable format for transmitting data over various media. There is an 11-pin I/O interface with integrated hardware and firmware within a Neuron Chip for connecting to application-specific external hardware. These pins may be configured in numerous ways to provide flexible input and output functions with a minimum of external circuitry. There are 5 kinds of I/O objects including 34 different I/O

objects available. Various I/O objects of different types may be used simultaneously. The programming model allows the programmer to declare one or more pins as I/O objects. Pins IO4 through IO7 have programmable (on/off) pull-up resistors. Pins IO0 through IO3 have high current (20 mA) sink capability. All pins (IO0 through IO10) have TTL-level inputs with hysteresis. Pins IO0 through IO7 also have low-level detect latches. More details can be found on [www.echelon.com](http://www.echelon.com).

## **A.2 Echelon TP/FT-10F Control Module**

Echelon's TP/FT-10F control module provides a simple, cost-effective method of adding LonWorks® technology to any control system. The small size of the control module permits them to be mounted on or inside an OEM's product, directly adjacent to the sensors, outputs, or displays that the module will control. Using the control module can save hundreds of hours of development time compared with designing customer modules. The control module is economically priced for both low and high volume users.

The control module is supplied as compact circuit board already including the surface-mount technology (SMT) Neuron 3150 Chip and crystal clock circuit, eliminating the need for the customer to operate an SMT board assembly operation. The Neuron 3150 Chip is operated at 10MHz clock speed. The control module includes circuitry to support an Atmel 29C257 (32K) or 29C512 (64K total, 56K usable), or 29C010A (128K total, 56K usable) flash memory. This feature allows new parameters and applications to be downloaded into the module via the network, and is ideal for applications that require field programming changes or where nodes will be physically inaccessible.

The control module uses an Echelon FTT-10 twist pair transceiver, which is a free topology, transformer-isolated, 78kbps, and differential Manchester encoded communication transceiver. This design provides excellent common mode rejection and permits the system to operate in electrically noisy

environments. It also reduces the susceptibility of the system to ground loops caused by the use of multiple node power supplies that are floating relative to ground. This architecture makes this module ideal for communicating over long distances in industrial environments.

Figure A-0-3 is a simplified block diagram of the TP/FT-10F Control Module. Figure A-0-4 shows a top view of the TP/FT-10F control module and its mechanical dimensions. The control module interfaces to the node application electronics and to the network through two connectors, P1 and P2 respectively. P1 provides access to the Neuron Chip I/O,  $\sim$ RESET, and  $\sim$ SERVICE pins and the power connection for the control module. P2 supports connections to the twisted pair data network.

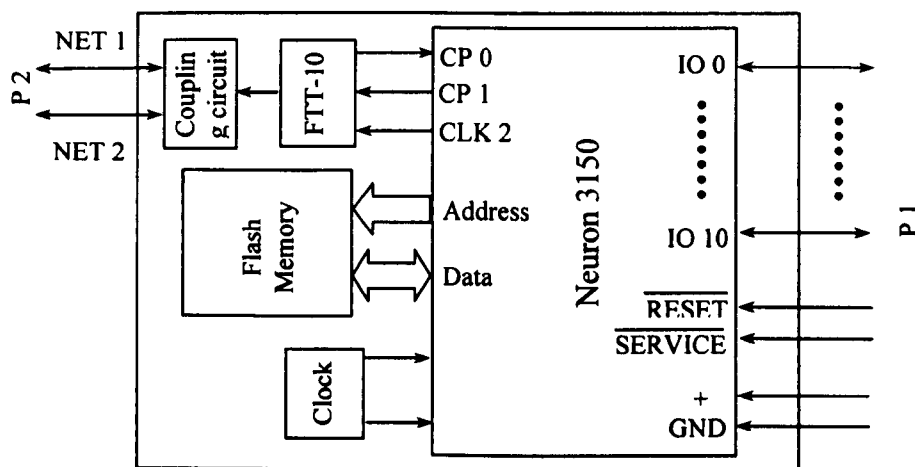


Figure A-0-3 Simplified block diagram of TP/FT-10F Control Module



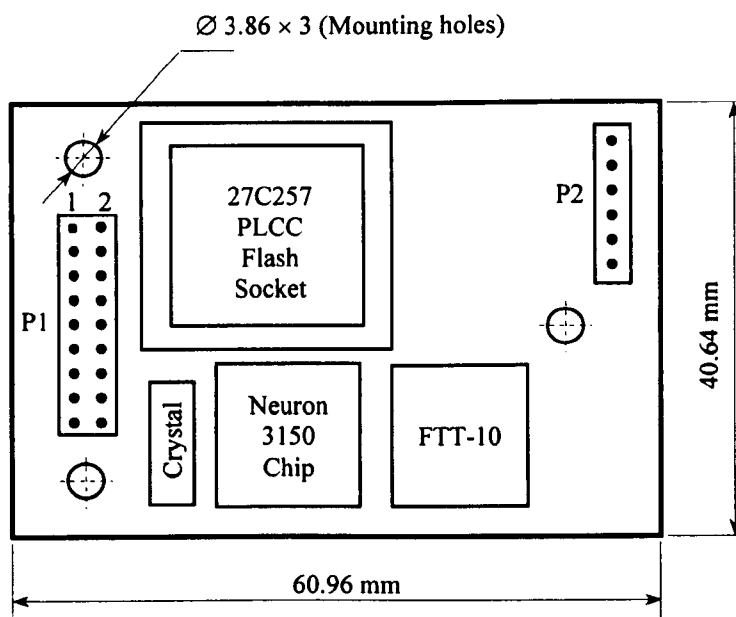


Figure A-0-4 Top view of TP/FT-10F Control Module

### A.3 Programming language - Neuron C

The primary programming language used to write applications for the Neuron Chip is Neuron C. Neuron c is a derivative of the C programming language and based on ANSI C, enhanced to support I/O, event processing, message passing, and distributed data objects. Neuron C includes extensions to ANSI C that directly support the Neuron Chip firmware, which make it a powerful tool for the development of LonWorks applications. Within Neuron C, the new class of objects, network variables simplify the data sharing among nodes on a LonWorks network; the explicit control of I/O operations, through declaration of I/O objects, standardize multi-functional I/O specific to Neuron Chips.

Each Neuron Chip has its own event scheduler which handles task scheduling for the Neuron Chip. The scheduling of Neuron Chip tasks is event driven: when a given condition becomes true, a body of code (called task) associated

with that condition is executed. The scheduler allows you to define tasks that run as the result of certain events, such as a change in the state of an input pin, receiving a new value for a network variable, or the expiration of a timer. Programmer can also specify certain tasks as priority tasks, so that they receive preferential service.

Events are defined through *when* clauses. A when clause contains an expression of an event followed by a body of code. The code will be executed when the expression is true. The following is an example of *when* clause and its associated task.

```

when ( io_changes (home_switch))      ← When clause
{
  //stop load;
  output (valve_A) = off;
  output (valve_B) = off;
}

```

} Task

In this example, when the state of the I/O (`home_switch`, defined elsewhere in the program), which connected to a home position switch is updated, that means that the load just reached the home position, the body of code (the task) that follows the `when (io_changes(home_switch))` clause is executed to close the specified I/O object, `valve_A` and `valve_B` (defined elsewhere in the program). After this task has been executed, the event is cleared. Its task is then ignored until the state of I/O (`home_switch`) is changed and the `when(io_changes(home_switch))` clause again evaluates to TRUE.

Neuron C adheres closely to the ANSI C language standard, however, Neuron C is not a “conforming implementation” of the Standard C. there are some difference between Neuron C and ANSI C, for example, Neuron C does not support floating point computation with C syntax of operators. However, a

floating point library is provided to allow use of floating point data conforming to IEEE 754. Further details can be found in “Neuron C Programmer’s Guide” and “Neuron c Reference Guide” which are available on [www.echelon.com](http://www.echelon.com).

#### **A.4 Network communications**

LonWorks devices communicate with other LonWorks devices through Network Variables (NV) or Application Messages (AM). A network variable is an object that represents a data value and may be connected to multiple devices on a network. Network variables greatly simplify the process of developing and installing distributed systems because devices can be defined individually, then connected and reconnected easily into many new applications. Application messages are used for creating a proprietary interface to a device. Application messages can be used for transfer of data that would not fit into a network variable.

##### ***A.4.1 Communications between devices using network variables***

A network variable is an object on one device that can be connected to network variables on one or more additional devices. A device’s network variables define its inputs and outputs from a network point of view and allow the sharing of data in a distributed application. Whenever a program writes into one of its output network variables (with the exception of output network variables being declared with the **polled** modifier), the new value of the network variable is propagated across the network to all devices with input network variables connected to that output network variable. In case the output network variable is not currently a member of any network variable connection, no transaction and no error occurs. Although the propagation of network variables occurs through LonWorks messages, these messages are sent implicitly. The application program does not require any explicit instructions for sending, receiving, managing, retrying, authenticating, or acknowledging network variable updates.

A neuron C application provides the most recent value by writing into an output network variable, and it obtains the most recent data from the network by reading an input network variable. A writer device (a device that writes to a particular network variable which is an output network variable) can change the value of a network variable. The connected network variables in all reader devices (devices that read a particular network variable which is an input network variable) are then updated to reflect this change. A writer device can also read from its last copy of the network variable, but it will only see the value it wrote last. In other words, two writers of the same network variable cannot change each other's value.

Up to 62 network variables (including array elements) may be declared on a device in a Neuron C program. Programmer can declare an array of network variable. Each element of the array is treated as a separate network variable for purposes of events, transmissions on the network, and so on. Therefore, each element counts individually towards the maximum number of network variables on a given device.

A reader device can also request that the writer device send its latest value for a network variable. A reader device's program may poll any input network variables at any time, including initial power-up and when transitioning from offline to online. Polling on initial power-up can cause network congestion if many devices are powered-up at the same time, and they all do power-up polling.

Connections between network variable outputs and inputs in different devices are specified by user after the device design is complete. The specification of the desired connections is used by a network tool to generate the appropriate network addresses. When these addresses are downloaded into the devices, they ensure that updates sent by writer reach all of the intended readers.

The new value if a network variable received by a reader device does not take

effect immediately upon reception and processing of the message. Similarly, assignment of a new value to an output network variable does not cause a message to be sent immediately.

When a writer device writes a value to an output network variable, the Neuron firmware causes a LonWorks message to be sent to all readers of the variable, informing them of the new value. By default, the message is sent using the acknowledged service.

#### ***A.4.2 Communications between devices using application messages***

Application messages are used for creating a proprietary interface (i.e. non-interoperable) to a device. The same mechanism used for application messaging may also be used to create foreign-frame messages (for proprietary gateways) and explicitly addressed network variable messages.

There is one interoperable use for application messages, and that is the LonWorks file transfer protocol. This protocol is used to exchange large blocks of data between devices or between devices and tools, and may also be used to implement configuration files.

Functional blocks, network variables, and configuration properties are used for creating an open interoperable interface to a device. A device interface may include an interoperable portion and a proprietary portion. For example, a device may implement a proprietary interface for use solely during manufacturing, and an interoperable interface for use in the field.

The content of an application message is defined by a proprietary message code that is sent as part of the message. This code is followed by a variable-sized data field. The same message code can have one byte of data in one instance and 25 bytes of data in another instance.

User can use a request/response service with application messages to enable an application on one device to cause an application on another device to respond to it. The request/response mechanism is similar to a network variable poll. When a network variable is polled, the application scheduler on the pooled device provides the most recent value for that network variable, without intervention of (or knowledge by) the application program. When an application message is sent with the request service, the application program on the remote device takes some action as a result of receiving the request message, and then provides a new value for its response. The request/response service can also be used to implement remote procedure calls, since it provides a way for an application on one device to invoke an action on another device.

Application messages use less EEPROM table space than network variables, but performing the equivalent tasks using application messages always consumes more code space than using network variables because of the amount of support code built-in to the Neuron firmware for the network variables. In addition, using application messages is a more complicated way of accomplishing such a task. User must explicitly build, send, and receive application messages. Message attributes such as service type, authentication, and priority are defined at compile time or run-time, and are not configurable by a network tool after device installation.

Application messages do allow for transfer of data that would not fit into a network variable. A network variable can accommodate up to 31 bytes of data. Application messages allow for up to 228 bytes of data to be transmitted within one message. However, large messages will not pass through most LonWorks routers, because are typically configured for messages with smaller amounts of data.

## List of References

1. Akagi, T., Dohta, S., Matsushita, H. and Tachibana, S. I. (1999). Studies on opto-pneumatic servo system. *JSME International Journal, Series C*, 42(1), p.171
2. Alonso, J. M., Ribas, J., Coz, J. J. D., Calleja, A. J., Corominas, E. L., and Rico-Secades, M. (2000). Development of a distributive control scheme for fluorescent lighting based on LonWorks technology. *Industrial Electronics, IEEE Transactions on*, 47(6), p.1253
3. Bachmam, R. J. and Surgenor, B. W. (1997). On the design and performance of a closed circuit pneumatic positioning system. *The Fifth Scandinavian International Conference on Fluid Power (SICFP '97)*, 1, Linköping, Sweden, p.309
4. Backé, W. (1986). The application of servo pneumatic drives for flexible mechanical handling techniques. *Robotics*, 2, p.45
5. Backé, W. (1993). The present and future of fluid power. *Journal of Systems and Control Engineering*, 207(4), p.193
6. Badea, L. and Daripa, P. (2004). A Domain Embedding Method Using the Optimal Distributed Control and a Fast Algorithm, *NUMERICAL ALGORITHMS*, 36(2), p.95
7. Balasubramanian, K., Guven, K., and Altun, Z. G. (1994). Microprocessor based new technique for measuring pneumatic pressure using optocoupler controlled vibrating wire transducer. *Instrumentation and Measurement Technology Conference, IMTC/94*. p.464
8. Bashir M. Y., Farid A., Swevers, J., Vanherck, P. and Hendrik V. B. (2000). Modelling a pneumatic servo positioning system with friction. *Proceedings of the American Control Conference, Chicago*, 2, p.1067

9. Bhakta, B., Brown, M., Levesley, M. C., and Richardson, R. (2003). Design and control of a three degree of freedom pneumatic physiotherapy robot. *Robotica*, 21 (6), p.589
10. Bowns and Ballard. (1972). Digital computation for the analysis of pneumatic actuator systems. *Proc. Instn. Mech. Engrs*, 186(73/72) p.881
11. Bublitz, W., Pindel, J. and Brunner, P. (1992). Integrating fluid power into control networks. *Hydraulics and Pneumatics*, 45(5), p.35
12. Burrows, C. R. and Webb, C. R. (1966). Use of root loci in design of pneumatic servo-motors. *Control*, p.423
13. Burrows, C. R. and Webb, C. R., (1968), Simulation of an on-off pneumatic servomechanism. *Proc. Instn. Mech. Engrs.*, 182(29) p.631
14. Burrows, C. R. (1969). Effect of position on the stability of pneumatic servo mechanisms. *J. Mech. Eng. Sci.*, 11(6), p.615
15. Burrows, C. R. and Webb, C. R. (1969). Further study of a low-pressure on-off pneumatic servomechanism. *Proc. Instn. Mech. Engrs.*, 184(45), p.849
16. Burton, R. V. (1996). Designing closed-loop circuits for stability. *Hydraulics & pneumatics*. September. p.53
17. Callen, J. N. (1998). Distributed control for unmanned vehicles. *Concurrency, IEEE [see also IEEE Parallel & Distributed Technology]*, 6(2), p.16
18. Callen, J. N. (1998). Distributed control enables flexible intelligent system development. *Intelligent Systems, IEEE*. 13(4), p.14
19. Carter, C. (2000). Distributed control as the way forward. *Control and Instrumentation*. 32(5), p.28
20. Chan, F. T. S. and Chan, H. K. (2004). Analysis of dynamic control strategies of an FMS under different scenarios. *Robotics & Computer-Integrated Manufacturing*, 20(5), p.423
21. Chapman, C. M. (1990) Distributed control for distributed systems.



- Control in Building Energy Management Systems*. IEE Colloquium. p.1/1
22. Chaudhury, A. and Rathnam, S. (1992). Informational and decision processes for flexible manufacturing systems. *Expert, IEEE [see also IEEE Intelligent Systems]*, 7(6), p.53
  23. Chen, C. C., Chen, P. C., and Chen, C. K. (1993). A pneumatic model-following control system using a fuzzy adaptive control. *Automatics*, 29(4), p.1101
  24. Chen, F. F. and Adam, J. E. E. (1991). The impact of flexible manufacturing systems on productivity and quality. *Engineering Management, IEEE Transactions*, 38(1), p.33
  25. Chen, L. and Wang, Y. (2002). Design and implementation of a Web-based distributed control system. *Electrical and Computer Engineering*, 2, p.681
  26. Choi, S. B. and Yoo, J. K. (2004). Pressure control of a pneumatic valve system using a piezoceramic flapper. *Proceedings of the Institution of Mechanical Engineers. C*, p83
  27. Dai, H. (2002). *Distributed control system architecture and smart sensing for intelligent semi-autonomous vehicles*. Doctoral thesis, De Montfort University, Leicester, UK.
  28. Darwish, M. G. and Soliman, H. M. (1988). Design of decentralized reliable controllers for large-scale systems. *International Journal of System Science*, 19(8), P.1529
  29. Deane, J. N. S. (1980). Computer aided design and manufacture. *The management of automation conference, the British management data foundation*, London, U.K.
  30. Diedrich, C., Simon, R., and Riedl, R. (2000). Engineering of distributed control systems. *Industrial Electronics, Proceedings of the 2000 IEEE International Symposium*, 2, p.661
  31. Draper, C. (1984). *Flexible manufacturing systems handbook*. Automation and management systems division. The Chares Stark Draper Laboratory, Inc., Noyes Publications.

32. Echelon, "*NodeBuilder User's Guide*", Revision 2, Echelon Corporation, 078-0141-01B, Document No. 19200
33. El-Demerdash, S. M. and Crolla, D. A. (1996). Effect of non-linear components on the performance of a hydro-pneumatic slow-active suspension system, *Proceedings of the Institution of Mechanical Engineers D, Journal of Automobile Engineering*. 210(D1), p. 23
34. Ellis, J. E. (1996). Distributed control systems-standards and availability for process control. *Measurement and Control*. 29(2), p.41
35. Eriksson, P. T. and Moore, P. R. (1994). Improved computer aided robotics with simulation of sensors, *Proceedings Mechnronics and Machine Vision in Practice*, IEEE Computer Society Press, ISBN 0-8186-6300-6
36. Errahimi, F., Cherrid, H., M'Sirdi, N. K., and Abarkane, H. (2002). Robust adaptive control and observer for a robot with pneumatic actuators, *Robotica*. 20(2), p.167
37. Eun, T., Cho, H. S. and Lee, C. W. (1982). Stability and positioning accuracy of a pneumatic on-off servomechanism. *Proceedings of American Control Conference*, p.1189
38. Fok, S. C., Wang, Z. and Dransfield, P. D. (1995). A digital simulation study of an adaptive controller for a pneumatic cylinder system. *International Journal of Computer Applications in Technology*, 8(3-4), p.163
39. French, M. and Ramirez, A. C. (1996). Towards a comparative study of quarter-turn pneumatic valve actuators. *Proceedings of the Institution of Mechanical Engineers B, Journal of Engineering Manufacture*. 210(B6), p. 543
40. Fujiwara, A., Katsumata, K. and Ishida, Y. (1995). Neural network based adaptive IPD controller for pneumatic cylinder. *Proceedings of the SICE Annual Conference*, p26
41. Gillard, P. (1994). Distributed control. *Control and Instrumentation*. 26(5), p.25

42. Gross, D. C. and Rattan, K. S. (1997). Feedforward MNN controller for pneumatic cylinder trajectory tracking control. *Proceedings of IEEE International Conference on Neural Networks*, 37 p.794
43. Gruhler, G. (1998). CAN open based distributed control systems. *Industrial Automation and Control: Distributed Control for Automation (297)*, IEE Colloquium, March, p.4/1
44. Hamdan, M. and Gao, Z. (2000). A novel PID controller for pneumatic proportional valves with hysteresis. *Proceeding of IEEE Industry Applications Conference*, 2, p1198
45. Harissis, A., Abdelrazik, M. B. E. and Ambler, A. (1990). Connectivity analysis of the benes network under distributed control. *Circuits and Systems, Proceedings of the 33rd Midwest Symposium*, 2, p.732
46. Heck, B. S., Wills, L. M. and Vachtsevanos, G. J. (2003). Software technology for implementing reusable, distributed control systems. *Control Systems Magazine, IEEE*, 23(1), p.21
47. Hirose, Michitaka. (1985). A study on optiona structure of a distributed control system. *Bulletin of the JSME*, 28(246), p.3028
48. Huliehel, F. A., Lee, F. C., Cho, B. H., Sable, D. M. and Choi, B. (1993). New design approach for distributed power systems. *Proceedings of the 28<sup>th</sup> Intersociety Energy Conversion Engineering Conference*, 1, Atlanta, GA, USA
49. Hunt, S. D. (2000). A general theory of economic growth: Resource, competences, productivity, economic growth. *Thousand Oaks, CA: Sage Publications*. p.209.
50. Huntsberger, T. L., Trebi-Ollennu, A., Aghazarian, H., Schenker, P. S., Pirjanian, P., and Nayar, H. D. (2004). Distributed Control of Multi-Robot Systems Engaged in Tightly Coupled Tasks. *Autonomous robots*. 17(1), p.79
51. Huvenoit, B., Bourey, J. P. and Craye, E. (1995). Design and implementation methodology based on Petri net formalism of flexible

- manufacturing system control. *Production Planning and Control*, January – February, Taylor & Francis Ltd. P.51
52. IEEE Committee report. (1993). A review of manufacturers recommendations for the grounding of distributed control system in generating stations. *Energy Conversion, IEEE Transactions*, 8(1), p.1
  53. Jung, B., Jeong, Y. and Burleson, W. P. (1994). Distributed control synthesis for data-dependent iterative algorithms. *Application Specific Array Processors. Proceedings of International Conference on 22-24 Aug.* p.57
  54. Kai Jin, Ping Liang, and Beni, G. (1994). Stability of synchronized distributed control of discrete swarm structures. *Robotics and Automation. Proceedings of IEEE International Conference on 8-13 May.* p.1033
  55. Karl J. Åström and Tore Hägglund (1995). *PID controllers: Theory, Design, and Tuning*. 2<sup>nd</sup> Edition, ISA International Society for Measurement and Control, North Carolina 27709.
  56. Kawakami, Y., Kimura, S., Kawai, S. and Machiyama, T. (1989). Some considerations on the oscillatory behaviour of pneumatic cylinders. *Proceedings of the First JHPS International Symposium on Fluid Power*, Tokyo. p.251
  57. Kawakami, Y., Masuda, S. and Kawai, S. (1993). Some considerations on the position control of pneumatic cylinders. *Proceedings of the Second JHPS International Symposium on Fluid Power*, Tokyo. p.563
  58. Kawakami, Y., Takeda, R. and Kawai, S. (1991). Some considerations on the generalized conditions for high speed driving of pneumatic cylinders. *ASME Proceedings of FLUCOME'91*. p.543
  59. Kernighan, B. W. and Ritchie, D. M. (1988) *C programming language*, Prentice Hall P.T.R., ISBN 0-13-110362-8.
  60. Kimura, T., Hara, S., Fujita, T., and Kagawa, T. (1997). Feedback linearization for pneumatic actuator systems with static friction. *Control Engineering Practice*. 5(10), p.1385

61. Knecht, T., Leszinski, R., and Webe, F.A. (1993). *Making profits after the sale*. The McKinsey Quarterly 4, p79.
62. Krejnin, G. V., Krivz, I. L., and Smelov, L. A. (1992). Improved positioning of pneumatic cylinder by using flexible coupling between the piston and rod, *Proceedings of the Institution of Mechanical Engineers C, Journal of Mechanical Engineering Science*. 206(6), p. 431
63. Lai, J. Y., Menq, C. H., and Singh, R. (1990). Accurate position control of a pneumatic actuator. *ASME J. of Dynamic systems, Measurement and Control*, 112, p.734
64. Lázaro, J. L., García, J. C., Mazo, M., Gardel, A., Martín, P., Fernández, I., and Marrón, M. (2001). Distributed architecture for control and path planning of autonomous vehicles, *Microprocessors and Microsystems*, 25(3), p.159
65. Lee, K.Y. (1997) Intelligent distributed control of power plants. *Advances in Power System Control, Operation and Management. APSCOM-97. Fourth International Conference*, 1. p.66
66. Lesser V. R. and Corkill D. D. (1981). Functionally accurate, co-operative distributed systems. *IEEE Transactions on Systems, Man, Cybernetics*, SMC-11(1), p.81
67. Lui, S. and Bobrow, J. L. (1988). An analysis of a pneumatic servo system and its application to a computer-controlled robot. *ASME, J. of Dynamic System, Measurement, and Control*, 110, p.228
68. Mahalik, N. G. P. C. and Lee, S. K. (2002). A study on production line automation with LonWorks™ control networks. *Computer Standards & Interfaces*, 24(1), p.21
69. Mannetje, J. J. (1981). Pneumatic servo design method improves system bandwidth twenty fold. *Journal of Control Engineering*, 28(6), p.79
70. Marcus, R. D., Leung, L. S., Klinzing, G. E. and Rizk, F. (1990). *Pneumatic conveying of solids* St. Edmundsbury Press, Bury St. Edmunds, Suffolk. ISBN 0-412-21490-3.

71. Mattiazzo, G., Mauro, S., Velardocchia, and Raparelli, T. (1998). On line autotuning for fuzzy logic controlled pneumatic positioners. *Mechatronics '98*, p. 43
72. Mo, P. T. J. (1989). *Modelling of servo-controlled pneumatic drives – A generalised approach to pneumatic modelling and applications in servo-drives design*. Doctoral thesis, the Loughborough University of Technology.
73. Moore, P. R. and Pu, J. (1996). Pneumatic servo actuator technology, Actuator Technology: Current Practice and New Developments. *IEE Colloquium*, p.3/1
74. Moore, P. R., Weston, R. H., and Thatcher, T. W. (1984). Control of pneumatic servo drives using digital compensation. *Proceedings of IASTED Int. Symp. On Telecommunication and Control*, Halkidiki, Greece, p.264
75. Morgan, G. (1985). Programmable positioning of pneumatic actuators. *Applied Pneumatics*, May, p.16
76. Moriwaki, T., Ueda, K., Sugimura, N., Martawirya, Y., and Ninagawa, T. (1993). Design and management of automous distributed manufacturing systems (2<sup>nd</sup> report, Application to scheduling problems considering unscheduled disruptions). *Transaction of the Japan Society of Mechanical Engineers, Series C*, 59, p3976
77. Narraway R. (1982). Making a start in CAD. *Engineering Materials and Design*, July/August, p.15
78. Noritsugu, T. (1987). Development of PWM mode electro-pneumatic servomechanism, *Part II: Position control of a pneumatic cylinder*. *J. of Fluid Control*, 66, p.65
79. Ogata Katsuhiko (1997). *Modern control engineering, (3rd edition)*. Publisher: Tom Robbins, ISBN: 0-13-261389-1.
80. Pan, H. (2002). *A further study on high-speed gantry type pneumatic driven pick-and-place system*. Thesis of M.Phil, De Montfort University, 2002.

81. Pascal L., Frederique M., and Gerard M., (1993), Reference modelling for distributed intelligent control system. *Man and Cybernetics Proceedings of the IEEE International Conference on Systems, Man and Cybernetics*. 5(3), p.17
82. Piuri, V. (1994). Design of fault-tolerant distributed control systems. *Instrumentation and Measurement, IEEE Transactions*, 43(2), p.257
83. Prior, S. D. and Warner P. R. (1991). A new development in low-cost pneumatic actuators. *Proceedings of the 5th International Conference on Advanced Robotics*, 2, p.1590
84. Pu, J. and Weston, R. H. (1988). Motion control of pneumatic drives. *Microprocessors and Microsystems*. 12(7), p373
85. Pu J. and Weston R. H. (1990). Steady state analysis of pneumatic servo drives. *Proc Instn Mech Engrs*, 204, p377
86. Pu, J. and Moore, P. R. (1998). Towards paradigm shift in machine design and control. *Mechatronics '98*, proceedings of the 6<sup>th</sup> UK mechatronics forum international conference, Skövde, Sweden, September 1998, p.23
87. Pu, J., Moore, P. R. and Wang, J. H. (1998). Smart components-based servo pneumatic actuation systems. *Mechatronics '98*, p.61
88. Pu, J., Moore, P. R. and Weston, R. H. (1991a). Digital servo motion control of air motors. *Int. J. of Production Research, Taylor-Francis*, 29(3), p.599
89. Pu, J., Moore, P.R., Weston, R. H., and Chen, C. (1991). Profile-planning in digital motion control of servo pneumatic drives. *ASME Winter Annual Meeting* December, Atlanta, GA
90. Pu, J., Moore, P.R., and Weston, R. H. (1991b). High gain control and tuning strategy for vane-type reciprocating pneumatic servo drives. *Int. J. of Production Research, Taylor-Francis*, 29(8), p.1587
91. Pu, J., Wang, J.H., Moore, P. R., and Wong, C. B. (1997). A new strategy for closed-loop control of servo-pneumatic systems with improved energy efficiency and system bandwidth. *The Fifth Scandinavian International*

- Conference on Fluid Power, (SICFP'97), Linköping, Sweden*
92. Pu, J., Wong, C. B., Moore, P. R., and Zhang, Z. (1998). Energy-efficient control of servo-pneumatic systems. *Invited paper on OLEODINAMICA-PNEUMATICA, Motion Control in Pneumatics*, Publisher Techniche-Nuove, Milan
  93. Purkayashta, P., Sood, S., and Padmanabhan, K., (1995). Computer aided engineering of distributed control systems. *Industrial Automation and Control, (I A & C'95)*, IEEE/IAS International Conference (Cat. No.95TH8005), p.441
  94. Quaglia, G. and Gastaldi, L. (1995). Model and dynamic of energy saving pneumatic actuator. *The Fourth Scandinavian International Symposium on Fluid Power*, Tokyo, Japan, p.731
  95. Raouf B. and Carlos M. (1997). Designing distributed control system on industrials networks, *Expersys-97 Industrial Application*, p.163
  96. Richer Edmond and Hurmuzlu Yildirim. (2000a). A high performance pneumatic force actuator system: Part I – nonlinear mathematical model. *Transactions of the ASME, Journal of Dynamic System, Measurement, and Control*. 122, p. 416
  97. Richer Edmond, Hurmuzlu Yildirim, (2000b), A high performance pneumatic force actuator system: Part II – nonlinear mathematical model. *Transactions of the ASME, Journal of Dynamic System, Measurement, and Control*, 122, p. 426
  98. Safaric, R., Uran, S., and Winther, T. (2004). Control of rigid and flexible objects on a pneumatic active surface device. *Transactions of the Institute of Measurement and Control*; 26 (2), p.139
  99. Sandoval D. and Latino F. (1997). Servopneumatic system stress simplicity, economy for motion solutions. *Control Engineering*, May.
  100. Sanville, F. E. (1986). Two-level compressed air systems for energy saving. *7th International Fluid Power Symposium*, University of Bath, Bath, England, paper 43.



101. Schwarzenbach, J. and Gill, K. F. (1992). *System modelling and control (3rd edition)*, ISBN 0 340 54379 5
102. Shearer, J. L. (1956). Study of pneumatic processes in the continuous control of motion with compressed air, I, II. *Trans. ASME*, Feb, p.233
103. Shearer, J. L. (1957). Nonlinear analogue study of a high pressure servomechanism. *Trans. ASME*, April, p.465
104. Shih, M. C. and Ma, M. A. (1998). Position control of a pneumatic rodless cylinder using sliding mode M-D-PWM control the high speed solenoid valves. *JSME. International Journal. Series C*, 41(2), p.236
105. Shih, M. C. and Ma, M. A. (1998). Positional control of a pneumatic cylinder control by fuzzy PWM control method. *Mechatronics*, 8, No.3, p.241
106. Shih, M. C. and Tseng, S. I. (1994). Pneumatic servo-cylinder position control by PID-self-tuning controller. *JSME International Journal, Series C*, 37, No.3, p.565
107. Sinh, M. C. and Huang, Y. F. (1992). Pneumatic servo-cylinder position control using a self-tuning controller. *JSME International Journal, Series B*, 35, No.2, p.247
108. Sinopoli, B., Sharp, C., Schenato, L., Schaffert, S., and Sastry, S. S. (2003). Distributed control applications within sensor networks. *Proceedings of the IEEE*. 91 , Issue: 8, p.1235
109. Slotine J. J. (1984). Sliding controller design for non-linear system. *International Journal of Control*, 40, No. 2, p. 421
110. Slotine J. J. and Sastry S. S. (1983). Tracking control of non-linear systems using sliding surfaces, with application to robot manipulators. *International Journal of Control*, Vol. 38, No. 2, p. 465
111. Slotine Jean-Jacques E. and Li, Weiping. (1991). *Applied nonlinear control*, Prentice-Hall. Inc, ISBN 0-13-040049-1
112. Smith, S. M. (1994). An approach to intelligent distributed control for autonomous underwater vehicles. *Autonomous Underwater*

- Vehicle Technology, Proceedings of the 1994 Symposium*, July, p.105
113. Suzumori, K. (1999). Pneumatic rubber actuator driven by elastic traveling waves. *JSME International Journal, Series C*, 42(2), p.398
114. Suzumori, K., Hashimoto, T., Uzuka, K. and Enomoto, I. (2002). Pneumatic direct-drive stepping motor for robots. *Intelligent Robots and System, IEEE/RSJ International Conference*, 2, p.2031
115. Suzumori, K. and Hori, K. (1999). Development of pneumatic wobble motors. *JSME International Journal, Series C*, 42(2), p.392
116. Taira, T. and Yamasaki, N. (2004). Functionally Distributed Control Architecture for Autonomous Mobile Robots. *Journal of robotics and mechatronics*, 16(2), p.217
117. Tillett, N. D., Vaughan, N. D. and Bowyer, A. (1997). A non-linear model of a rotary pneumatic servo system. *Proceedings of the Institution of Mechanical Engineers I, Journal of Systems and Control Engineering*. 211(I2), p.123
118. Tizzard, Keith. (1992). *C for professional programmers*. Ellis Horwood Limited, ISBN 0-13-116997-1.
119. VanDoren, V. J. (1998). Basics of proportional-integral-derivative control. *Control Engineering*, March, p.135
120. Vaughan, D.R. (1965). hot-gas actuators: some limits on the response of speed. *ASME J. of Basic Engineering*, March, p.113
121. Virvalo, T. (1989). Designing pneumatic position servo system. *Power International*, 35(408), p.141
122. Wang, H., Mo, J. P. T., and Chen, N. (1998). On the estimation of on - off valve parameters for control of programmable pneumatic actuators. *Transactions of the Institute of Measurement and Control*. 20(5), p. 211
123. Wang, Y. T. and Chang, M. K. (1999). Experimental implementations of decoupling self-organizing fuzzy control to a TITO pneumatic position control system. *JSME International Journal, Series C*, 42(1), p.85

124. Warring, R. H. (1969). Pneumatic engineering calculations. 621.5, 85461 030 3
125. Weston, R. H., Moore, P. R., Thatcher, T. W., and Morgan, G. (1984). Computer controlled pneumatic servo drives. *ImechE*, 198B(14), p.275
126. Williams, S. J. and Mason, B. (1988). The impact of control system design on a flexible manufacturing system for colliery arches. *CONTROL 88, International Conference*, p.189
127. Wise, R. and Baumgartner, P. (1999). Go downstream-the new profit imperative in manufacturing. *Harvard Business Review* 77(5), p133.
128. Wong, C. B., Pu, J., Moore, P. R., and Zhang, Z. (1998). Modelling study and servo-control of air motor systems. *Int. J. Control*, 71(3), p.459
129. Xiang, F. and Wikander, J. (1998). Synthesis and analysis of feedback linearization for pneumatic actuator control systems. *Mechatronics '98*, p. 37
130. Xie, C., Pu, J., and Moore, P. R. (1998), A case study on the development of intelligent actuator components for distributed control systems using LonWork neuron chips, *Mechatronics*, 8(2), p.103
131. Xie, Changwen. (1999). *Methods, tolls and components paradigms for the design and building of distributed machine control systems*, Doctor of philosophy thesis, De Montfort University, Leicester, UK.
132. Yamada, Y., Tanaka, K., Sakamoto, M., and Shimizu, A. (1997). Improved design scheme of adaptive pole-placement control for pneumatic servo systems. *Advanced Intelligent Mechatronics '97*, IEEE/ASME International Conference, p.139
133. Yamasaki, N. (2004). Design Concept of Responsive Multithreaded Processor for Distributed Real-Time Control. *Journal of robotics and mechatronics*. 6(2), p.194
134. Zhang, Zhongmao. (1999). *Further advancements in modelling study of servo pneumatic drives and energy-efficient control schemes*. Doctor of philosophy thesis, De Montfort University, Leicester, UK.

135. Zheng W. B., Wang M. Q., (2000). Enterprise network and distributed control network platform, *Intelligent Control and Automation*, Proceedings of the 3rd World Congress, 5, p.3632